Climatological trends and predictions in snowfall over the Canadian snowbelts of the Laurentian Great Lakes Basin

by

Janine A. Baijnath-Rodino

A thesis
presented to the University of Waterloo
in fulfillment of the
thesis requirement for the degree of
Doctor of Philosophy
in
Geography

Waterloo, Ontario, Canada, 2018

Examining Committee Membership

The following served on the Examining Committee for this thesis. The decision of the Examining Committee is by majority vote.

External Examiner	Dr. Jia Wang
Supervisor(s)	Dr. Claude R. Duguay
Internal Member	Dr. Ellsworth LeDrew
Internal Member	Dr. Richard Kelly
Internal-external Member	Dr. Andrea Scott

AUTHOR'S DECLARATION

This thesis consists of material all of which I authored or co-authored: see Statement of Contributions included in the thesis. This is a true copy of the thesis, including any required final revisions, as accepted by my examiners.

I understand that my thesis may be made electronically available to the public.

Statement of Contributions

This thesis contains six chapters. Chapters 1, 2, and 6 provide a general introduction, background, and overall conclusion, respectively. Chapters 3,4, and 5 comprise three separate journal articles that examine the role of lake-induced snowfall within the understudied region of the Canadian Laurentian Great Lakes Basin. The first paper focuses on the climatological trends of snowfall over the Laurentian Great Lakes Basin and is published in the peer reviewed journal*, International Journal of Climatology*. The second paper assesses the historical spatiotemporal trends in snowfall extremes over the Canadian domain and has been submitted to the international peer reviewed journal entitled, *Advances in Meteorology*. Finally, the third paper, which evaluates a regional climate model's capability to reproduce lake-induced snowfall, has been submitted to the international peer reviewed journal entitled *Theoretical and Applied Climatology.*

The work presented in this thesis is a result of direct supervision from Dr. Claude Duguay at the University of Waterloo. Dr. Duguay helped with the initial research proposal and facilitated collaboration with the Canadian Network for Regional Climate and Weather Processes (CNRCWP) at the Université du Québec à Montréal (UQAM), Canada, which was funded by the Natural Science and Engineering Research Council (NSERC) from 2013-2017. In addition, Dr. Ellsworth LeDrew, a co-author on manuscript 1, provided beneficial suggestions in the atmospheric processes. Furthermore, Dr. Andrea Scott aided in the final version of Manuscript 1 by providing beneficial suggestions in error analyses methods. Manuscript 2 and 3 are joint collaborations between Janine and Dr. Duguay. However, model data obtained for analysis in manuscript 3 was provided by the CNRCWP working group in direct communication with Dr. Oumarou Nikiema and Ms. Katja Winger. Revisions on manuscript 3 were provided by Dr. Oleksandr Huziy from UQAM. These collaborative efforts were beneficial in the final outcome of this thesis.

Abstract

The leeward shores of the Laurentian Great Lakes are highly susceptible to lake-induced snowfall that is either driven by extratropical cyclones or lake effect processes. During the late autumn and winter season, cold air advection over relatively warm lakes induces instability in the lower planetary boundary layer (PBL). This process facilitates the exchange of moisture and energy fluxes and fuels the development of snowfall. In addition, the large thermal capacity of the lakes can enhance existing precipitation that is associated with frontal boundaries moving over the Great Lakes Basin (GLB). Lake-induced snowfall can produce whiteout snowsqualls and heavy snowfall accumulations in highly localized areas, which can affect residential, agricultural, economic, and recreational sectors within the GLB. Therefore, the dangerous impacts of lake-induced snowfall on snowbelt communities warrant the need for improved spatiotemporal investigations in observed and predicted snowfall.

Despite many snowfall studies, three gaps have been identified. The first gap suggests that minimal snowfall research has been conducted for the Ontario snowbelts of Lake Superior and Lake Huron-Georgian Bay (hereinafter referred to as Lake Huron). The second gap identifies that there has been limited investigations conducted on climatological trends in snowfall and LES predictor variables. The third gap suggests that most lake-induced snowfall studies have employed coarse global climate models (GCMs) and regional climate models (RCMs) at spatial resolutions that make it difficult to delineate meso-beta scale LES snow bands. Thus, the objective of this study is to conduct historical spatiotemporal trends in snowfall and LES predictor variables, and to examine the predictive performance of a RCM in capturing LES events for the under-studied regions of the Canadian Laurentian Great Lakes' snowbelts.

Manuscript 1 investigated 1980-2015 spatiotemporal trends in monthly total snowfall and total precipitation over the GLB using the Daymet (Version 3), hereinafter referred to as Daymet, gridded dataset. Results showed a significant decrease in snowfall (at the 95%

confidence level), at a rate of 40 cm/36yrs, and a significant decrease in total precipitation of 20 mm/36yrs, along the Ontario snowbelts of Lake Superior and partially along that of Lake Huron. Attributions to these negative spatiotemporal trends are explored using data from the North American Regional Reanalysis (NARR) and the Canadian Ice Service (CIS). Predictor variables showed significant warming in lake surface temperature (LST) at a rate of over 6 °K/36yrs for Lake Superior; significant decrease in ice cover fraction for both lakes; and an increase in the vertical temperature gradient (VTG). While the resultant trends of these variables are believed to enhance snowfall in these regions, through increased evaporation into the lower PBL, there are other complex processes involved, such as inefficient moisture recycling and increased moisture storage in warmer air masses that inhibit the rapid production of precipitation.

Following the identification of trends in monthly snowfall totals, the second manuscript explored whether historical spatiotemporal trends in monthly snowfall extremes were also changing. Manuscript 2 assessed the intensity, frequency, and duration of snowfall within Ontario's GLB. Monthly spatiotemporal snowfall and total precipitation trends were computed for the 1980-2015 period using Daymet. Results showed that extreme snowfall intensity, frequency, and duration have significantly decreased, at the 90% confidence level, predominantly in December and January along Lake Superior's snowbelt. Intensity has decreased at a rate of approximately 6 cm/36yrs and 2 cm/36yrs for December and January, respectively. The frequency in extreme snowfall events has decreased by 5 days/36yrs. Furthermore, the number of consecutive days of extreme snowfall events have decreased at a rate of 1 day/36yrs. The Canadian snowbelts of Lake Superior and Lake Huron exhibited different spatiotemporal patterns, and even within a particular snowbelt region, trends in extreme snowfall are not spatially coherent. Discussions into the local and large-scale surface-atmosphere variables that influence these spatiotemporal trends were presented.

Finally, in order to investigate future trends in snowfall over the GLB, reliable high-resolution RCMs are required to accurately predict historical LES events. Thus, Manuscript 3 conducted validation testing on the high resolution, 0.11° (12 km), Canadian Regional

Climate Model Version 5 (CRCM5), interactively coupled to the one-dimensional Freshwater Lake model (FLake). Predictions of snow water equivalent (SWE) and precipitation along the Canadian snowbelts of Lake Superior and Lake Huron during the months of December and January were tested for the period 1995-2014. This study assessed the model's performance in predicting the timing, location, and precipitation accumulation of specific lake-induced events during a high (2013-2014) and a low (2011-2012) ice season. Findings showed that December SWE had a negative mean bias difference (MBD) $\leq$ -10 mm along both snowbelts, with values $\leq$ -30 mm in January. Similarly, December precipitation showed MBD $\leq$ -5 mm and January's precipitation MBD $\leq$ -10 mm for both snowbelts. Comparison of lake-induced precipitation events also showed that the model mostly under-predicts the daily accumulated precipitation associated with each event but tends to accurately capture the timing and the general location of the snowsqualls along the snowbelts, though not for highly localized snow bands. The findings gained from this thesis, through exploring historical spatiotemporal snowfall trends and RCM validation analyses, are essential for sustainability and adaptation studies.

Acknowledgments

It has been a distinct privilege to be associated with the persons named herein for the duration of this research. I owe a depth of gratitude for their collective efforts on this journey.

This experience would not have been possible without the opportunity granted by Dr. Claude Duguay, under whose supervision I became a member of the Canadian Network for Regional Climate and Weather Processes. His guided direction on my research and patience in mentoring me throughout this process have motivated me towards this final academic outcome.

I would sincerely like to thank all of my committee members for their unlimited support throughout my academic pursuit at the University of Waterloo. Particular thanks go to Dr. Richard Kelly who readily availed himself for meetings and provided references, one of which offered me the unique opportunity to intern at the NASA Ames Research Center. My gratitude is also extended to Dr. Ellsworth LeDrew, whose knowledge on atmospheric sciences and climatology made it a pleasure to partake in enriching discussions. It was also very rewarding acting as a teaching assistant for his climatology classes. I am also thankful to Dr. Andrea Scott for her unwavering support and timely suggestions for overseeing some of the technical aspects of my research.

I would be remiss without recognizing my parents and sister, who have resiliently stood by me from the very beginning. Their unconditional and unflinching support has been my motivation to this end. I hope to be equally inspirational to my niece, Incy, and nephew, Zoogies.

Finally, a heartfelt thank you to my supportive husband, Christian, who has always patiently considered my whirlwind of life ideas. His calm and encouraging nature is unmatched and has been truly appreciated throughout this academic journey.

Dedication

To the angels I have gained throughout my academic pursuit

Table of Contents

List of Figures

List of Tables

List of Abbreviations

3D-VAR	Three-Dimensional Variation
AMIP	Atmospheric Model Inter-comparison Project
AMO	Atlantic Multidecadal Oscillation
AR3	Third Assessment Report
ARM	Atmospheric Radiation Measurement
AVHRR	Advanced Very High Resolution Radiometer
CAPE	Convective Available Potential Energy
CanSISE	Canadian Sea Ice Evolution
CCM1	Canadian Climate Centre Coupled Ocean-atmosphere model
CIS	Canadian Ice Service
CLASS	Canadian Land Surface Scheme
CNRCWP	Canadian Network for Regional Climate and Weather Processes
CRCM5	Canadian Regional Climate Model Version 5
DOE	Department of Energy
ECCC	Environment and Climate Change Canada
EDLORA	Electra Doppler Radar
ENSO	El Niño-Southern Oscillation
ERA	European Reanalysis
EST	Eastern Standard Time
FLake	Freshwater Lake Model
GCM	Global Climate Model
GEM	Global Environmental Multi-scale
GHCN	Global Historic Climatology Network
GLB	Great Lakes Basin
GLERL	Great Lakes Environmental Research Laboratory
GLSEA	Great Lakes Surface Environmental Analysis
GOES	Geostationary Operation Environment Satellite
GR1	Global Reanalysis 1
HadCM2	Hadley Centre Coupled Model Version 2

IPCC	Intergovernmental Panel on Climate Change
LES	Lake Effect Snowfall
LST	Lake Surface Temperature
MAE	Mean Absolute Error
MBD	Mean Bias Difference
MERRA	Modern-Era Retrospective analysis for Research and Applications
MK	Mann Kendall
MODIS	Moderate Resolution Imaging Spectroradiometer
NARR	North American Regional Reanalysis
NASA	National Aeronautics and Space Administration
NAO	North Atlantic Oscillation
NCAR	National Center for Atmospheric Research
NCEP	National Centers for Environmental Prediction
NDJFM	November, December, January, February, March
NEMO	Nucleus for European Modelling of the Ocean
NOAA	National Oceanic and Atmospheric Administration
NWP	Numerical Weather Prediction
NWS	National Weather Service
PBL	Planetary Boundary Layer
PDO	Pacific Decadal Oscillation
PVA	Positive Vorticity Advection
RCM	Regional Climate Model
RegCM4	Regional Climate Model Version 4
RMSD	Root Mean Square Difference
SLR	Snow Liquid Ratio
SNODAS	Snow Data Assimilation System
SRES	Special Report Emission Scenarios
SWE	Snow Water Equivalent
UQAM	Université du Québec à Montréal
VIIRS	Visible Imaging Radiometer Suite
VTG	Vertical Temperature Gradient

WRF	Weather Research Forecast

List of Symbols

C_p	Heat capacity of dry air at a constant pressure (1004 $J \bullet K^{-1} \bullet kg^{-1}$)
f	Coriolis parameter
H	Sensible heat flux
H_n	Estimated height of new snowfall
k	Von Kármán's constant
L	Latent heat per unit of evaporation
LE	Latent heat flux
o	Observed variable
P_1	Daily total precipitation (mm)
P_n	New snowfall
p	Air pressure
pr	Predictor variables
q_a	Water vapor mixing ratio
q_w	Saturation mixing ratio at the water surface temperature
$q*$	Frictional mixing ratio
R	Ratio of daily snowfall to the total daily precipitation
R	Ideal gas constant for dry air (287 $J \bullet K^{-1} \bullet kg^{-1}$),
$R*$	Universal gas constant (8.3145 x 103 $J \bullet K^{-1} mol^{-1}$)
s	Flux adjustment
T	Temperature
$Tair_{850}$	Temperature at 850 mb level
$Tair_{1000}$	Temperature at 1000 mb level
T_{LST}	Lake surface temperature
T_{max}	Maximum air temperature
T_{mid}	Midpoint air temperature
T_{min}	Minimum air temperature
U	Wind speed
$U*$	Frictional velocity
V_g	Geostrophic wind vector

X	Average value of a variable
z	Height above surface
z_o	Roughness length
θ_a	Potential air temperature
θ_w	Potential water surface temperature
$\theta *$	Frictional temperature
μ	Median value of a variable
ρ_{air}	Density of air
ρ_{snow}	Density of snowfall assigned
$\sigma *$	Standard deviation
σ	Static stability
ς_g	Geostrophic vorticity
ω	Vertical motion

Chapter 1
General Introduction

Lakes influence weather and climate by affecting spatiotemporal patterns in air temperature and precipitation at local to regional scales. Lake-induced snowfall is a meteorological phenomenon driven, in part, by lakes, and can have significant and detrimental impacts on local residents and the economy. Therefore, it is important to monitor and predict the response of lake effect processes to climate change in highly populated, lake-rich regions, such as the Laurentian Great Lakes Basin (GLB). Many snowfall studies within the GLB have focused on the United States domain of the Great Lakes, with minimal attention paid to the Canadian snowbelts. Furthermore, most of these investigations have been case studies that generally lacked in analyses of spatiotemporal trends in observed or simulated snowfall. Therefore, the purpose of this thesis is to assess the historical changes of snowfall patterns in response to a warming climate and to evaluate a climate model's performance in predicting snowfall along the under-studied Canadian snowbelts of the GLB.

Climate change, driven by either natural or anthropogenic forcings, can lead to changes in the occurrence or strength of extreme weather and climate events, such as extreme precipitation (Cubasch et al., 2013). It is therefore essential to assess the spatiotemporal response of precipitation to climate change, in particular, for lake-rich regions. This is because lakes influence regional climate and weather by modulating the local surface energy budget, hydrological budget, and atmospheric circulation patterns (Anyah and Semazzi, 2004; Obolkinm and Potemkin, 2006; Dupont et al., 2012; Martynov et al., 2012). As a result, lakes can influence the production of snowfall known as lake-induced snowfall.

Lake-induced snowfall describes both lake effect snowfall (LES) and lake-enhanced processes, as defined by Suriano and Leathers (2016). Lake effect snowfall is a meso-beta scale system that develops when boundary layer convection is initiated as a result of a cold and dry continental air mass advecting over relatively warm and ice-free lakes. This advection generates turbulent moisture and heat fluxes into the atmosphere, through

evaporation and conduction respectively, and destabilizes the lower part of the planetary boundary layer (PBL). The increase of moisture into the PBL, along with downwind frictional convergence, initiate convection and produce cloud formation and precipitation along the leeward shores of lakes (Wiggin, 1950; Eichenlaub, 1970, 1979; Holroyd, 1971; Hozumi and Magono, 1984; Pease et al., 1988; Leathers and Ellis, 1993; Niziol et al., 1995; Ballentine et al., 1998; Kristovich and Laird, 1998; Notaro et al., 2013; Campbell et al., 2016). Lake effect bands can range from approximately 5 km to a few hundred km in size (Notaro et al., 2013). The vertical atmospheric lake effect profile often features a moist-neutral or unstable convective boundary layer that extends to a shallow 1 to 4 km in height above the lake surface. After an approximate height of 4 km, the capping stable layer, or inversion, limits the vertical extent of convection (Niziol, 1987; Byrd et al., 1991; Kristovich et al., 2003; Schroeder et al., 2006; Campbell et al., 2016).

In contrast to lake effect snowfall, lake-enhanced snowfall is driven by a large synoptic scale system that is already associated with snowfall, such as extratropical cyclones. Extratropical cyclones are generated by quasigeostrophic forcing from positive temperature advection or positive vorticity advection (PVA) (Notaro et al., 2013) and are associated with a low-pressure centre tracking zonally following the jetstream. Lake-enhanced snowfall occurs when these cyclones move over relatively warm and ice-free lakes. Thus, frequent wintertime extratropical storms, such as the Alberta Clipper, Colorado Low, and Nor'easter, track from west to east, affecting surface-atmosphere processes within the GLB region. These systems can increase the altitude of the capping inversion, producing deeper cloud convection, and as a result, enhance existing snowfall.

1.1 Motivation

The lake effect process is observed over many water bodies worldwide, such as Lake Baikal in Russia and the Aral Sea in Western Asia (Obolkin and Potemkin, 2006; Hartman, 2013). Lakes of North America that produce lake-enhanced snowfall include, Great Salt Lake, Lake Tahoe, Lake Champlain, the Finger Lakes, Lake Athabasca, Lake Winnipeg, and Lake Winnipegosis, Great Bear Lake, and Great Slave Lake (Carpenter, 1993; Cairns et al., 2001; Payer et al., 2007; Laird et al., 2009; Laird et al., 2010; Hartmann et al., 2013).

Canada is the country with the greatest number of lakes (ECCC, 2017b). Over 500 of these lakes are larger than 100 km^2, with some of the Laurentian Great Lakes ranked among the largest freshwater lakes, by area, worldwide (ECCC, 2017b).

The Laurentian Great Lakes were formed at the end of the last ice age, over 10 000 years ago, when immense glaciers carved and gouged a number of basins, which filled as the melting glaciers began to retreat. Today, the Canadian leeward shores of the Laurentian Great Lakes are of prime importance. Cumulatively, the Great Lakes contain approximately 60% of the world's freshwater, with a total surface area of approximately 244 000 km^2 (Notaro et al., 2013; ECCC, 2017b). These lakes support 40% of Canada's economic activities, 25% of its agricultural capacity, and 45% of its industrial capacity. The Laurentian Great Lakes also support approximately 400 million dollars in cumulative recreational and commercial fishing industries and 180 billion dollars in Canada and United States trade (ECCC, 2017b). Furthermore, over 33 million people reside within the GLB, including 90% of Ontario's population. Approximately 1.5 million live along the Canadian shores of Lake Huron and 200 000 along Lake Superior (NOAA, 2017). Thus, heavy lake-induced snowfall downwind of the highly populated Great Lakes can pose danger to life, property, and transportation. Lake-induced snowfall can also affect multimillion-dollar recreational industries, agricultural activities, water supplies, and hydroelectric generation (Norton and Bolsenga, 1993; Kunkel et al., 2000; Burnett et al., 2003; Kristovich and Spinar, 2005; Hartmann et al., 2013)

Because these lakes are situated in a climatologically favourable geographic location for producing lake-induced snowfall (Comet, 2015), snowstorms can affect many communities along the populated leeward shores of the Great Lakes during late autumn and winter months (Hartmann et al., 2013; Burnett et al., 2003). Examples of extreme lake-induced snowfall events include the Southern Ontario storm of December 2010. This event produced heavy westerly snowsqualls off Lake Huron-Georgian Bay (hereinafter referred to as Lake Huron), producing between 75 and 100 cm of snow during a four-day period in communities from Grand Bend to London, and Thornbury to Alliston. In Buffalo, New York, an unexpected snowstorm on October 2006 produced 60 cm of snow during a 12-

hour period. This event impacted over 1 million people within a highly localized, 40 km by 64 km, area (Hamilton et al., 2006). Separately, two consecutive November 2014 LES storms produced a cumulative 200 cm of snow in New York State. This led to l3 fatalities, hundreds of structural failures, power outages from downed wires and trees, and thousands of stranded motorists (NWS, 2014). These examples further reinforce that lake-induced snowfall can have devastating impacts on populated communities and businesses, giving credence to researching snowfall in a changing environment.

1.2 Gaps in the Literature

Published LES studies have increased over the last half of the 20th century (Hartman et al., 2013) and have utilized both observational and climate modelling approaches. However, despite research progress, three identifiable gaps within this field were recognized. The first gap is the lack of snowfall studies conducted for the Canadian snowbelt regions of the GLB. Secondly, few investigations on climatological trends in snowfall totals and extremes for the Canadian snowbelt have been conducted. Finally, a limited number of studies have evaluated regional climate model (RCM) predictions of lake-induced snowfall.

1.2.1 *Lack of Snowfall Investigations for the Canadian Snowbelts of the GLB*

The study regions for many lake-induced snowfall investigations within the GLB have been limited to the United States, with minimal focus on the Ontario snowbelts along the leeward shores of Lake Superior and Lake Huron. Examples of this disparity include work by Leathers and Ellis (1996), who examined mechanisms responsible for large observed snowfall amounts, but restricted their study area to the Eastern Great Lakes of the United States. Kristovich et al. (2000) investigated improvements in LES predictions, limiting their area of interest to Ohio and Illinois in the United States Midwest. Burnett et al. (2003) assessed LES trends over the last half of the 20th century, focusing their study sites around Syracuse and Buffalo, New York. Kunkel et al. (2009) performed a quality assessment of snowfall data in the GLB and identified a number of homogenous stations suitable for long-term trend analyses; however, these stations were solely located in the United States. Hartman et al. (2013) analysed LES forecasting techniques and focused only on Buffalo, New York. Finally, Hartnett et al. (2014) examined spatiotemporal snowfall patterns and

their underlying causes in Central New York. The regional disparity of LES research could be attributed to the relatively sparse networks of weather observation stations in Canada compared to the large spatial coverage in the United States. It is evident that LES analyses for the Canadian snowbelt is lagging compared to that of the United States and require an increase in research focus.

1.2.2 Lack of Climatological Lake-Induced Snowfall Investigations

The second gap highlights the under-examination of historical monthly total snowfall trends and extremes compared to case studies. The majority of LES publications have focused on analysing specific LES events and associated dynamic features. For example, Lackmann (2001), and Leathers and Ellis (1996) conducted case studies to identify key features that develop prior to LES events over Southern Ontario and Western New York. They found that the ideal synoptic setup includes a surface high pressure in the Midwest and a surface low over Eastern Canada. Another case study by Niziol et al. (1995) found that the presence of a 500 mb trough over the GLB was required for the production of LES. A study on a specific LES event by Hamilton et al. (2006) on the October 2006 lake effect snowstorm identified the presence of a cold front moving across Lake Erie. This study highlights the importance of investigating upper level synoptic systems. Hartmann et al. (2013) conducted a case study on LES in Buffalo, New York and outlined key synoptic features required for the development of LES by monitoring the geopotential height at the 1000, 925, 850, 700 mb, and 500 mb levels over James Bay. Furthermore, modelling case studies of short duration LES simulations have also been conducted and range in complexity from primitive equation models (Ellenton and Danard, 1979), cloud-resolving models (Maesaka et al., 2006), mixed layer models (Lavoie, 1972), to mesoscale models (Hjelmfelt, 1990; Warner and Seaman, 1990; Bates et al., 1993; Sousounis and Fritsch, 1994; Ballentine et al., 1998; Tripoli, 2005; Shi et al., 2010; Notaro et al., 2013). Case studies contain valuable information on the dynamics and key factors triggering the development of LES. However, assessing and monitoring lake-induced snowfall trends and extremes in response to climate change are of strong importance for sustainability and adaptation studies. This aspect of snowfall research still requires continued investigation.

1.2.3 Lack of RCM Studies in LES along the Canadian Snowbelt Regions

The third gap is the lack of LES studies using predictions from high spatial resolution regional climate models (RCMs). Climate model predictions are useful in simulating weather events such as ice storms and droughts, which are important in impact adaptation work. Many of these extreme events are accurately simulated in higher resolution modelling systems (Zadra et al., 2008). Testing the performance of high resolution RCMs in producing and delineating historical LES events and trends is needed to provide confidence in future snowfall scenarios.

Of the few modelling lake-induced snowfall studies, most have employed relatively coarse-resolution global climate models (GCMs). For instance, Cohen and Allsopp (1988) used an 8° x10° spatial resolution model to infer the reduction of snowfall downwind of Lake Huron and Lake Ontario in response to a doubled CO_2 scenario. Similarly, Kunkel et al. (2002) used two coarse GCMs to identify weather conditions related to LES off of Lake Erie and to investigate projected changes in the frequency of these favourable conditions for the late 20th and 21st centuries. Their results are consistent with Cohen and Allsopp (1988) who suggest that LES downwind of Lake Erie will become less abundant. However, the relatively coarse resolution of GCMs makes it challenging to accurately resolve meso-beta scale snow squalls and snow bands that are present with different LES morphologies.

Furthermore, Vavrus et al. (2013) employed the 25 km Regional Climate Model (RegCM4) to simulate ice cover concentrations over the Laurentian Great Lakes between 1976 and 2002. They observed negative trends, attributable to the warming in the 21st century and suggest that changes towards more open water should favour the production of lake-induced snowfall. In contrast, GCM ensemble predictions, under the special report emission scenarios (SRES) A1B greenhouse gas emission, project fewer extreme cold-air outbreaks by 50 to 100% over the Northern Hemisphere (Vavrus et al., 2006), a variable that may reduce the likelihood of LES development. Logically, these studies present contradicting projections of LES trends in response to climate change. However, prior to investigating future snowfall trends, high resolution climate models need to be evaluated

with historical snowfall data. This thesis addresses the three aforementioned gaps by fulfilling three objectives as discussed in the following.

1.3 Goals and Objectives

The overall goal of this research is to determine the historical spatiotemporal behaviours of lake-induced snowfall over the under-studied snowbelts of the Canadian GLB, and to determine whether regional climate models are capable of predicting these behaviours. Three specific objectives have been established for addressing the overall goal. The first objective is to determine historical (1980-2015) trends in cold season monthly snowfall totals over Ontario's snowbelts of Lakes Superior and Huron. A set of LES predictor variables are explored to provide explanations for the resultant snowfall trends (Chapter 3). The second objective is to assesses historical spatiotemporal trends (1980-2015) in extreme snowfall intensity, frequency and duration over the two Ontario snowbelts. Explanations of these results are provided by discussing potential surface-atmosphere controls (Chapter 4). Lastly, the third objective is to evaluate a regional climate model's performance in predicting the location, timing, and accumulation of contemporary (1995-2014) lake-induced snowfall events within the Canadian snowbelts of the GLB. Additional LES predictor variables are also explored to help diagnose issues within the model (Chapter 5). A detailed description of each objective and approach will be presented in the upcoming chapters.

1.4 Thesis Structure

This dissertation follows a manuscript-based thesis format that comprises six chapters. The current chapter (Chapter 1) presents the general introduction, provides the motivation of the thesis by outlining the major gaps within the research, and establishes the three objectives of this study. Chapter 2 discusses the physical and dynamic properties of lakes and their role in regional weather and climate. It also describes the dynamic and thermodynamic processes of lake-induced snowfall and related LES morphological structures, and the key surface-atmosphere predictor variables that influence the development of LES. Chapter 3 addresses objective one and presents manuscript one entitled:

***Baijnath-Rodino, J.A.**, C.R. Duguay, E. LeDrew:* Climatological Trends of Snowfall over the Laurentian Great Lakes Basin. *International Journal of Climatology. 2018.*

Chapter 4 addresses objective two and presents manuscript two entitled:

***Baijnath-Rodino, J.A.**, C.R. Duguay:* Historical Spatiotemporal Trends in Snowfall Extremes over the Canadian Domain of the Great Lakes Basin. *Advances in Meteorology. In review.*

Chapter 5 addresses objective three and presents manuscript three entitled:

***Baijnath-Rodino, J.A.**, C.R. Duguay:* Assessment of Coupled CRCM5-FLake on the Reproduction of Wintertime Lake-Induced Precipitation in the Great Lakes Basin. *Theoretical and Applied Climatology. In review.*

Finally, Chapter 6 concludes the thesis by summarizing the key results of the research. It also discusses some of the limitations on the current work and addresses areas of future research on lake-induced snowfall within the realm of meteorology and climatology.

Chapter 2
Physical and Dynamic Properties of Lake-Induced Snowfall and Forecasting Techniques

2.1 Physical and Thermodynamic Processes of Lakes

To understand lake-induced snowfall processes, Chapter 2 reviews the physical and thermodynamic properties of lakes, followed by details on the mechanisms of lake effect snowfall, and finally describes the forecast techniques for predicting snowfall along the leeward shores of the Laurentian Great Lakes.

Lakes can be divided into two types of mixing categories for transporting energy, holomictic and meromictic. Holomictic refers to all lakes that mix, while meromictic lakes have stable layers and dead zones. Holomicitic lakes include monomictic, polymictic, and dimictic lakes. Cold monomictic lakes are usually present in the Arctic and high altitudes and comprise one turnover annually. These lakes are ice covered for most of the year and turn over when warming occurs for a short duration during the ice-free summer period. Polymictic lakes are usually shallower and comprise multiple turnovers annually because of dynamic mixing caused by atmospheric winds. Dimictic lakes have two turnovers annually, once in the spring and once in the fall, and produce ice cover in the winter. This thesis focuses on dimictic lakes. The mixing properties of lakes are influenced by dynamic and thermodynamic properties, which are discussed next.

In general, thermodynamic mixing can occur in several ways, including heat transfer through radiation, conduction, convection, evaporation and condensation. Atmospheric mixing occurs when there is a gradient between lakes and contiguous landmasses, as well as lakes and overlying air masses, because of differences in each medium's heat capacity, transparency, and thermal conductivity (Eichenlaub, 1979). Lake-atmosphere heat exchange processes include the absorption of shortwave and longwave radiation and the emission of longwave radiation by the lake; the exchange of latent heat between lake and atmosphere as a result of evaporation and condensation; and convective exchange of sensible heat between the lake and atmosphere (Livingstone, 2010b).

Mixing can be influenced by the surface albedo, which can affect the amount of incoming shortwave radiation being absorbed or reflected by the surface. Lake surface albedo can be affected by water turbidity. The albedo for water surfaces can range between 2-3% for turbid waters and 6% for clear water (Schertzer, 1997). Lake surface albedo is also a function of the solar zenith angle, latitude, and surface roughness (Cogley, 1979). Lake surface albedo is highest when the sun is closest to the horizon, thus reflecting the majority of energy away from the lake. However, lakes are naturally good absorbers of incoming solar radiation and possess a certain degree of transparency, in contrast to land, which can lead to temperature and pressure gradients between lakes and nearby land surfaces.

The temperature gradient between land and water bodies is attributed to the thermal capacity of a substance. Thermal conductivity, which is the rate of penetration of heat from the surface into a substance, influences the thermal capacity of lakes. Thermal conductivity increases with greater water turbulence, which is induced by wind stresses, currents, and density differences. Mixing within the lake occurs through convection, which induces mass transport of fluid that permits heat exchange throughout the water body. Mixing efficiency distributes heat downward, absorbing and diffusing energy throughout the large water volume and preventing the surface from rapidly warming. As lakes absorb energy, some of it is used for evaporation, thereby cooling the surface and inhibiting an increase in lake temperature (Eichenlaub, 1979). At the top layer, evaporative cooling can destabilize the surface, thereby, further enhancing convective mixing (Oke, 1987).

Mixing and overturning occur when overlying water is denser than that below. Denser water sinks and is replaced with water that is less dense. The maximum water density, 1.0 g/ml^{-1}, occurs at a temperature of 4 °C. In spring, as the lake surface temperature (LST) rises from below freezing to 4 °C, the density of the water increases, causing it to sink, and allowing colder water from below to rise. This overturning contributes to a slower warming of lakes compared to land (Eichenlaub, 1979). As LSTs continue to warm above 4 °C, the density decreases and the warmer water floats on top of the colder and denser water beneath. Stratification begins to form as surface temperatures continue to warm rapidly

from June to mid-July (Figure 2.1). Finally, dynamic mixing from winds and currents deepen the stratified layer to depths of 12 to 15 m, and the downward dispersal of heat, is limited by depth (Eichenlaub, 1979). Shallower waters near the shores of lakes tend to warm faster than deeper waters, usually in the middle of lakes. Heat-absorbing and heat-retaining properties of water bodies also act to modify the climate of adjacent landmasses (Wetzel, 1975) due to variations in thermal heat capacity. These physical properties of lakes set up a thermal and pressure gradient with the surrounding environment that contribute to lake effect processes, which occur on different temporal scales.

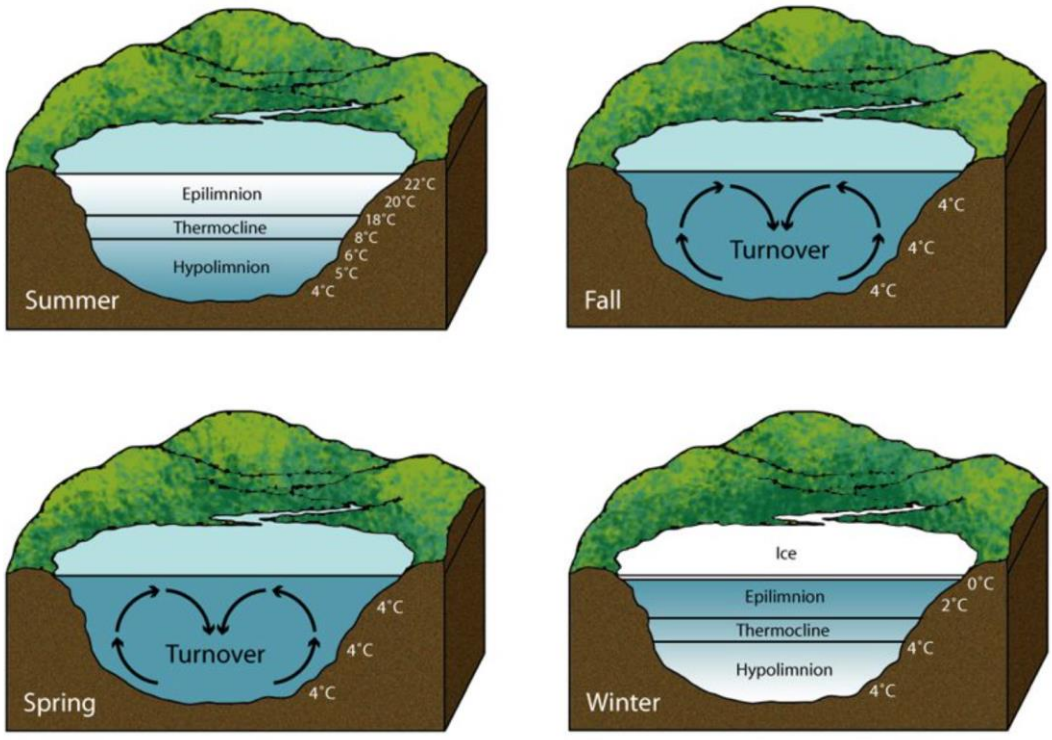

Figure 2.1: Seasonal water movement and turnover in lakes due to temperature and density changes (National Geographic, 2017).

Lakes modulate the local environment on multiple temporal scales, including diurnal and seasonal. On a diurnal scale, lakes can induce land and lake breezes, which are caused by differential heating between land and water bodies (Cuxart et al., 2014). Lake-breeze prevails during calm winds and clear sky conditions when maximum incoming solar radiation reaches the surface. As a result, land surface temperatures become higher than those of the air above and neighbouring LSTs (Cuxart et al., 2014). This temperature gradient induces pressure differences that drive lake-breeze. In addition to the diurnal variations, this phenomenon can take place on a seasonal scale. For example, in July, lakes in the Mackenzie River Basin are able to modify the regional distribution of specific humidity at the surface. Over the lakes the specific humidity is much lower due to the colder LSTs. In October, however, the LSTs are relatively warmer, and the specific humidity over the lakes is much higher than that of the surrounding land (Long et al., 2007). Increased humidity and saturation of an air parcel contribute to cloud formation, which can produce lake-induced precipitation.

2.2 The Lake-Induced Snowfall Process

With the correct climate and weather conditions, lakes can produce intense precipitation. Lake-induced precipitation will most likely fall as rain providing that a sufficient depth in the boundary layer exceeds 0 °C (Miner and Fritsch, 1997; Notaro et al., 2013); otherwise, solid-state precipitation will persist. The winter air temperatures need to be sufficiently cold for precipitation to fall as snow but not cold enough for a body of water to completely freeze over. The body of open water needs to be large enough to induce maximum fetch and warm enough to heat the overlying air, however, not large enough to warm the air above the freezing point. The ideal climate for lake-induced snowfall is also dependent on its geographic location. Land mass of continental dimensions must be upwind of water bodies to supply cold and dry air for lake effect process to occur (Eichenlaub, 1979). The spatial distribution of lakes can also influence snowfall in neighbouring areas. For example, Lake Ontario can enhance snowfall downwind towards the Finger Lakes in the United States (Laird et al., 2010), and the moisture of Lake Superior can influence the Lake Huron snowbelt. Thus, geographic location of lakes will modulate the intensity and morphology of lake-induced snowfall.

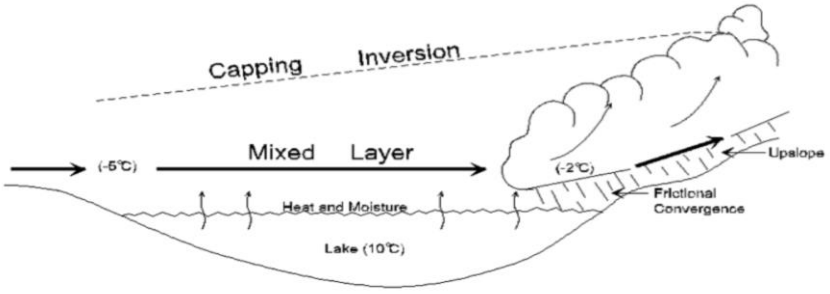

Figure 2.2: Surface-atmosphere interactions and forcing mechanisms required for the development of LES (iWeatherNet.com, 2017).

2.2.1 Lake Effect Snowfall Morphology

LES convective bands are typically long and narrow, between 50 and 300 km in length, and 5 to 20 km in width (Ballentine et al., 1998; Notaro et al., 2013). They can produce highly localized snowfall amounts on cities along the snowbelts of the GLB (Bluestein, 1992; Rauber et al., 2005; Theeuwes et al., 2010). These convective bands can organize into a spectrum of LES morphologies that range from discrete and disorganized cells to organized mesoscale bands (Campbell et al., 2016). Three types of morphologies include widespread coverage of wind parallel rolls, mid-lake shore-parallel bands, and mesoscale vortices (Passarelli and Braham, 1981; Hjelmfelt and Braham, 1983; Kristovich and Laird, 1998; Laird, 1999; Spinar and Kristovich, 2007; Notaro et al., 2013).

Wind-parallel rolls predominantly spawn off Lakes Superior, Huron, and northern Lake Michigan (Figure 2.3). These rolls develop when winds cross the short axis of the lake. The exchange of mass momentum balance, due to convection, produces patterns of surface convergence and divergence that result in rolls of clouds that are separated by bands of relatively clear sky. In general, the rolls are approximately 1 to 2 km wide and spaced between 4 and 10 km (Rauber et al., 2005).

Mid-lake shore-parallel bands form in the middle of lakes and run parallel to shorelines. Unlike wind-parallel bands, this spatial setup only generates a single snowband (Figure

2.3). Commonly observed over Lake Erie and Ontario, shore-parallel bands develop from weak lower level winds. Furthermore, heat from the lake rises by ushering in surface level air from either side of the shore, allowing surface convergence to occur in the middle of the lake. The bands can extend to an altitude of 3 km and can produce over 25 cm of snow in one location (Rauber et al., 2005).

Finally, mesoscale-vortex morphology resembles a cyclonic rotation and spans a diameter between 10 and 100 km. The heaviest bands of snow occur on the outwards spiral and can exist for several hours. Despite occurring on all of the Laurentian Great Lakes, these vorticity developments are less understood in comparison to the other morphologies and are more difficult to forecast due to their great uncertainty in storm track. This lake effect pattern is dependent on horizontal wind shear, wind speed, shoreline variation, and topography (Rauber et al., 2005) (Figure 2.3). In conclusion, the development of different LES morphologies are dependent on LES surface-atmosphere variables that will be discussed next.

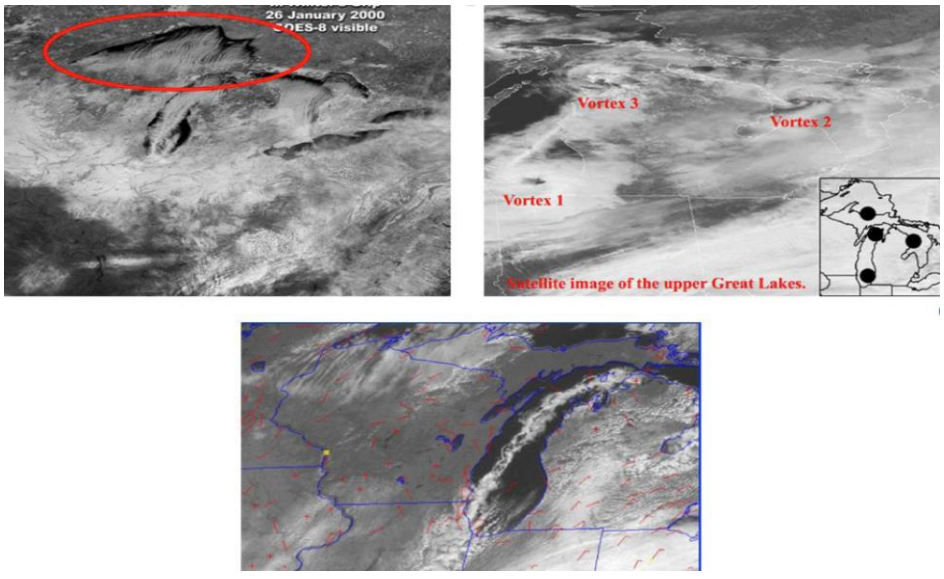

Figure 2.3: LES morphology of wind parallel rolls off of Lake Superior (top left), vortices over the GLB (top right), and mid-lakef shore-parallel band over Lake Michigan (bottom) (Spinar and Kristovich, 2007).

2.2.2 Surface-Atmosphere Predictor Variables

LES predictor variables are defined as the key parameters required for lake-induced snowfall development. The specific values of LES predictor variables will differ depending on the lake's location and snowbelt examined. This section describes known predictor variables required for the development of LES over the GLB. These variables include vertical temperature gradient (VTG) between the lake and overlying atmosphere, and lake-ice cover concentration as suggested by Notaro et al. (2013). In addition, Hartman et al. (2013) suggested the following key predictor variables: LST, air temperature over the lake of interest and surrounding areas at the 1000, 925, 850, and 700 mb levels; the east-west (U) and north-south (V) wind components affecting the eastern and the western portions of the lake at the aforementioned pressure levels; geopotential height for each of the aforementioned vertical pressure levels; and sea level pressure over the lake and surrounding regions. Some of these predictor variables are investigated in this thesis.

2.2.2.1 Energy Fluxes

Instability parameters are key components in lake-induced snowfall. An unstable lapse rate is generated from moisture and heat fluxes into the lower PBL. The transfer of sensible heat flux (temperature) into the atmosphere and latent heat flux (moisture) is directly related to wind speed, temperature gradient between the air and water, and the moisture contrast between the air and water interface. The energy fluxes can be calculated using a method proposed by Croley (1989) and Lofgren et al. (2000).

$$H = C_p \rho_{air} U^* \theta^* \qquad (2.1)$$

$$LE = -L \rho_{air} U^* q^* \qquad (2.2)$$

where H represents the sensible heat flux penetrated into the lake surface and LE represents the latent heat flux out of the lake surface. C_p denotes the heat capacity of air at constant pressure; L is the latent heat per unit of evaporation; ρ_{air} is the air density; U^* represents the frictional velocity; θ^* denotes the frictional temperature; and q^* represents the frictional mixing ratio. In addition, frictional velocity (U^*), frictional temperature (θ^*), and the mixing ratio (q*) are calculated as follows:

$$U* = \frac{kU}{[\ln\left(\frac{z}{z_o}\right) - s_1]} \qquad (2.3)$$

$$\theta* = \frac{k(\theta_a - \theta_w)}{[\ln\left(\frac{z}{z_o}\right) - s_2]} \qquad (2.4)$$

$$q* = \frac{k(q_a - q_w)}{[\ln\left(\frac{z}{z_o}\right) - s_2\,]} \qquad (2.5)$$

Note that U represents the wind speed at a reference height z, which is usually taken at 8 m above the surface. The variable, k, is Von Kármán's constant; z_o denotes the roughness length; s_1 and s_2 represent adjustments to the fluxes and depend on the static stability and wind shear of the atmospheric boundary layer (Croley, 1989; Lofgren and Zhu, 2000). Furthermore, θ_a represents the potential air temperature at the reference height; θ_w is the potential water surface temperature; q_a is the water vapor mixing ratio at the reference height; and q_w is the saturation mixing ratio at the water surface temperature. The Charnock relation is applied to represent water surface roughness as a function of $U*$ (Croley, 1989; Lofgren and Zhu, 2000). In addition to the frictional velocity, temperature, and mixing ratio, the potential temperature (θ) is given by the following:

$$\theta = T\left(\frac{p_0}{p}\right)^{R/C_P} \qquad (2.6)$$

where T is the in-situ temperature; p is the air pressure; p_0 denotes the reference air pressure at the 1000 mb level; R is the ideal gas constant for dry air (287 J•K^{-1}•kg^{-1}); and C_p represents the thermal capacity of dry air at a constant pressure (1004 J•K^{-1}•kg^{-1}) (Lofgren and Zhu, 2000).

The aforementioned variables influence the instability of the overlying advecting air parcel. Empirical investigations by Phillips (1972) suggests that most modifications of an air parcel's temperature and moisture occur within the first 30 minutes over the lake. On average, most air parcels take between 1and 3 hours to traverse the Great Lakes. The sensible and latent energy fluxes into the lower atmosphere are modulated by low-level

wind speed over the water body, moisture contrast, and VTG between the LST and overlying 850 mb air temperature.

VTG between the relatively warm lakes and colder air mass aloft allows for the lakes to destabilize the colder and lower atmosphere through vertical moisture heat flux (Burnett et al., 2003; Hartmann et al., 2013). According to Lavoie (1972), the most important factor in forcing LES convection is the VTG. In general, destabilization occurs when VTG is ≥ 13 °C, and this gradient approximately follows the vertical dry adiabatic laps rate. A 13 °C lapse rate in the boundary layer can develop if the residence time of cold air over the water is sufficiently long. This cold air parcel can result in absolute instability, lifting the parcel higher into the atmosphere and initiating lake effect precipitation (Holryoyd, 1971; Niziol, 1987; Theeuwes et al., 2010; Hartman, 2013). Other authors have suggested various temperature gradients. For example, Rauber (2005) proposed that a 10 °C temperature gradient between the lake-surface and 2-m height is required for sufficient evaporation and destabilization of the air mass, and Wilson (1977) found that LES over Lake Ontario is induced by a 7°C gradient between the lake surface and the 850 mb level. However, meteorologists often use a VTG of 13°C as a general rule of thumb for predicting LES over the GLB.

Another instability parameter is the omega forcing that represents the vertical ascent or descent of air at the synoptic scale level, such as in lake-enhanced systems. Despite being applied to synoptic scale systems, omega is still an important variable in analysing lake-induced processes because large-scale extratropical systems assist in the development of lake-enhanced snowfall. The omega equation is, thus, used to calculate the amount of instability associated with these systems and comprises two terms that pertain to vertical motion: thermal advection and differential vorticity advection. Thermal advection can be divided into cold and warm air, and differential vorticity advection can be either positive or negative. Cold air advection in the lower part of the atmosphere is attributed to sinking motion because the air tends to be denser, while warmer and less dense air is associated with rising motion. Negative vorticity advection is associated with sinking air while differential positive vorticity is associated with upper level divergence and rising motion.

Moreover, cold air masses are relatively shallow, as determined by the height of the capping subsidence inversion. This inversion height will determine the altitude to which convective cloud growth will occur. Strong low-level inversions can inhibit deep convective growth. Consequently, both strong energy flux and moisture flux can modify and change the strength of the capping inversion, promoting cloud growth and lake-induced snowfall.

2.2.2.2 Wind Fetch

Fetch, another key predictor variable that influences lake-induced snowfall, is the distance an air parcel advects over a lake between the 850 and 500 mb level. Fetch is determined by the cross section length of the lake and the wind speed of the air parcel. The advective residence time of an air parcel over the lake is inversely proportional to the wind speed. For example, assuming a fixed fetch distance, the residence time will decrease with increased wind speed, or, the residence time will increase with a decreased wind speed. Persistent fetch is required in order to facilitate the transfer of moisture and energy to the atmosphere (Notaro et al., 2013). The maximum length of the lake determines the effective length for winds advecting over lakes without interruptions from land (Wetzel, 1975).

Fetch along the major axis of lakes results in intense snowband development. The major axis allows for the longest fetch time of an air parcel, while winds oriented along the minor axis of lakes will produce less intense bands (Steenburgh et al., 2000). In general, mean 10-m winds over lakes have to be prominent for at least 6 hours to produce lake-induced snowfall because this amount of time allows for sufficient fetch. Minimal directional wind shear is also preferred because directional shear constitutes a significant change in wind direction with height. Apart from wind speed and wind shear, ideal fetch time will differ for each lake due to each lake's surface-atmosphere controls, such as shoreline variation and surrounding topography. For example, Kunkel et al. (2002) suggest that over Lake Erie, a wind velocity $\geq$ 6 m/s from 230° to 340° is required for heavy LES production. In contrast to Lake Erie, Lake Ontario requires wind directions of 80° or 230° in order to create maximum fetch and produce heavy LES (Hartmann et al., 2013). However, fetch is applicable only if ice cover concentration over lakes is minimal. The next section discusses

how ice cover on lakes can affect the production of lake-induced snowfall.

2.2.2.3 Ice Concentration

Ice concentration influences the exchange of energy fluxes between the lake surface and the overlying atmosphere (Surdu et al., 2014). The duration and spatial extent of ice on lakes control the seasonal lake-atmosphere heat budget and the magnitude of evaporation. A longer open-water season leads to increased exposure of solar radiation that can increase lake-to-atmosphere latent heat release through the process of evaporation (Mendez et al., 1998; Surdu et al., 2014). Alternatively, the presence of lake ice can act as a barrier between the lake surface and lower PBL, thereby inhibiting the transport of these fluxes into the atmosphere. An increase in ice cover results in a linear decrease in latent heat flux over the lakes. However, the sensible heat flux tends to stay relatively constant for ice cover extent up to 70% and then rapidly decreases with a further increase in ice cover. Complete ice cover can significantly reduce lake effect snowfall by over 80% (Gerbush et al., 2008; Vavrus et al., 2013; Wright et al., 2013). The presence of lake-ice and snow-on-ice contribute to an increase in surface albedo that peaks between 0.8-0.9. Snow-ice has a high albedo, limiting the penetration of incoming solar radiation into the ice and water (Duguay et al., 2003). However, the penetration of radiation through the ice can heat the water below, resulting in ice melt at its underside, and induce convective mixing within the lake (Brown and Duguay, 2010). Ice cover concentration is affected by surface-atmosphere controls, such as lake bathymetry. The next section discusses the key surface-atmosphere controls affecting LES predictor variables.

2.3 Surface-Atmosphere Controls

Surface and atmospheric processes are highly coupled; for example, changes in surface processes can influence the dynamic and thermodynamic state of the atmosphere. Surface-atmosphere controls include lake morphology, surrounding topography, and synoptic scale features. Lake bathymetry is a lake morphometric property that influences the horizontal and vertical mixing of lakes, LST, and the development of ice cover concentration. As a result, lake volumes and depths can influence the onset of the LES season through modulating ice cover and thermal lake regimes.

2.3.1 Lake Morphometric Influences on Lake-Induced Snowfall

The Laurentian Great Lakes have different onset times of stable and unstable seasons due to the size, depth, and latitudinal extent (Figure 2.4). The stable (unstable) season refers to the period when the lake is colder (warmer) than the ambient temperature. In shallow lakes, for example, LST rises faster than deeper lakes, allowing for strong evaporation to occur earlier in thaw season (Rouse et al., 2005).

However, Lake Superior is a larger deeper lake that is farther north than the other Great Lakes. As a result, the warming season for Lake Superior begins relatively later in the spring and rarely ever attains a high LST value similar to that of the lower Great Lakes. With the shear volume and depth of Lake Superior, it takes a longer time for the LSTs to cool and produce ice cover, thereby leading to a prolonged unstable season lasting from November to early April (Notaro et al., 2013). Lake depth is thus a controlling factor that also influences ice freeze-up and break-up dates at high latitudes (Duguay et al., 2003; Duguay et al., 2006). Unlike the greater depths of Lake Superior, shallower lakes promote faster ice growth due to shorter thermal turnover rates, in the period of a week, thus storing less heat. Shallower lakes permit rapid and early cooling of LST in the fall and winter (Eichenlaub, 1979). For example, although Lake Erie is the most southern of the Great Lakes it usually forms the most extensive ice cover in comparison to the other Great Lakes, ceasing the production of lake-induced snowfall sooner in the winter season than most of the other Lakes.

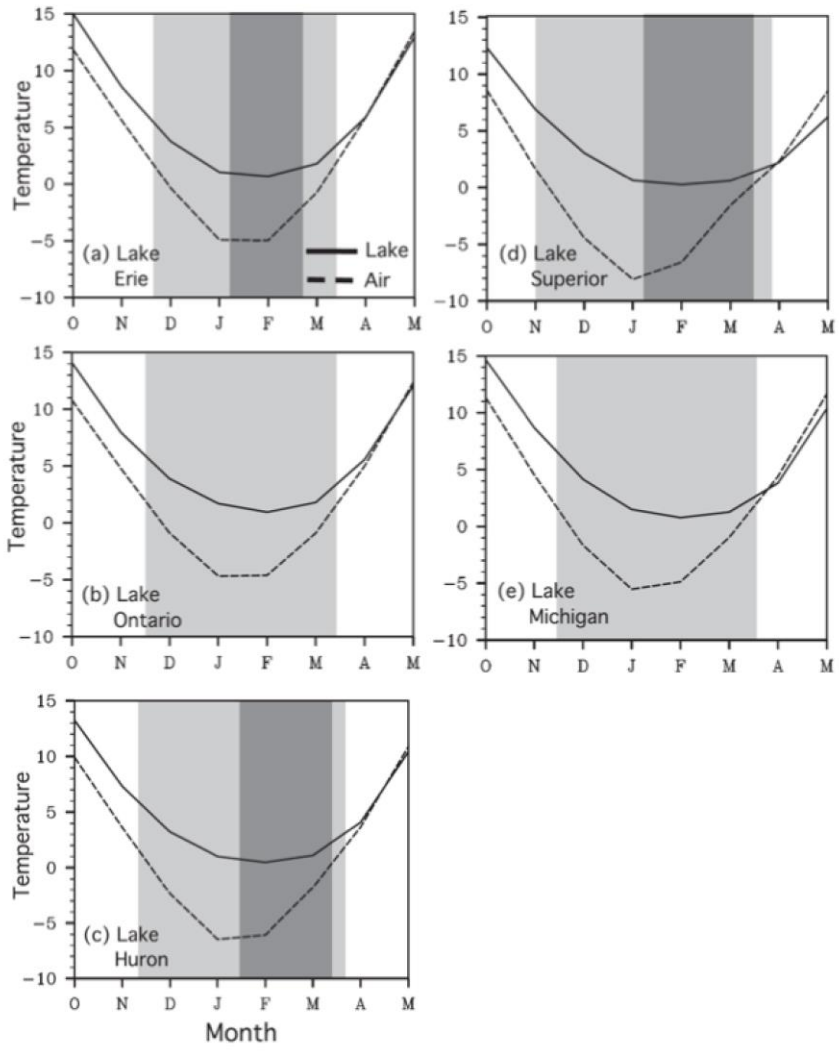

Figure 2.4: Regional Climate Model (RegCM4) simulation of mean seasonal cycle of LST (solid line) and 2-m air temperature (dashed) over each of the Laurentian Great Lakes during 1977-2002. Light gray shading indicates the unstable period when LES season is present. Dark gray indicates when the lakes are more than 70% ice covered, limiting LES (Notaro et al., 2013).

2.3.2 Topographic Factors on Lake-Induced Snowfall

Other surface controls include topographic characteristics of surrounding lakes. The topography of surrounding landmasses, such as surface roughness and mountain features, can modify the production and intensity of LES by influencing the lift of an advected air parcel. Surface roughness types can act to accelerate or decelerate airflow. For instance, winds approaching the upwind shores of lakes begin to accelerate due to decreased surface friction. Surface divergence and subsidence occur, resulting in clear sky conditions. As the

air mass crosses the downwind shoreline, the surface roughness increases, thereby decelerating the air mass and inducing surface convergence. This convergence further leads to instability of the air parcel (Rauber et al., 2005; Lofgren, 2006). In addition, mountain features can also result in increased instability of the air parcel due to orographic lift. Orographic lift can provide an additional 13 to 20 cm of mean annual snowfall for every 30-m increase in elevation (Hill, 1971; Hartmann, 2013).

Strength of a parcel's vertical ascent is also dependent on fetch duration. Fetch, however, is dependent on lake morphometric properties, such as the shape of the shoreline and the lake areal extent. Maximum lake fetch differs among lakes of varying shorelines and orientation. For example, an elliptically shaped lake that is oriented from east to west, as opposed to north to south, will produce maximum fetch in a region with prevalent westerly winds. Morphometric parameters can influence LES morphology, and as a result, snowfall intensity (Laird et al., 2003a and b; Laird and Kristovich, 2004). It is apparent that the surface controls of lake morphology and topography influence the intensity and onset of lake-induced snowfall.

2.3.3 Synoptic Scale Influences on Lake-Induced Snowfall

Two additional surface-atmosphere controls include temperature and pressure fields associated with synoptic scale features. Changes in air temperature can modify the VTG, while atmospheric pressure influences vertical and horizontal wind flow. The preferred air-surface temperature for generating lake-induced snowfall is between 0 and -10°C because the air is cold enough to permit frozen precipitation but mild enough to hold sufficient moisture. However, air temperature that is conducive to the production of LES differs for various locations. For example, LES over Lake Erie and Ontario forms due to cold surges that are between -8 and -18 °C at the 850 mb level and are usually derived from the Canadian Northwest. However, Lakes Superior and Michigan typically require milder air temperatures that range between -1 and -13°C. This is because larger lakes take a longer time to cool (Notaro et al., 2013), leaving LSTs relatively warm. Because the LST is warmer for these lakes, the air temperature does not need to be as cold to facilitate a VTG of 13 °C.

Finally, synoptic systems are associated with changes in surface pressure, which induces advection over the GLB, for example, directing cold and dry northwesterly air behind a cold front. An associated occluded front from this system can also facilitate northwesterly advection over the GLB, assuming the center low-pressure is east of the Laurentian Great Lakes. Furthermore, a northwesterly flow is often generated when an anticyclone is situated over North Dakota or Manitoba and a cyclone is present over southern Quebec or northeastern United States. The clockwise rotation, from the anticyclone, and the counter-clockwise rotation, from the cyclone, advect continental polar air masses over the GLB (Notaro et al., 2013).

Furthermore, to facilitate maximum fetch, the wind direction of an air parcel will differ for each lake, thus requiring slightly different synoptic configurations. Many case studies have analysed the different synoptic setups required for LES along various snowbelts within the GLB. For example, results from case studies conducted by Lackmann (2001), Leathers and Ellis (1996), and Niziol et al. (1995) identified three distinct synoptic features that occur prior to the development of LES along the region of Southern Ontario and Western New York and Rochester: firstly, the presence of a surface high-pressure in the Midwest United States; secondly, a surface low pressure system over eastern Canada; and finally, a trough extending over the GLB at the surface. At upper levels, a 500 mb trough is also present over the GLB.

The importance of assessing upper level synoptic features in the production of lake-induced snowfall is reiterated in Hamilton et al. (2006). They identified several features prior to a high intensity lake effect snowstorm in Buffalo of 2006. The features included an upper level trough and an associated cold front moving across Lake Erie. It was noted that upper-level troughs can cause synoptic-scale ascent that spurs widespread clouds and precipitation (Mahoney and Lackmann, 2007). Thus, synoptic features associated with this snowbelt include monitoring the geopotential height over the GLB and surrounding regions at the 1000, 925, 850 and 700 mb levels; geopotential height at the 500 mb level over James Bay, Canada, and sea level pressure measurements over the Great Plains, GLB, and

surrounding areas (Hartmann et al., 2013). These surface-atmosphere controls, along with the predictor variables are useful when forecasting lake-induced snowfall. The next section elaborates on the approaches and techniques employed for forecasting snowfall within the GLB.

2.4 Lake-Induced Forecasting Techniques and Prediction Models

The unique location, orientation, shape, and size of the Laurentian Great Lakes pose a challenge for developing standard techniques for predicting lake-induced snowfall (Notaro et al., 2013). However, scientists over the last half of the 20th century have worked to understand the processes that drive LES formation (Hartmann et al., 2013). This section discusses the operational forecasting methods for predicting lake-induced snowfall. Operational forecasters utilize a plethora of tools, including observations from in-situ measurements, soundings, synoptic charts, radars, satellites, and numerical weather prediction models.

2.4.1 Operational Forecasting Approaches

In-situ measurements from buoys and ground-based weather station data are used to acquire many meteorological observations, such as surface temperature, wind speeds, atmospheric pressure, and humidity. In addition, weather balloon soundings are used to measure vertical profiles of the atmosphere to identify adiabatic lapse rates, lifting condensation level, dew point temperature, and convective available potential energy (CAPE). Soundings can also provide information on temperature at the 850 mb level, as well as the presence and height of the inversion layer, which are all helpful for predicting lake-induced snowfall.

Synoptic charts are also useful tools because they can aid meteorologists in delineating frontal thermal and pressure boundaries (Figure 2.5). Synoptic charts are ideal for determining temperature and vorticity advection into the Great Lakes region, monitoring Arctic air outbreaks, and locating regions of instability. Observing and monitoring these meteorological conditions are crucial when forecasting lake-induced snowfall.

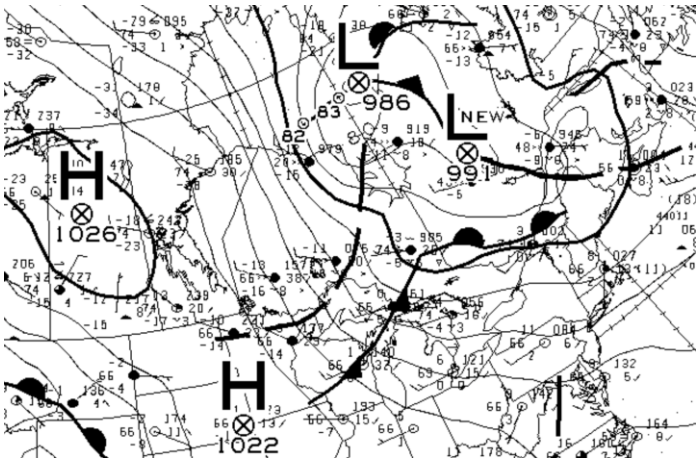

Figure 2.5: An example of Environment and Climate Change Canada's mean sea level pressure chart used as an operational forecasting tool for surface analysis, indicating regions of surface highs, lows, cold and warm fronts, and troughs over the GLB (ECCC, 2015).

When conditions are favourable for the development of LES, nowcasting tools such as radar and satellite imagery are utilized to determine directional fetch, location, and onset of snowfall. Also, satellite and ground-based weather radars are useful for assessing developments of an air parcel's trajectory and snow squalls. For example, the airborne dual-doppler, Electra Doppler Radar (EDLORA) was utilized by Kristovich et al. (2003) to examine the mesoscale convective structures of LES bands across Lake Michigan. Also, satellite imagery helped to determine the highly localized and intense LES of November 2014. Visible Imaging Radiometer Suite (VIIRS) showed a maximum fetch of an air parcel across the major axis of Lake Erie. The imagery showed that the squall band was becoming narrower and converging as it moved closer to the leeward shores of Lake Erie. This is because of the protruding landmass of Long Point Island in Lake Erie, which helped to funnel the squall band to a convergent point. This imagery helped meteorologists determined that the snowstorm would be highly localized and amplified in a very narrow region of Lake Erie's snowbelt. Finally, Barjenbruch et al. (1997) also suggested that the use of both space-borne satellite imagery and ground-based radar can aid in snowfall forecast predictions by correlating cloud top temperatures from snowsquall bands, seen on satellite infrared imagery, with reflectivity echoes from radar. This correlation can help

infer snowfall intensity beyond the effective radar range. Satellite and radar imagery is beneficial in nowcasting, but numerical weather prediction models are useful for short-term forecasting of major lake-induced snowstorms.

2.4.2 Model Predictions

General Circulation Models (GCMs) have been used for LES climatology studies. For example, Kunkel et al. (2002) employed two GCMs, the second generation Hadley Centre Coupled Model Version 2 (HadCM2) and the first generation Canadian Climate Centre Coupled Ocean-atmosphere model (CCM1), to study the response of LES to climate change in the 21st century. They concluded that the resolution of GCMs constrains the spatial and temporal features of LES. The average spatial resolution of GCMs ranges between 150 and 200 km. LES, however, requires spatial resolutions that can capture the narrow snow squall bands that are less than approximately 25 km in width. LES forecasts require a number of meteorological conditions that are not well resolved by GCMs due the GCM's coarse spatial and temporal resolutions (Kunkel et al., 2002).

Advancement in regional climate models (RCMs) and numerical weather prediction (NWP) models have provided the requisite spatial and temporal resolutions for resolving LES features such as mesoscale processes, thereby improving LES predictability (Lavoie, 1972; Hjelmfelt, 1990; Bates et al., 1993; Niziol et al., 1995; Ballentine et al., 1998). For instance, NWP models with resolutions of a few kilometers, such as 10 km, can realistically capture the spatial distribution of precipitation events, as confirmed by weather radar observations. Another RCM is the Canadian Regional Climate Model Version 5 (CRCM5). This thesis assesses the predictive capabilities of the CRCM5 in reproducing contemporary LES events and will be covered in Chapter 5.

In conclusion, this chapter has provided a general background on the dynamic and thermodynamic properties of lake-induced snowfall, outlining surface-atmosphere controls, and LES predictor variables. This chapter has also provided a brief overview of forecasting techniques and tools used for lake-induced snowfall predictions. The next chapter will investigate trends in monthly snowfall totals over the GLB

Chapter 3

CLIMATOLOGICAL TRENDS OF SNOWFALL OVER THE LAURENTIAN GREAT LAKES BASIN

3.1 Introduction

Chapter 3 presents the first manuscript, which focuses on determining the historical climatological trends of snowfall for the Canadian snowbelts of Lakes Superior and Huron. Recall, from Chapters 1 and 2 that the leeward shores of the Laurentian Great Lakes are highly susceptible to lake-induced snowfall during the late autumn and winter seasons. During the lake effect season, it is extremely dangerous for motorists traversing busy highways along the snowbelt region, such as highway 400 that connects Southern Ontario to Cottage Country. This is because the highly localized nature of LES can produce snowsqualls amidst patches of clearer sky, leaving motorists in blinding and whiteout conditions. Thus, the impacts of LES on residents and local communities give credence to studying these storms. However, most LES studies have been conducted for the United States snowbelts of the GLB with minimal focus on the Canadian domain.

Furthermore, most LES research was in the form of case studies with limited findings on observed climatological trends. Therefore, the objective of this study is to determine historical climatological snowfall and precipitation trends over Lakes Superior and Hurons' snowbelts and to further examine a series of key surface-atmosphere LES predictor variables that will provide explanations for the resultant spatiotemporal trends. In this paper, spatiotemporal snowfall and total precipitation trends using Daymet (Version 3), hereinafter referred to as Daymet, gridded interpolated datasets were computed for the 1980-2015 period over the GLB.

In this study, 1 km gridded snowfall data is analysed from the total precipitation dataset attained by Daymet (https://daymet.ornl.gov) to assess historical spatiotemporal trends in snowfall and total precipitation over the Ontario snowbelt of the GLB from 1980 to 2015. Snowfall trends are assessed for the months of the cold season (November, December, January, February, and March). The mechanisms influencing the resulting snowfall trends

are explained through further trend analyses of LES predictor variables. While previous studies, for example Burnet et al. (2003), have suggested 20th century increases in annual snowfall along the United States lake effect snowbelts of the GLB, it is suggested that changes in LES may respond differently for the Ontario snowbelts of Lakes Superior and Huron. These differences are due to various influential factors, including geographic locations of lakes, lake bathymetry, surface-atmosphere interactions, and downwind topography. This is the premise for evaluating regional LES trends and its predictor variables within the Canadian domain of the GLB.

Section 3.1 presents the introduction, which provides a background on the gaps and objectives of this research. The data and methodology are provided in section 3.2, which describes the data sources and derivations of the variables used in this study. This is followed by the results and discussion in section 3.3 and ends with the conclusion in section 3.4 that summarizes the results of the current work and provides suggestions for future research.

3.2 Data and Methodology

A comprehensive investigation into the climatological trends in snowfall along the Ontario snowbelt of the GLB requires the analysis of multiple atmospheric and surface variables from various sources (Table 3.1). The variables used to analyse snowfall trends include gridded 1-km snowfall derived from Daymet's estimated precipitation and 2-m air temperature dataset. Potential explanations for resultant snowfall trends are explored by examining LES predictor variables based on previous investigations from Niziol et al. (1995), Cosgrove et al. (1996), Hamilton et al. (2006), Hartmann et al. (2013), and Notaro et al. (2013). These variables include omega, VTG, LST, and air temperature at the 1000 mb level from the North American Regional Reanalysis (NARR) dataset, and ice cover concentration from the Environment and Climate Change Canada (ECCC) Canadian Ice Service (CIS). While it is acknowledged that there are many LES predictor variables such as fetch and wind velocity, these variables are beneficial to assess on a shorter temporal scale, such as during specific LES events. The purpose of this study is to evaluate long-

term climatological trends, and thus, certain LES variables are more appropriate for long-term climatological analysis such as LST, instability parameters, and ice cover.

Table 3.1: Description of resolution, sources, and units of each variable analysed in this study.

Variables	Resolution	Source	Units
Snowfall	1km x=1614 y=1320	Daymet	cm
Precipitation	1 km x=1614 y=1320	Daymet	mm
Omega	32 km x=56 y=47	NARR	Pa/s
VTG	32 km x=56 y=47	NARR	°K
$Tair_{1000}$	32km x=56 y=47	NARR	°K
LST	32km x=56 y=47	NARR	°K
Ice Cover	-	CIS	-

3.2.1 Snowfall and Precipitation from Daymet

Daymet is a collection of software and algorithms that provide gridded estimates of daily meteorological observations, including maximum and minimum 2-m air temperature and daily precipitation, which are used in the derivation of estimated snowfall. Daymet interpolates and extrapolates observational data to produce 1-km resolution weather parameters over larger regions (Thornton et al., 1997, 2000). Daymet requires input from models such as a digital elevation model and uses ground-based observations from weather stations. The digital elevation model is a subset of the National Aeronautics and Space Administration's (NASA) Shuttle Radar Topography Mission 2.1 (SRTM). The in-situ weather observations are acquired from the Global Historical Climatology Network (GHCN) under the National Oceanic and Atmospheric Administration (NOAA) (Menne et al., 2012a and b). The interpolation method is based on the spatial convolution of a

truncated Gaussian weighting filter with sets of station locations. The dataset was developed by the Environmental Sciences Division at the Oak Ridge National Laboratory (Thornton et al., 1997, 2000). A detailed description of this dataset can be found at http://daymet.ornl.gov.

Gridded daily total precipitation, P_1 (mm), daily 2-m maximum air temperature (T_{max}) and minimum air temperature (T_{min}) are acquired from Daymet and are used to derive gridded snowfall. First, an estimate of the fraction of total daily precipitation falling as snowfall is computed by determining the ratio (R) of daily snowfall to the total daily precipitation, where $0 \leq R \leq 1$ (Legates and Willmott, 1990; Rawlins et al., 2006).

$$R = [1.0 + 1.61(1.35)^{T_{mid}}]^{-1} \quad (3.1)$$

Daymet does not offer daily mean 2-m air temperature; thus, a midpoint value is used instead and is calculated by taking the sum of T_{max} and T_{min} and dividing by 2, as follows:

$$T_{mid} = \frac{T_{max}+T_{min}}{2} \quad (3.2)$$

The product of P_1 and R yields the water equivalent of new snowfall, P_n (mm).

$$P_n = P_1 \cdot (R) \quad (3.3)$$

If $T_{mid} \geq -15\,℃$, then a density value is computed as a function of T_{mid} and denoted as ρ_{snow}

$$\rho_{snow}(T_{mid}) = 0.05 + 0.0017[T_{mid}+15]^{1.5} \quad (3.4)$$

When $T_{mid} < -15\,℃$, the density of snowfall is assigned to 0.05 g/cm^3. Finally, the estimated height of new snowfall, H_n (cm), is as follows:

$$H_n = [0.1 \cdot P_n]/\ \rho_{snow} \quad (3.5)$$

Error analysis of the estimated Daymet variables and derived snowfall were considered in this study. Annual summary cross-validation statics for Daymet were generated by station-based daily observations and predictions for 2° x 2° tiles over North America (Thornton et al., 2016). Each tile provides period-of-record mean absolute error (MAE) and bias statistics for input weather observations of maximum and minimum temperature and precipitation for each year. Furthermore, published studies have trusted and employed Daymet for climatological analysis, including Mote et al. (2017) who used Daymet to examine the 2015 spatial distribution of daily rainfall in eastern Puerto Rico. Further details on Daymet's data validation can be found at https://daac.ornl.gov/DAYMET/guides/Daymet_V3_CrossVal.html#revisions.

In this study, additional error analysis was conducted to quantify the annual uncertainty in the derived snowfall. As discussed above, derived snowfall (H_n) is a function of R, P_1, T_{mid} , and ρ. Uncertainty values of these variables were calculated and inputted into the equations above to determine the annual sensitivity of H_n to ρ, H_n to P_1, R to T_{mid} , ρ_{snow} to T_{mid} , H_n to R, H_n to T_{mid} (if $T_{mid} \geq -15$ ℃) and H_n to T_{mid} (if $T_{mid} < -15$ ℃). In order to calculate the initial uncertainty of precipitation and T_{mid}, two 2° x 2° tiles that contained Wawa, a city within the snowbelt of Lake Superior, and Wiarton, a city within Lake Huron's snowbelt were selected from Daymet's cross validation data resources. Both tiles provided the MAE of precipitation, which were converted to the error of standard deviation before being inputted into the derivation equations. T_{mid} was derived from Daymet's T_{max} and T_{min} temperatures, recall equation (3.2). Annual uncertainty measures of T_{mid} were calculated by computing the annual standard deviation between Daymet's calculated T_{mid}, and T_{mid} calculated from an independent dataset, NARR, for the cities of Wawa and Wiarton. These annual uncertainty errors of T_{mid} were then inputted into the derivation equations. The uncertainty estimate of density was given 0.005, 10% of its initial value.

The overall 36-year annual uncertainties in H_n relative to T_{mid} are 1.7 cm for Wiarton and 6.2 cm for Wawa. It is expected that the tile containing Wawa, farther North, would have a higher snowfall uncertainty than that of Wiarton. This is because there are fewer weather

observation stations within Lake Superior's snowbelt tile than that of Lake Huron's. Thus, a system is established for which the search radius of stations is reduced in data-rich regions and increased in data-poor regions. In addition, when predicting snowfall accumulation, meteorologists usually provide a predictive range in snowfall, for example 1-5 cm or 10-15 cm of snow. Thus, having an uncertainty value of 1.7 cm for Wiarton and 6.2 cm for Wawa are within a reasonable range. Furthermore, the sensitivity of H_n to P_1 is 0.03 cm for Wiarton and 0.12 cm for Wawa. The sensitivity of snowfall to R averages 1.4 cm for both Wiarton and Wawa. These uncertainties are fairly low and provide confidence in the derived snowfall method used in this study.

After determining H_n, the derived gridded daily snowfall is then aggregated over each month of the cold season November, December, January, February, and March (NDJFM) to determine monthly snowfall totals over land in the GLB. Similarly, daily total precipitation (mm) over land is aggregated to compute the total monthly precipitation for each month of the cold season. Spatiotemporal trends of total precipitation are also analysed to determine whether there are noticeable changes within the atmospheric moisture stores. Differences between snowfall and total precipitation spatiotemporal trends may suggest shifts in precipitation types, while similar spatiotemporal trends may suggest an overall change within the atmospheric moisture storage.

3.2.2 Air Temperatures, Omega, VTG, and LST from NARR

Some atmospheric and surface variables used in this study are provided by NARR. The NARR dataset includes long-term, high resolution, high frequency, and dynamically consistent atmospheric and land surface hydrology information for North America, making it ideal for gridded climatological analyses. Components of the NARR system include the National Centers for Environmental Prediction (NCEP) Eta model, at 32 km resolution and 45 vertical layers, data assimilation schemes, the Noah land-surface model, and lateral boundary forcing from the NCEP-Department of Energy (DOE) Global reanalysis. The NARR assimilates precipitation observations and produces land and surface model updates. Given an estimate of the present state of the environment, also known as the first guess, three hourly observations are collected and assimilated using a three-dimensional

variation (3D-Var) approach with a model integration period of 3 hours for which a short range forecast is produced. This result is then fed, as the initial condition, into the next cycle for which the system repeats itself with updated observational data (Mesinger, 2006).

It is noted that the quality of the NARR data has been validated with both surface stations and sounding measurements and was used in numerous North American validation climate studies. For example, Kennedy et al. (2011) compared a number of the NARR variable, which include temperature and omega and found a temperature bias only within 0.5 °K when compared to data gathered by the Modern-Era Retrospective analysis for Research and Applications (MERRA) and the Atmospheric Radiation Measurement (ARM) program. While the NARR's omega values were similar to that of MERRA, it mainly differed to that of ARM by not capturing the amplitude, but by capturing the overall seasonal patterns of omega. Furthermore, all three sources agree on the hour-to-hour variations in vertical velocity and its relationship to cloud occurrence. Additional studies, such as Mesinger (2006), have discussed the improvements of the NARR's outputs, including LST, from the earlier NCEP-National Center for Atmospheric Research Global Reanalysis 1 (NCEP-NCAR GR1). NARR is, thus, a trustworthy source for atmospheric reanalysis data (Mesinger, 2006; Lo et al., 2008; Gula and Peltier, 2012) and justifies its use in this study. The NARR system is produced by NOAA-NCEP in Boulder, Colorado, USA and is accessible through the NOAA website http://www.esrl.noaa.gov/psd/.

Monthly averaged omega, 1000 mb and 850 mb air temperatures, and LST are directly extracted from the NARR dataset, while VTG is computed using several surface and atmospheric NARR variables. Firstly, omega was analysed because it represents vertical motion and instability, which are two factors required for cloud and precipitation development. In the current study, omega is assessed at the 700 mb level for all grid cells over lakes. This is because the current study is interested in determining instability over lakes for the production of lake-induced snowfall. Furthermore, measuring omega at the 700 mb altitude is indicative of whether instability is sufficient for generating clouds. Omega is given as follows:

$$[(\sigma\nabla_p^2) + f_0^2\frac{\partial^2}{\partial p^2}]\omega = -f_0\frac{\partial}{\partial p}[-V_g.\nabla_p(\varsigma_g + f)] - \frac{R*}{p}\nabla^2[-V_g.\nabla_p T] - \frac{R*}{pC_p}\nabla^2\mathrm{H} \quad (3.6)$$

Note that C_p is the specific heat at constant pressure; f denotes the coriolis parameter; p represents pressure; H signifies the diabatic heat transfer; $R*$ is the universal gas constant; T denotes temperature; V_g represents the geostrophic wind vector; ς_g is the relative geostrophic vorticity; σ signifies the static stability; and ω, the vertical motion. The first term, on the right hand side of equation 3.6, represents the positive vorticity advection (PVA), the second is temperature advection, and the third, diabatic heat changes (Zamg, 2017). PVA and a negative ω are attributed to ascending motion and the development of cloud cover. In synoptic meteorology, a ω value $\leq$ - 0.2 pa/s produces a very strong ascent, which can result in heavy LES storms (OWO, 1994).

VTG is another instability measure but at the meso-beta scale. VTG is frequently used in forecasting LES events; however, it is adopted in this climatological study to aid in assessing localized monthly instability over the Great Lakes. Climatological VTG may average between 7 to 8 °C but can exceed 30 °C during intense cold air outbreaks. Average monthly VTG is calculated by taking the difference between the monthly mean LST and the 850 mb air temperature for each grid cell over the GLB domain using the NARR dataset and is calculated as:

$$\mathrm{VTG} = \mathrm{T_{LST}} - \mathrm{Tair_{850}} \quad (3.7)$$

The LST is acquired from the NARR's monthly mean surface temperature grid cells over the lakes and masked over land. The NARR's surface temperature is defined as the skin temperature, which is generated from the land surface model. Grid cells over water are denoted as sea surface temperature and over land it is denoted as the radiative temperature of the surface. These aforementioned variables were acquired from the NARR dataset and are used as LES predictor variables to help evaluate historical climatological LES trends.

3.2.3 Ice Cover Concentration from CIS

Another predictor variable is ice cover over the Great Lakes. Ice cover concentration is derived from ECCC CIS. Weekly ice charts provide mapped median ice cover concentration fractions, (ECCC, 2017c). For this study, historical monthly total accumulated ice extents were selected for each month of the cold season over Lake Superior, and separately, for Lake Huron. The ice cover data are offered as a single percentage value over the entire lake for each year (1980-2015). It should be noted that the authors are aware of the NOAA Ice Atlas gridded data but chose to use the CIS dataset instead. This is because data for the month of November was not available by NOAA ice atlas, and the authors wanted to maintain the temporal consistency among all variables analysed.

Separate standardized ice cover concentration time series were generated for each month of the cold season for Lake Superior and Lake Huron. The standardized score is given by equation 3.8:

$$\frac{X-\mu}{\sigma*} \quad (3.8)$$

X represents the average ice cover concentration over the entire 36-years, μ denotes the monthly median ice cover concentration for a particular year, and $\sigma*$ signifies the standard deviation of the time series. The standardized score technique is adopted to better visualize and compare the ice cover concentration trends among the months.

3.2.4 Methodology

In this section, the steps taken to analyse snowfall, precipitation, and LES predictor variables are explained. First, monthly snowfall and precipitation totals are computed for each month of the cold season (NDJFM). These months were chosen because lake effect season over the GLB usually occurs between November and January. The later months, February and March, were also analysed because they can provide additional information on the temporal changes of snowfall during this time. Monthly averages of LES predictor variables were also computed.

Spatiotemporal trends analyses for each variable were conducted by taking the monthly totals and averages over 36 calendar years. The temporal analysis period was from the beginning of 1980 to the end of 2015 because of the common overlap among all datasets and served as an adequate time period to study recent climatological trends in response to climate change. Spatial trends were calculated over the gridded domain of the GLB at 94ºW, 74ºW, 40ºN, and 50ºN. The Mann Kendall (MK) statistical test was applied to snowfall, precipitation, and predictor atmospheric time series to assess whether there are monotonic upward or downward climatological trends. The Kendall-Theil method was used to calculate the Sen slope at each grid cell over the 36-year period. The P-value was also computed at the 95% confidence level. The MK test was used because it evaluates the Sen slope of an estimated linear regression non-parametrically, which does not require that the residual from the fitted regression line be normally distributed, like that of a parametric linear regression. Furthermore, the MK test is less sensitive to outliers, thereby making it an ideal test for assessing long-term climatological trends (Kendall, 1975; Gilbert, 1987).

3.3 Results and Discussion

3.3.1 Snowfall and Total Precipitation

Thirty-six-year trends in monthly snowfall totals were computed for regions over the GLB. The observed changes in the snowfall trends were most apparent during December and January, which are noted as the prime months of the LES season (Figures 3.1b and c). In comparison to all months of the cold season, December and January's snowfall trends have significantly decreased, at the 95% confidence level, along the eastern shores of Lake Superior and Lake Huron by a rate of over 40 cm/36yrs (Figures 3.1b, c, g, and h). In March, the snowbelt along Lake Huron also exhibits a significant decrease in snowfall, but at a lesser rate of approximately 15 cm/36yrs (Figures 3.1e and j). However, the months of November and February show non-significant changes in snowfall amounts along Lakes Superior and Huron's snowbelts (Figures 3.1f and i).

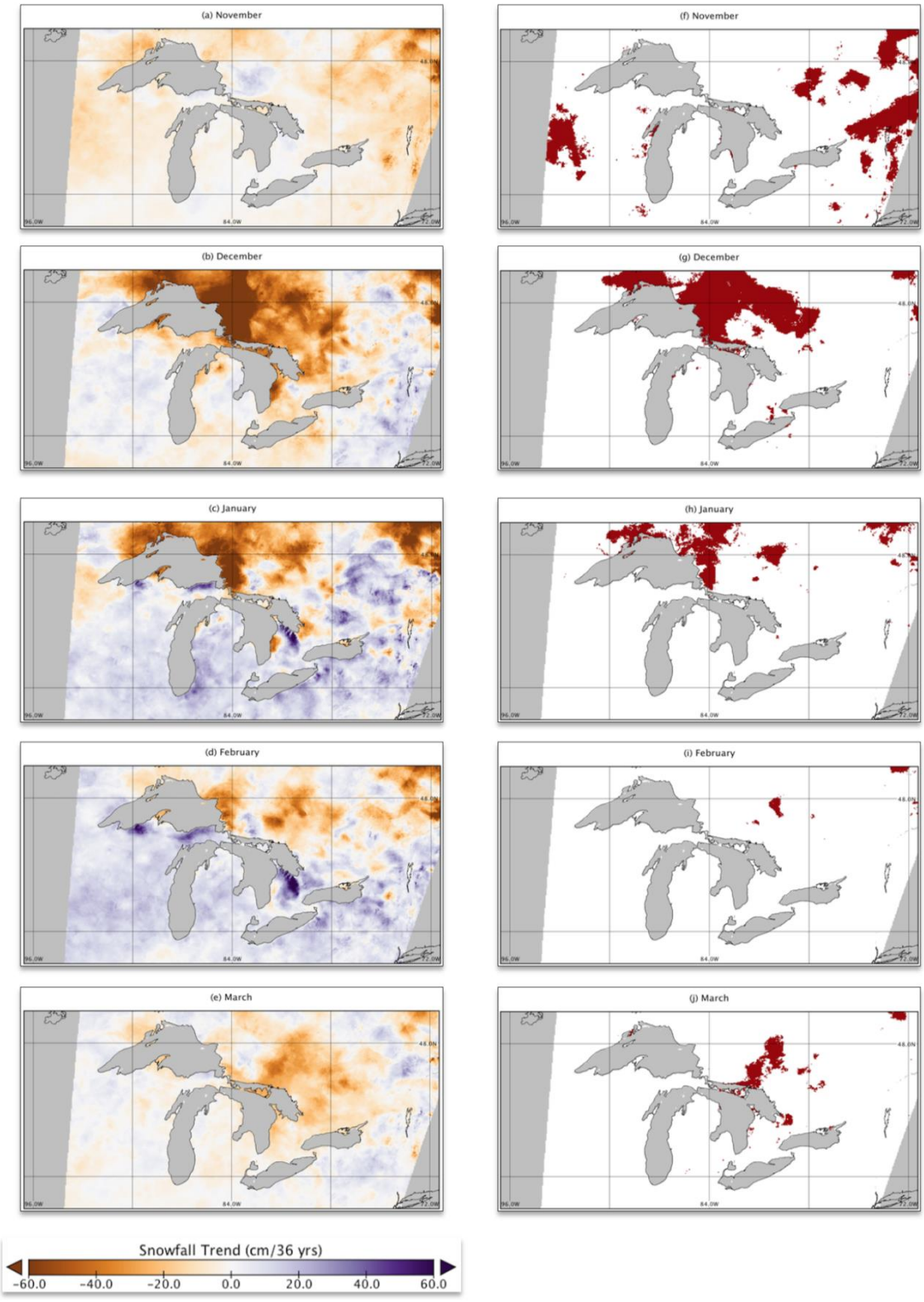

Figure 3.1: Spatiotemporal snowfall trends (cm) over 36 years (1980-2015) of total monthly snowfall (left) and the corresponding areas of significant decrease at the 95% confidence level (right).

Results of the significant negative snowfall trends along Lake Superior's snowbelt are in agreement with several studies. Researchers have examined trends in snowfall patterns across the GLB during the 20th century and found a snowfall trend reversal. While, the first half of the 20th century exhibited an increase in snowfall, recent studies have shown a decline through the later half of the 20th and early 21st century. As suggested by Suriano and Leathers (2016), previous studies indicated an increase in snowfall over the GLB (Leathers and Ellis, 1993; Norton and Bolsenga, 1993; Leathers and Ellis, 1996; Kunkel et al., 2009). In addition, investigations by Burnett et al. (2003) and Kunkel et al. (2009) have also suggested increases in annual snowfall along the United States lake effect zones of the GLB during the 20th century and are in agreement with Ellis and Johnson (2004); and Notaro et al. (2013). Furthermore, Scott and Kaiser (2004) examined snowfall trends over North America from 1948 to 2001 and observed a snowfall increase over a narrow band from Colorado to the lee of Lake Erie and Ontario.

In the later half of the 20th and early 21st century, however, studies have shown a decrease in snowfall, for example, Bard and Kristovich (2012) showed a decrease in snowfall along the leeward shores of Lake Michigan between 1980-2005, and Hartnett et al. (2014) also showed a snowfall decrease for Central New York between 1971-2012. In southern Canada (less than 55ºN) a negative trend of 0.65 cm per decade during this period was discovered, with the most decrease occurring in the 1980s (Krasting et al., 2013). Thus, the resultant negative trends in snowfall for the Ontario domain is in agreement with previously published analyses of snowfall over the later half of the 20th and early 21st century.

The observed decrease in monthly snowfall warranted further investigation to determine whether snowfall was transitioning into liquid precipitation, or whether the overall moisture storage was changing, both of which are likely scenarios within the context of climate change. If the spatiotemporal trends in total precipitation exhibit different behaviours to that of snowfall, for example, if there are no significant changes in total precipitation, then this result is indicative of snowfall transitioning to a different precipitation state. However, if total precipitation exhibits similar trends to that of snowfall, then this may suggest changes to the overall moisture budget within the atmosphere.

Total precipitation results, in this study, show similar spatiotemporal trends to that of snowfall. The leeward shores of Lake Superior exhibit a significant decrease in total precipitation of over 20 mm/36yrs predominantly for the months of December and January (Figure 3.2b-c, and g-h). The leeward shores of Lake Huron also show a significant decrease of snowfall at a rate of 20 mm/36 yrs, but to a lesser spatial extent and only for the month of December and March (Figures 3.2b, e, g, and j). Furthermore, negligible total precipitation changes occur for the month of November along the snowbelts of Lakes Superior and Huron. Because the total precipitation trends exhibit similar behaviours to that of snowfall, these results suggest that snowfall is not necessarily transitioning into rainfall during the cold season, and that the observed changes in snowfall and precipitation may result from other surface-atmosphere interaction factors.

In the context of snowfall within the seasonal cycle, Notaro et al. (2013) analysed the mean seasonal cycle of snowfall downstream of Lakes Superior and Huron and showed that March produces less snowfall in comparison to the months of December to February. For Lake Superior, the months of November through March have mean snowfall amounts of 35, 80, 85, 50, and 45 cm, respectively. For Lake Huron, the mean snowfall for the months November through March show mean snowfall amounts of 35, 80, 85, 50, and 35 cm, respectively. Thus, given that the decrease in snowfall trends are more apparent for the months with the greatest mean snowfall, which are during the LES season, this warrants investigations into whether the resultant changes in snowfall may be influenced by potential lake-effect predictor variables.

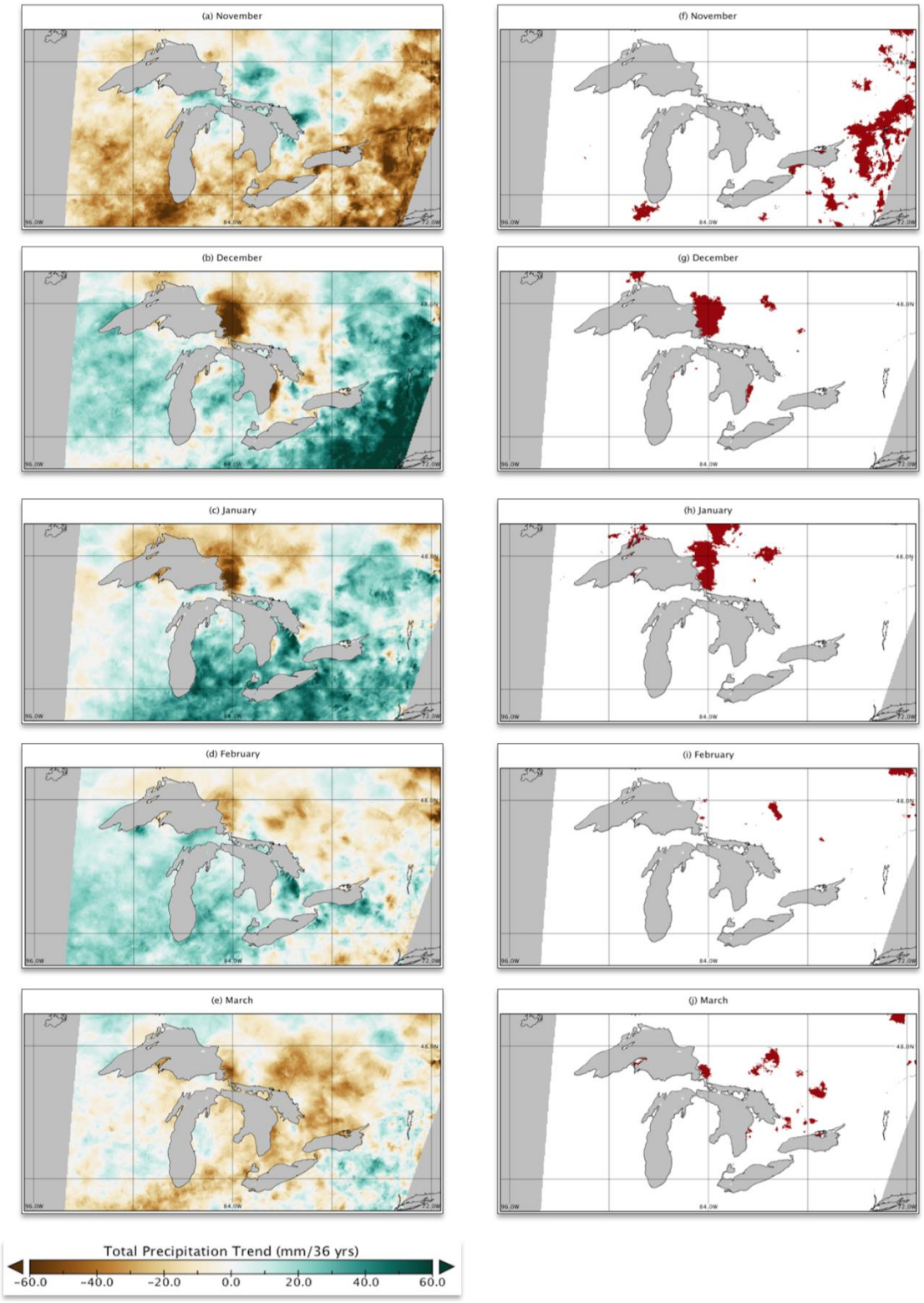

Figure 3.2: Spatiotemporal monthly total precipitation trends (mm) over 36 years (1980-2015) (left) and the corresponding areas of significant decrease at the 95% confidence level (right).

3.3.2 Surface-Atmosphere LES Predictor Variables

Spatiotemporal trends in LES predictor variables are also computed to examine whether the dynamic and thermodynamic changes in lake-induced processes influence the monthly snowfall totals. The surface-atmosphere variables include instability parameters and lake processes.

3.3.2.1 Instability Parameters

The two instability parameters investigated in this paper are omega and VTG. Recall, from section 2 that measuring omega at the 700 mb level provides information about the state of the atmosphere and whether there is enough instability to facilitate the production of clouds. Most of Lake Huron shows a significant increase in instability at values greater than -0.02 pa/s·36yrs for all months of the cold season, suggesting an increase in ascending motion within the PBL (Figure 3.3a-j). Lake Superior shows similar trends, but at a lower rate. Furthermore, there is no significant increase in omega over Lake Superior for the month of March (Figure 3.3e and j).

For Lake Superior, the non-significant trend in March, and the overall weaker omega trend for the rest of the cold season suggest that PVA and temperature advection associated with synoptic scale systems are not as pronounced over Lake Superior as they are over Lake Huron at this time. Within the PBL, these advection processes influence the inversion height that facilitates deeper levels of convection and produce lake-enhanced snowfall. Based on the results, it is suggested that the month of March does not experience an increase in the capping inversion height, limiting deep layer convection that is required for heavy lake-enhanced snowfall. However, during the mid to late LES season, PVA and temperature advection are dominant for both Lakes Superior and Huron, indicating a potential increase in the capping inversion height, which could facilitate deeper layer convection for the production of lake-enhanced snowfall.

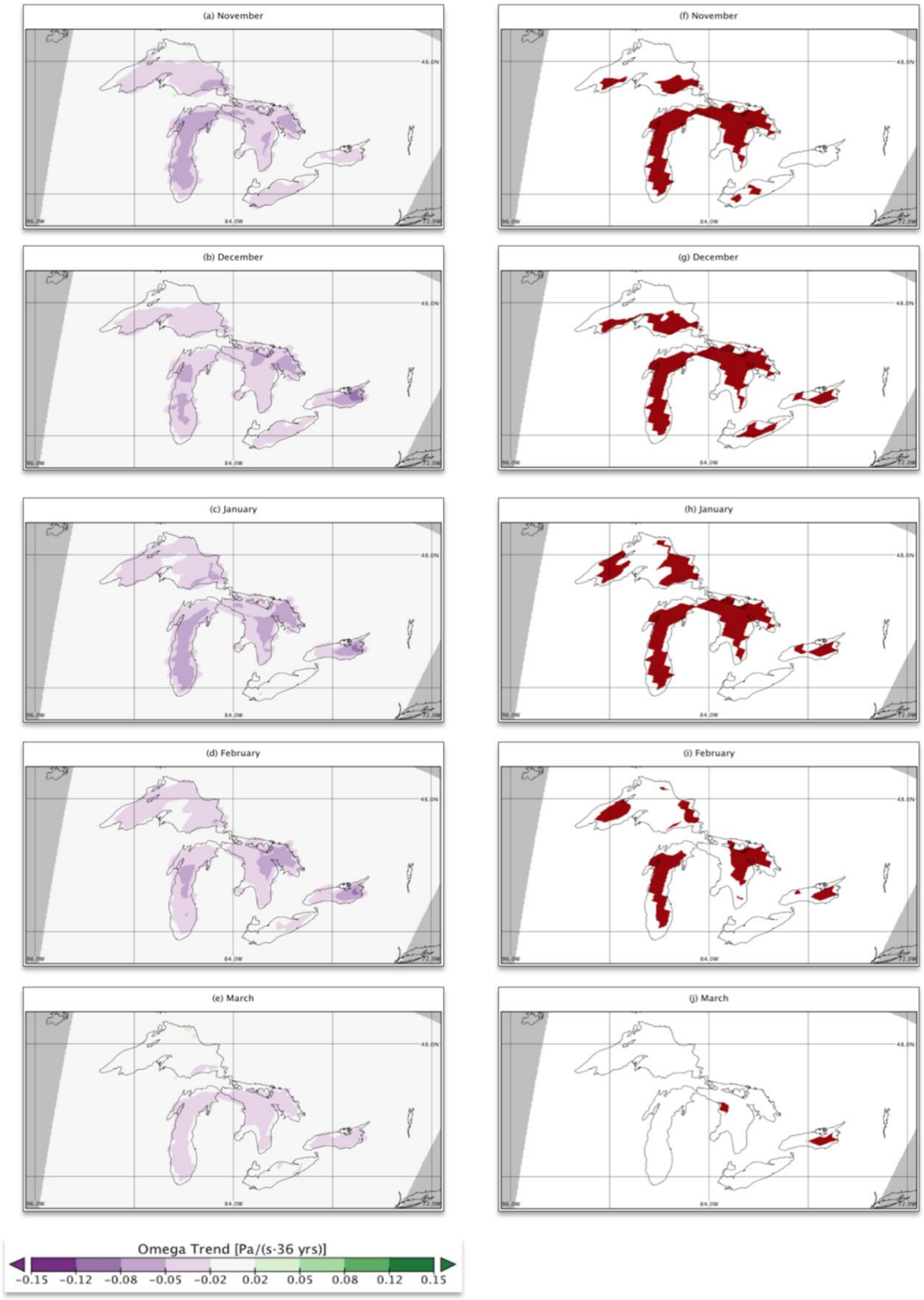

Figure 3.3: Spatiotemporal omega trends (Pa/s) over 36 years (1980-2015) of average monthly omega (left) and the corresponding areas of significant strengthening at the 95% confidence level (right).

Conversely, at the meso-beta scale, VTG is evaluated to determine instability within the PBL. According to Lavoie (1972), the most important factor required for the production of LES is the temperature gradient between the lake surface and the 850 mb level. Evident from Figures 3.4a-e is the predominant increase in VTG over the lakes and not over land. This increase occurs because lakes, in general, are efficient at absorbing incoming solar radiation (insolation) and have a high degree of transparency in contrast to land. A portion of the energy penetrates and disperses downward to great depths and is absorbed and diffused through a large water volume. Some of the energy received by the water body is used in evaporation, thereby cooling the surface and inhibiting the increase of lake temperature (Eichenlaub, 1979). Thus, in the context of climate change and a warming climate, air temperature with a lower heat capacity, will increase faster than will a water body with a higher heat capacity. Therefore, the VTG, over time, will begin to increase, as seen in the current results for the cold months.

LES occurs during the unstable season when the LST is warmer than the 850 mb air temperature. The Great Lakes have different onset times for the unstable season due to lake bathymetry and geographic location. Bathymetry influences LST due to the proportional relationship between heat capacity and water depth (Assel et al., 2003; Lacey et al., 2016). Lake Superior is larger by area, deeper, and located farther north than the rest of the Great Lakes, making it more susceptible to a prolonged unstable season that lasts from mid November to early April (Notaro et al., 2013).

Analysis of Figures 3.4f-j indicates that both Lakes Superior and Huron experience the greatest increase in VTG during January and February. There is a strong increase in VTG, upwards of 10 °K/36yrs, along the shores of Lake Superior in January, which gradually spreads over most of the lake by February. The monthly temporal variations in VTG within the cold season are correlated with a higher increase in LST, occurring in February in comparison to November for Lake Superior. However, there are no significant changes in the 850 mb air temperature that occur during the cold months of the 36-year period, not shown. February experiences a higher increase in VTG compared to November because LST increases at a faster rate in February, and the 850 mb stays relatively consistent. These

results are in agreement with Austin and Colman (2007) and Wang et al. (2014) who observed that LSTs have been increasing faster than regional air temperatures over Lake Superior and are, thereby, evidence of climate forcing mechanisms, such as the increased instability seen in this study.

In November, Figure 3.4a shows that VTG trends over lakes are similar to that over land. When lakes are statically stable, water warmed by incoming solar radiation (before reaching 4°C) will decrease density in the shallow layer of the lake surface, thereby making the LST behave similar to that of land. Furthermore, shallower waters near the shores of lakes tend to respond faster to ambient temperatures than deeper waters in the middle of lakes. As lakes respond to climate change, LST along lakeshores may warm relatively faster than the rest of the lake, inducing a larger VTG along the shores, as seen for Lake Superior in January (Figure 3.4c). The increase in the instability parameters of omega and VTG suggests the intensification of moisture and energy fluxes into the PBL. Thus, instability is influenced by LST and is another predictor variable that will be discussed next.

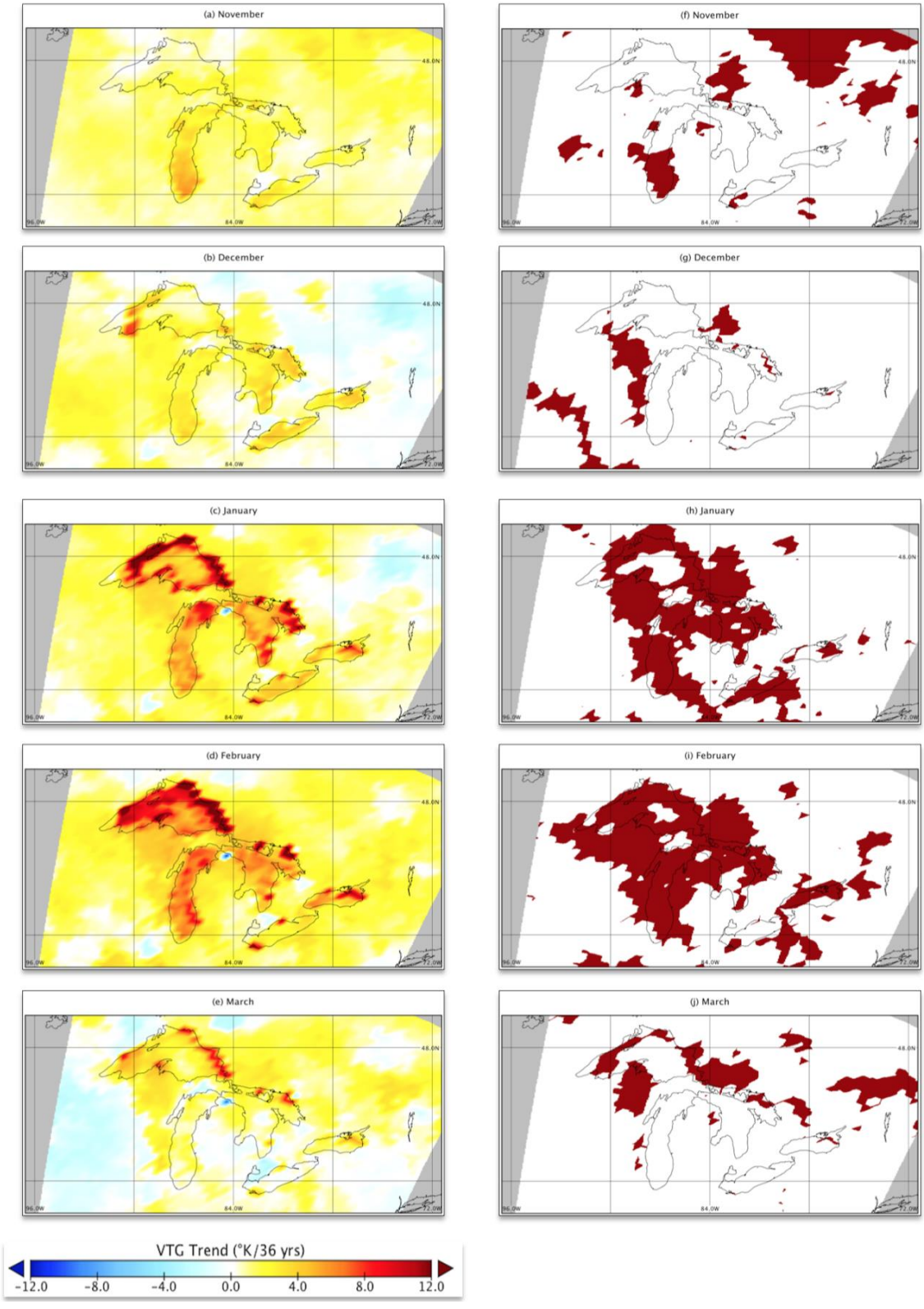

Figure 3.4: Spatiotemporal VTG trends (°K) over 36 years (1980-2015) of average monthly VTG (left) and the corresponding areas of significant increase at the 95% confidence level (right).

3.3.2.2 Lake Processes

Apart from the instability parameters, thermal and dynamic lake variables, including LST and ice cover concentration, were also explored to help diagnose changes in snowfall along Ontario's snowbelt of Lakes Superior and Huron. Results show that LST is significantly warming over regions of Lakes Superior and Huron, at rates exceeding 2 °K/36yrs for all months of the cold season (Figures 3.5a-j). The greatest warming in LST is predominant during the months of January and February for Lakes Superior and Huron (Figures 3.5c, d, h, and i).

The increases in cold season LSTs are also consistent with studies that have found an increase in summer surface water temperatures across the GLB (Austin and Colman, 2007; Dobiesz and Lester, 2009; Lacey et al., 2016). Lacey et al. (2016) found that 1994 to 2013 LSTs have been increasing significantly over the Great Lakes, with the fastest warming occurring around the coastline of Lake Superior, at a median rate of 0.2 °K/yr during the summer months. Furthermore, lake-wide averages of LSTs also show a significant increase in LST over Lake Superior between 1979 and 2006, as determined by Austin and Colman (2007). LSTs are also increasing in the winter months due to enhanced warming during the previous summer and the thermal lag of the lakes. The lack of ice and the larger areas of open water during summer can increase the exposure of lakes to incoming solar radiation, thereby warming and increasing the lake's heat storage, producing less ice cover during the cold season.

Evidently, ice cover concentration is another predictor variable that influences lake-induced snowfall because of its feedback effects on the energy exchanges between the lake-surface and atmosphere (Surdu et al., 2014). Ice extent and duration on lakes can control the seasonal lake-atmosphere heat budget and the magnitude of evaporation into the PBL, all of which are required for the development of LES. Conversely, warmer air temperatures, which are associated with seasons of less ice cover, can also limit the production of LES because of a reduced VTG. The total accumulated ice cover for each month of the cold season is plotted for Lake Superior and separately for Lake Huron (Figures 3.6a, and b), respectively.

Lake Superior experiences a decrease in ice cover for all months of the cold season except for November over the 36-years (Figure 3.6a and Table 3.2). Lake Huron exhibits a decrease in ice cover from January through March, with a slight increase in December and no changes in November (Figure 3.6b and Table 3.3). The rate of ice cover decline is higher for Lake Superior than Lake Huron and can contribute to a stronger increase in LST for Lake Superior than Huron (Wang et al., 2005; Wang et al., 2014). A significant decrease in ice cover concentration over the 36-year period is predominant for the later months, for both lakes, and can be attributed to LST. Recall that LST trends have increased during the cold season, a probable cause for the observed decrease in ice cover concentration.

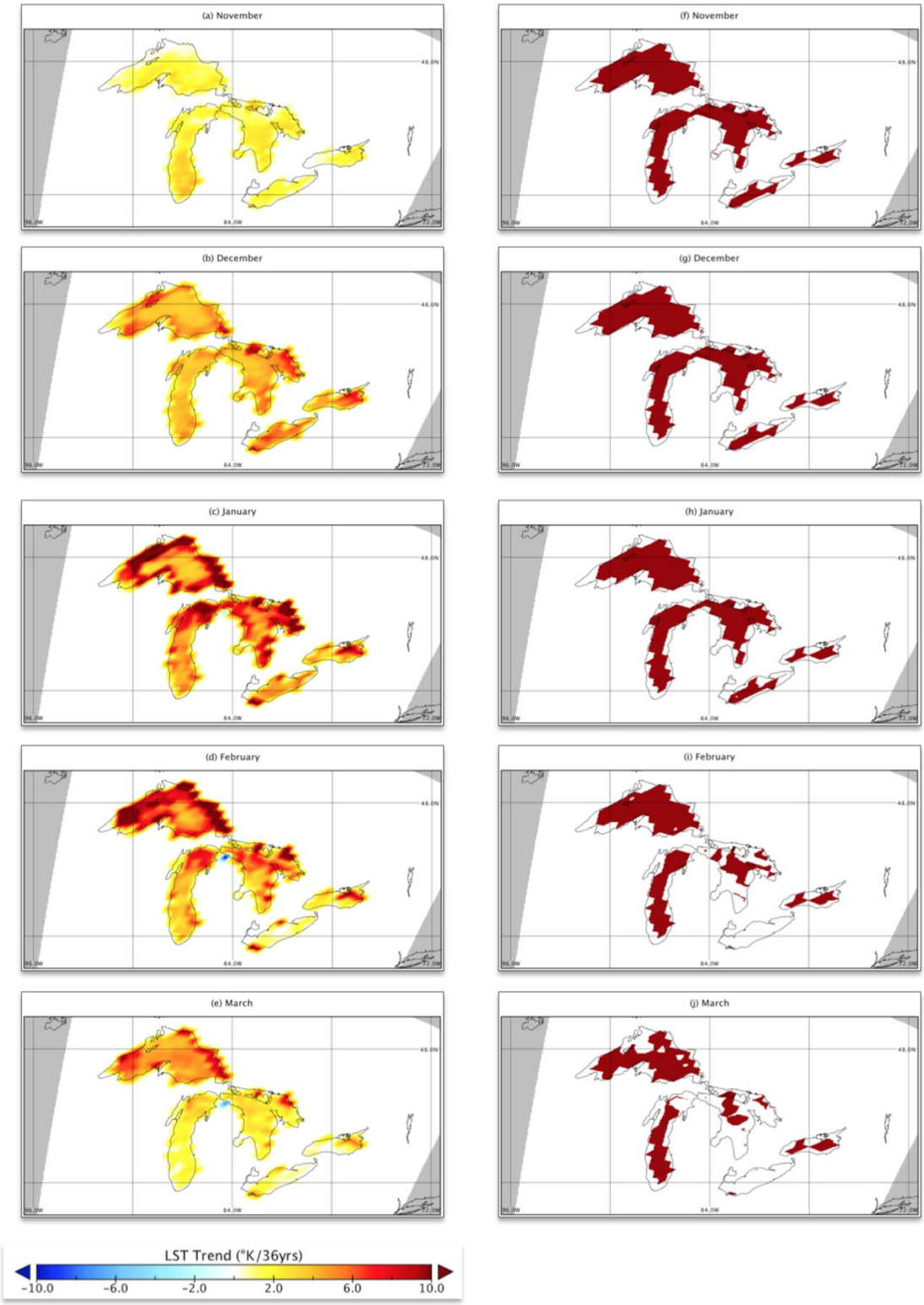

Figure 3.5: Spatiotemporal LST trends (°K) over 36 years (1980-2015) of average monthly LST (left) and the corresponding areas of significant increase at the 95% confidence level (right).

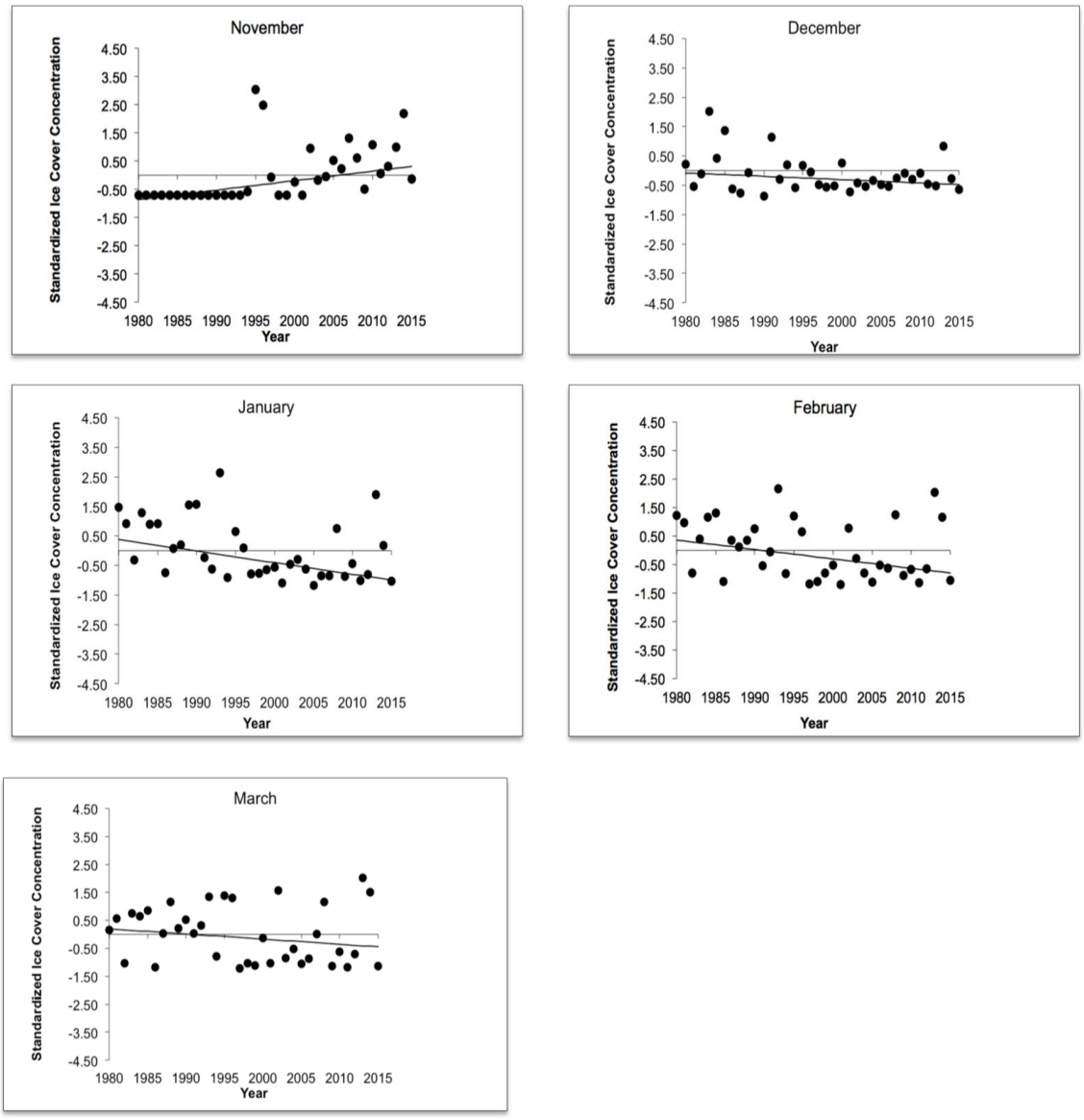

Figure 3.6a: Lake Superior's historical (1980-2015) total accumulated ice cover for each month of the cold season shown by plotting the standardized score and computing the climatological trend.

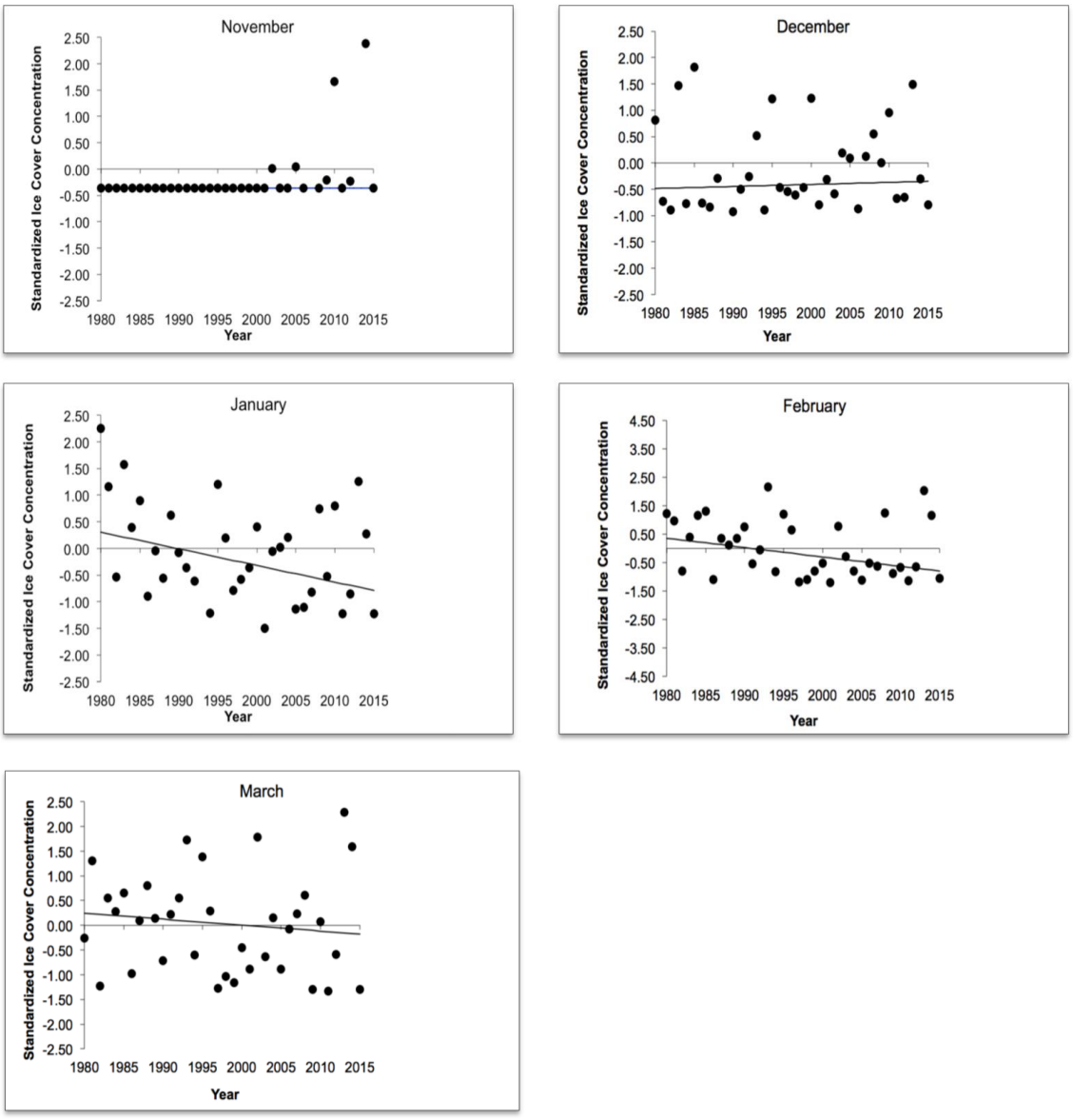

Figure 3.6b: Lake Huron's historical (1980-2015) total accumulated ice cover for each month of the cold season shown by plotting the standardized score and computing the climatological trend.

Table 3.2: The Sen slope and significance of total accumulated ice cover trend over the 1980-2015 period for each month (November through March) for Lake Superior.

Months	**Sen Slope & Significance**
November	0.034***
December	-0.011
January	-0.039**
February	-0.033+
March	-0.018
***	*0.001 level of significance*
**	*0.01 level of significance*
+	*0.1 level of significance*

Table 3.3: The Sen slope and significance of total accumulated ice cover trend over the 1980-2015 period for each month (November through March) for Lake Huron.

Months	**Sen Slope & Significance**
November	0**
December	0.004
January	-0.031+
February	-0.024
March	-0.012
**	*0.01 level of significance*
+	*0.1 level of significance*

Incoming solar radiation can penetrate through lake-ice and warm the water below. This melts the underside of the ice and induces convective mixing within the lakes (Brown and Duguay, 2010). The decrease in ice cover is in agreement with previous studies from Magnuson et al. (2000), Assel et al. (2003), Austin and Colman (2007), Titze and Austin (2014), Jensen et al. (2007), Wang et al. (2012), Lacey et al. (2016). Lacey et al. (2016) suggest that seasonal ice cover duration has decreased by 0.96 days/yr for Lake Superior, and 0.67 days/yr for Lake Huron during the 1994-2013 period. Furthermore, Lacey et al. (2016) argue that Lakes Superior and Huron's decrease in ice cover since the 1970s can be attributed to a shift in ice cover mainly during the 1990s and coinciding with the strong El Niño Southern Oscillation (ENSO) winter of 1997-1998.

Thus, a decrease in ice cover is not only correlated with a direct increase in LST. For example, results indicate that during the month of November, the ice cover did not change for Lake Huron and actually increased for Lake Superior, despite the increase in LST. Furthermore, during the month of December, Lake Huron's ice cover also increased, although not significantly. Notable ice cover variability is apparent over this 36-year period, with above-normal ice concentration recorded over the Great Lakes during the winter of 1994. Extensive mid-lake ice formation started forming two weeks earlier than usual at this time. This example, along with several other cold air outbreaks in the early 1990s, constituted an increase in ice cover trends during November. The increase in ice cover was a result of anomalously strong anticyclonic circulation over the central North Pacific, which extended to the North Pole, and a strong polar vortex centered over Hudson Bay. These synoptic setups can frequently advect Arctic and polar air masses into eastern North America and over the Great Lakes Region (Assel et al., 2003), producing unusually larger ice cover extent. Synoptic scale systems also have an influential role on the predictor variables, which will be discussed in the next section.

3.3.2.3 Predictor Variables and their Connections to Changes in Snowfall

Predictor variables show a significant increase in instability for the omega parameter over the GLB but little spatial coherency and a weak trend over Lake Superior during the months of DJF. The VTG parameter significantly increases over Lake Superior during the later

part of the cold season. The LST increases significantly over Lake Superior during NDJ, and ice is significantly reduced during the month of January for this lake. These predictor variable results lead towards a favourable increase in evaporation and energy fluxes into the lower PBL.

The results are in agreement with those of Hunter et al. (2015), who observed an over lake decrease in precipitation for the past 20 years for Lake Superior. They also observed an abrupt increase in over-lake evaporation at the beginning of the late 1990s for the Laurentian Great Lakes and an increase in evaporation, for a longer period, over Lake Superior. Wang et al. (2012), Austin and Colman (2007), Blanken et al. (2011) and Spence et al. (2011) have also found these evaporation estimates to be consistent with observations of both ice cover and surface water temperature, similar to the results attained in this study.

Rauber (2005) suggests that a temperature gradient of approximately 10°C between the LST and 2-m air temperature is sufficient for the destabilization of the overlying atmosphere. Additional analysis of the air temperature at the 1000 mb level shows a significant 2-4 °K/36yrs warming, predominantly over Lake Superior, during the cold season (Figures 3.7a-j). The preferred air temperature for LES is between 273 °K and 263 °K because it is cold enough to permit frozen precipitation but mild enough to hold sufficient moisture. Precipitation will most likely fall as rain if a sufficient depth in the boundary layer exceeds 273 °K (Miner and Fritsch, 1997; Notaro et al., 2013). As air temperature warms, it can hold more moisture within an air parcel, increasing the atmospheric absolute humidity and the residence time of water vapour in the atmosphere.

These ideas are in agreement with Notaro et al. (2013), who suggested that although the Great Lakes can increase precipitation by 0.13 mm/day during the cold season, an increase in air temperature during the cold season could lead to a smaller fraction of snowfall accumulation and a decrease in snowfall by approximately 9%, hence the decrease in observed snowfall and precipitation along the immediate Ontario snowbelt of eastern Lake Superior. Furthermore, the reasons for these negative spatiotemporal trends in snowfall can be attributed to the fact that the precipitation response is approximately 2.3 times smaller

than evaporation over the Great Lakes during the cold season. In addition, there is inefficient moisture recycling and greater moisture entering the atmosphere as vapor and clouds during the LES season (Notaro et al., 2013).

This study suggests that an increase in evaporation over the lakes does not necessarily constitute the immediate production of precipitation in the same region. These air parcels can be advected to downwind regions of the Great Lakes and to zonally eastward locations before becoming saturated and precipitating. Landmasses of continental dimensions must be upwind of water bodies to supply cold and dry air (Eichenlaub, 1979). The spatial distribution of lakes can also influence LES in neighbouring areas due to multi-lake connections. For example, Lake Ontario influences LES downwind towards the Finger Lakes in the United States (Laird et al., 2010), and the moisture of Lake Superior can influence the Lake Huron and Lake Ontario snowbelts. It is acknowledged that over-lake fetch from the northern lakes and the increased moisture over Lake Superior may facilitate increased lake effect precipitation along Lake Erie's and Lake Ontario's snowbelts in the United States due to multi-lake connections. Air parcels can continue to advect until they become very saturated and precipitate heavy amounts of snowfall towards downwind regions. Thus, the decrease in snowfall for the Canadian snowbelt, and the increase in snowfall seen over parts of the United States, as observed by Burnett et al. (2003), Ellis and Johnson (2004), Kunkel et al. (2009) are perhaps attributable to the aforementioned phenomena, during overlapping analysis years.

The trajectories of advected saturated air masses are influenced by synoptic scale setups. Changes in snowfall can be related to variations in ocean-atmospheric oscillation patterns that can influence the location and behaviour of synoptic scale features, which in turn inhibit or facilitate cold air outbreaks over the GLB. Changes in synoptic scale systems that influence LES are shown to correlate with LES totals downwind of Lakes Erie and Ontario (Leathers and Ellis, 1996). Suriano and Leathers (2017) have investigated the trends in seven synoptic features that influence LES over the cold season of 1950 to 2009. They found that the frequency of synoptic systems influencing LES have decreased or exhibit no trends in frequency from 1980 to 2009, the same period for which other studies

have shown a decrease in snowfall over parts of the GLB, example, Hartnett et al. (2014). While Suriano and Leathers (2017) have made great progress in attributing changes in LES synoptic features to ocean-atmosphere oscillation patterns, further research is required to study the changes in these synoptic patterns to that of snowfall over the GLB. Thus, teleconnection trends in response to climate change are a topic area that requires additional research (Kunkel et al., 2009; Brown and Duguay, 2010) and is beyond the scope of the current study.

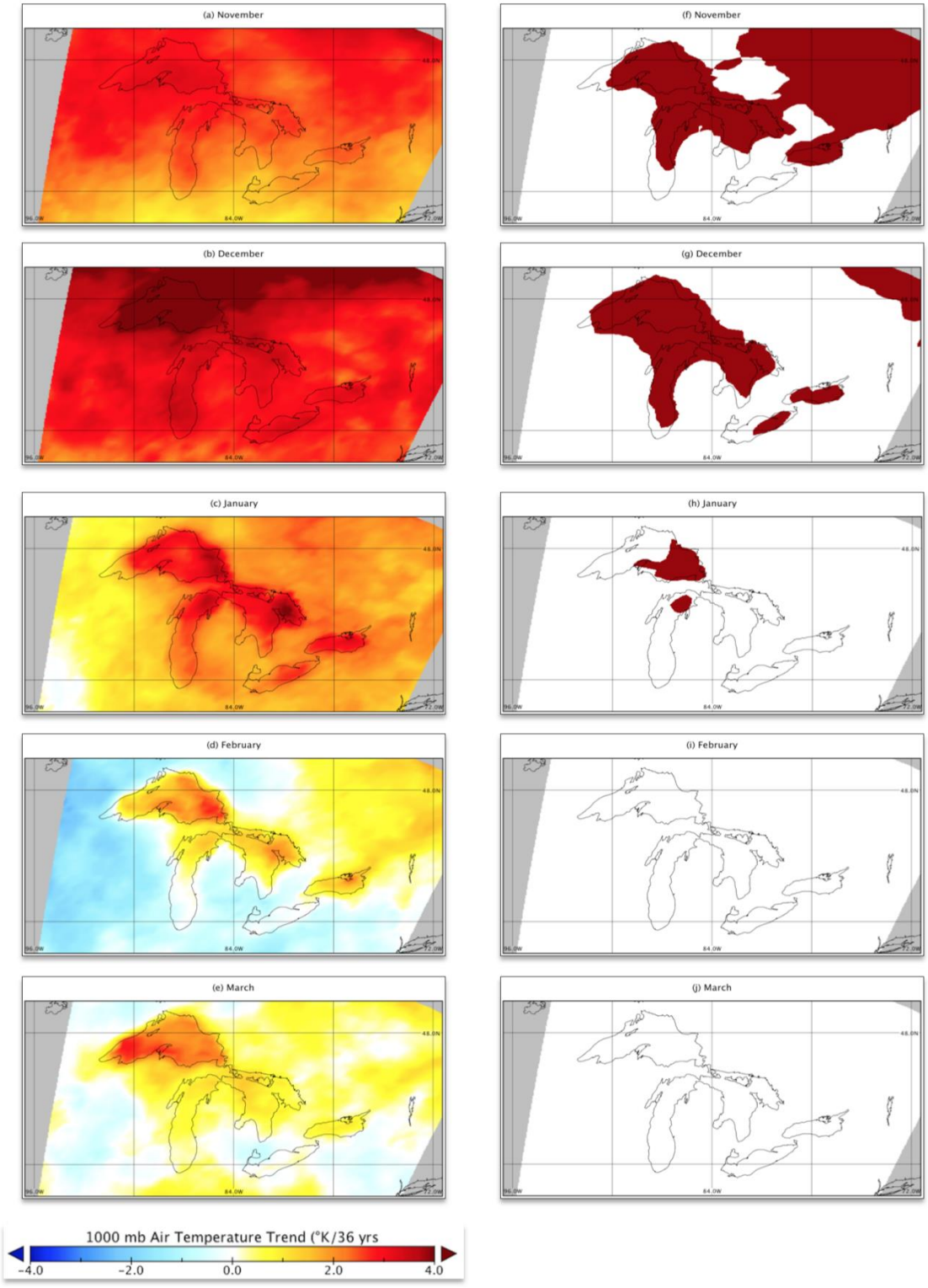

Figure 3.7: Spatiotemporal 1000 mb air temperature trends (°K) over 36 years (1980-2015) of average monthly air temperature (left) and the corresponding areas of significant increase at the 95% confidence level (right).

3.4 Summary and Conclusions

A comprehensive study of the climatological trends of snowfall from 1980 to 2015 was presented in this chapter. The region of study was focused on the understudied snowbelt region of Lake Superior and Lake Huron in Ontario, Canada. Multiple datasets were utilized, including the gridded datasets of Daymet, NARR, and ECCC CIS. Monthly totals of snowfall and precipitation trends were examined over a 36-year period using the MK statistics test. Surface-atmosphere LES predictor variable trends were also analysed by taking the monthly mean omega at the 700 mb level, VTG between the LST and 850 mb level, LST, monthly ice cover concentrations, and air temperature at 1000 mb to help diagnose the changes in snowfall for these regions.

This study suggests that snowfall and precipitation have significantly decreased from 1980 to 2015 along the Ontario snowbelts of Lake Superior and Lake Huron. However, for snowbelts within the United States, observed snowfall trends have increased during the 20^{th} and early 21^{st} century. Furthermore, investigations into the predictor variables during the cold season, which influence lake-induced snowfall, show an increase in 1000 mb air temperature over Lake Superior, an increase in instability in the lower PBL, an increase in LST, and a decrease in ice cover. A decrease in ice cover can potentially enhance fetch and increase both sensible and latent fluxes into the PBL, promoting increased snowfall. However, warmer air temperatures can also decrease the sensible heat flux into the lower PBL. Warmer air masses also have the ability to hold more moisture, thereby limiting the further development of lake-induced precipitation (Notaro et al. 2015). It is suggested that the increase in moisture into the atmosphere does not necessarily lead to heavier precipitation over the same region. This may be due to inefficient moisture recycling, and the air parcel can continue to advect farther downwind to the southern Laurentian Great Lakes before saturating and precipitating.

While the current research examines trends in snowfall that are related to LES predictor variables, it is acknowledged that other regional processes, including cold air outbreaks from large scale synoptic shifts, can contribute to changes in snowfall trends; however, these assessments are beyond the scope of this study. Sensitivity analysis, such as that

conducted by Wright et al. (2013), suggests that an increase in LST will produce an increase in the intensity of LES and its propagation downwind of the Laurentian Great Lakes. Now that historical monthly total snowfall and precipitation trends over the Canadian snowbelts have been established, future work will focus on examining the extreme trends in snowfall intensity, duration, and frequency over the Canadian leeward shores of the Laurentian Great Lakes.

Chapter 4
Historical Spatiotemporal Trends in Snowfall Extremes over the Canadian Domain of the Great Lakes Basin

4.1 Introduction

Chapter 3 explored spatiotemporal trends in monthly snowfall totals and attributed the decrease in snowfall, in part, to rising air temperatures. Therefore, continued warming could significantly influence variability in temperature and precipitation during the 21st century. As monthly snowfall totals decrease another question arises. Are extremes in snowfall intensity, frequency and duration also changing? Assessing and monitoring spatiotemporal trends in snowfall extremes to a historically changing climate can provide knowledge as to future behavioural spatiotemporal trends in snowfall extremes within the densely populated Canadian GLB domain and can be useful for sustainability and adaptation studies.

However, under-examination of historical spatiotemporal snowfall extremes, compared to lake-induced snowfall case studies, are apparent. The majority of lake-induced snowfall investigations have analysed specific lake-induced events and associated features as opposed to lake-induced climatology, for example, Lackmann (2001), Niziol et al. (1995), Hamilton et al. (2006), Maesaka et al. (2006), Lavoie (1972), Hjelmfelt (1990), Warner and Seaman (1990), Bates et al. (1993), Sousounis and Fritch (1994), Ballentine et al. (1998), Tripoli (2005), and Shi et al. (2010). Furthermore, several studies have examined trends in snowfall patterns across the GLB over the 20th century and found a snowfall trend reversal, in which there was an increase followed by a decrease in snowfall. Scott and Kaiser (2004) investigated snowfall trends over North America from 1948 to 2001 and observed a snowfall increase over a narrow band from Colorado to the lee of Lake Erie and Lake Ontario. In addition, Karl and Knight (1998) found that the area-averaged snowfall across northern Canada (55ºN to 88ºN) significantly increased at a rate of 8.8 cm per decade in the late 20th century and early 21st century. In southern Canada (below 55ºN) a negative trend of 0.65 cm per decade during this period was discovered, with the most decrease occurring in the 1980s (Krasting et al., 2013). Suriano and Leathers (2016)

suggest that while some studies have shown a general increase in snowfall over the GLB (Leathers et al., 1993; Norton and Bolsenga, 1993; Leathers and Ellis, 1996; Burnett et al., 2003; Ellis and Johnson, 2004; Kunkel et al., 2009), recent studies have seen a decline in LES through the later half of the 20th century. For example, Bard and Kristovich (2012) showed a decrease in snowfall along the leeward shores of Lake Michigan between 1980-2005, and Hartnett et al. (2014) showed a decrease in Central New York between 1971-2012. While these studies outline trends in North American snowfall, there is still a lack in the examination of climatological snowfall extremes over the GLB. Little is still known about the physical processes influencing the past changes in daily snowfall extremes on the global and hemispheric scale. On a regional scale, observational studies show large inter-decadal variations in snowfall extreme measures; however, long-term trends remain unclear (Zhang et al., 2001; Kunkel et al., 2013; Gorman et al., 2014).

Thus, the objective of this study is to assess historical 1980-2015 spatiotemporal trends in snowfall extremes for the Canadian snowbelt zones of Lake Superior and Lake Huron (Figure 4.1). This will be conducted by examining snowfall intensity, frequency, and duration, and provide potential explanations of the results in the context of LES predictor variables. This paper commences with an introduction, in section 4.1, that provides a background on the development of snowfall within the GLB region; section 4.2 explains the data sources and procedures used to conduct this research; section 4.3 presents the results and discussions that will hone in on interpreting the findings; and finally, section 4.4 summarizes the current study and discusses future research investigations.

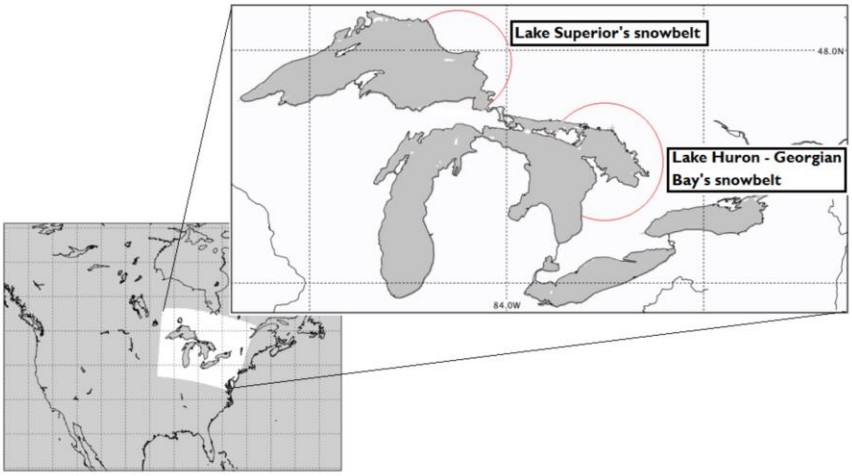

Figure 4.1: Map of the Laurentian Great Lakes in northeastern North America depicting the Canadian snowbelts of Lakes Superior and Huron analysed in this study.

4.2 Data and Methodology

This paper utilizes the Daymet dataset and the snowfall derivation method that were employed in Chapter 3. Recall section 3.2.1 for a description of the Daymet dataset and the snowfall derivation process. This section continues with an overview on defining snowfall extremes and the methods used in this paper.

Snowfall extreme analyses are evaluated in two folds; first by exploring the monthly spatiotemporal extremes in snowfall intensity, frequency, and duration over the 36-year period (hereinafter referred to as the 36-year extreme) and secondly by determining the trends in these extremes. Firstly, the 36-year extremes are explained. Snowfall intensity is defined as the rate of snowfall over time. The 99^{th} percentile of daily snowfall accumulation is computed over all time steps, that is, all days between 1980 and 2015 for each individual month. The 99^{th} percentile over the 36-year period is then spatially mapped to determine the extreme values of snowfall intensity and its location for each month of the cold season. Based on each month's extreme intensity snowfall, a midpoint value is chosen that best represents the extreme threshold snowfall intensity for the overall cold months.

The acquired threshold value is then used to evaluate the 36-year extreme in snowfall frequency and duration. Frequency is defined as the number of snowfall days over a

particular time period. In this study, the extreme snowfall frequency is determined by calculating the number of snowfall days that the given threshold is met or exceeded for each month over all time-steps of the 36-year period. Monthly maps are generated to determine regions within the GLB of high and low extreme snowfall frequencies during the 36-year period. Snowfall duration is described as the length of time it snows at a particular intensity. The 36-year duration extreme is presented by mapping the maximum number of consecutive snowfall days for which events equaled or exceeded the acquired snowfall threshold value over this time period. This procedure is repeated for each month of the cold season to determine spatial patterns in extreme snowfall duration throughout the season.

Secondly, the trends in 36-year extremes are calculated. Trends in extreme intensity are computed by applying a filter to extract daily snowfall events greater than or equal to the extreme threshold value for each month and for each year. The filtered values are aggregated and then divided by the total number of snowfall days in the month, yielding the monthly snowfall intensity. This procedure is repeated for each of the 36-years. The MK test is then applied to this time series to compute the trend in monthly extreme snowfall intensity. The trend is computed for each month of the cold season, and monthly spatiotemporal extreme intensity trends are produced. Trends in snowfall frequency are computed by counting the number of monthly extreme events (filtered values) for each year. The MK test is then applied over this time series to evaluate the spatiotemporal trends in monthly snowfall extremes. The trend in extreme snowfall duration is calculated by computing the MK test over each monthly time series. The time series comprise the monthly maximum number of consecutive snowfall days for which events equaled or exceeded the extreme snowfall threshold.

The MK test is applied to the extreme snowfall time series to determine whether there are monotonic upward or downward trends in intensity, frequency, and duration for each grid cell over the 36-year period. If grid cells do not have a complete 36-year time series of extreme values, then no trend analysis is computed for that grid cell, and it is assigned “not a number” and shaded gray. The MK test evaluates the slope of an estimated linear

regression line non-parametrically and does not require the residual from a fitted regression line to be normally distributed, like that of a parametric linear regression (Gilbert, 1987; Kendall, 1995). In this study, slope is calculated over the 36-year period for each grid cell in order to generate spatiotemporal trend maps. For the purpose of this study the significance of the trends is calculated at the 90% confidence level. This is because a higher confidence level may not be able to capture the highly episodic and disorganized spatial patterns of extreme lake-induced trends seen in the results.

4.3 Results

4.3.1 Snowfall Intensity Extreme Values

A predefined extreme intensity snowfall value is required in order to conduct extreme snowfall analyses. For this study, the extreme threshold value is computed by calculating the 99th percentile of daily snowfall for each month over the 36-year period (Figure 4.2a-e). Within the Canadian GLB domain, the eastern shores of Lake Superior and Lake Huron show the greatest value in snowfall intensity for all months. Along these shores, the lower snowfall intensity values range between 5 cm and 15 cm for the months of November and March (Figure 4.2a and e) and the higher values range between 15 cm and 30 cm for December and January (Figure 4.2b and c).

The threshold value of 15 cm of snowfall per day is adopted to evaluate extreme snowfall over the 36-year study period. The 15 cm threshold is ideal because it is the midpoint value among the cold months that are being analysed. This threshold is also in agreement with Environment Canada's warning criteria for Ontario, which issues a snowfall warning when the alerting snowfall parameter reaches or exceeds 15 cm of snowfall within 12 hours. The alerting parameter for Ontario's snowsquall warnings is similar but also factors in a reduced visibility criterion of 400 m with or without the presence of persistent blowing snow (ECCC, 2017a). Since this study is limited to a daily temporal resolution, 15 cm/day is used as the extreme threshold value. Furthermore, 15 cm/day is a reasonable threshold indicator for extreme daily snowfall intensity. For example, when separately considering historical 1981 to 2015 monthly snowfall average for the city of Barrie, which lies within Lake Huron's snowbelt, Barrie experiences its highest snowfall in January with an average

of 66 cm. This suggests an average of approximately only 2 cm/day with assumed continuous daily snowfall (Current Results, 2017). Therefore, a snowfall rate of 15 cm/day would be considered an extreme snowfall event of high intensity. This threshold is now applied to evaluate extremes in snowfall frequency and duration.

4.3.2 Snowfall Frequency Extreme Values

Results show that extremes in snowfall intensity are predominant along the leeward shores of Lake Superior and Lake Huron during the cold season. Next, the spatiotemporal frequency in extreme snowfall events is explored by determining the number of days that snowfall events equaled or exceeded the extreme threshold value of 15 cm/day over the 36-year period. At the start of the LES season, in November, the leeward shores of Lake Superior begin to experience higher frequencies in extreme snowfall events compared to other regions of the GLB (Figure 4.3a). The greatest spatial extent with highest frequencies upward of 50 days are seen on the eastern shores of Lake Superior and Lake Huron for the months of December (Figure 4.3b) and January (Figure 4.3c). The spatial and temporal onsets of high frequency snowfall behave similar to that of lake-induced snowfall spatiotemporal patterns. In February, (Figure 4.3d) the frequency is still high along Lake Superior's eastern lakeshore but, becomes highly localized, while both the spatial extent and higher frequencies along the snowbelt of Lake Huron have decreased. By March, both the high frequency values and spatial extent have decreased for both snowbelts with frequencies less than 10 days (Figure 4.3e). Similar spatiotemporal results are exhibited when examining extreme snowfall duration.

4.3.3 Snowfall Duration Extreme Values

Extreme snowfall duration plots show the maximum number of consecutive days when snowfall intensity equaled or exceeded 15 cm/day for the 36-year period. As early as November, highly localized areas along the eastern shores of Lake Superior experienced high duration of extreme snowfall events upwards of 3 days, while Lake Huron's snowbelt shows zero to one day of maximum snowfall duration (Figure 4.4a). In December and January, most of Northeastern Ontario experienced extreme events greater than 2 days. However, the duration of extreme snowfall events greater than 5 days were spatially

confined to the snowbelt regions. By February, the duration of extreme snowfall events have spatially decreased along the Lake Huron snowbelt, but continues to stay dominant along the leeward shores of Lake Superior. By March, both snowbelts show a spatial reduction and decrease in extreme snowfall duration (Figure 4.4e).

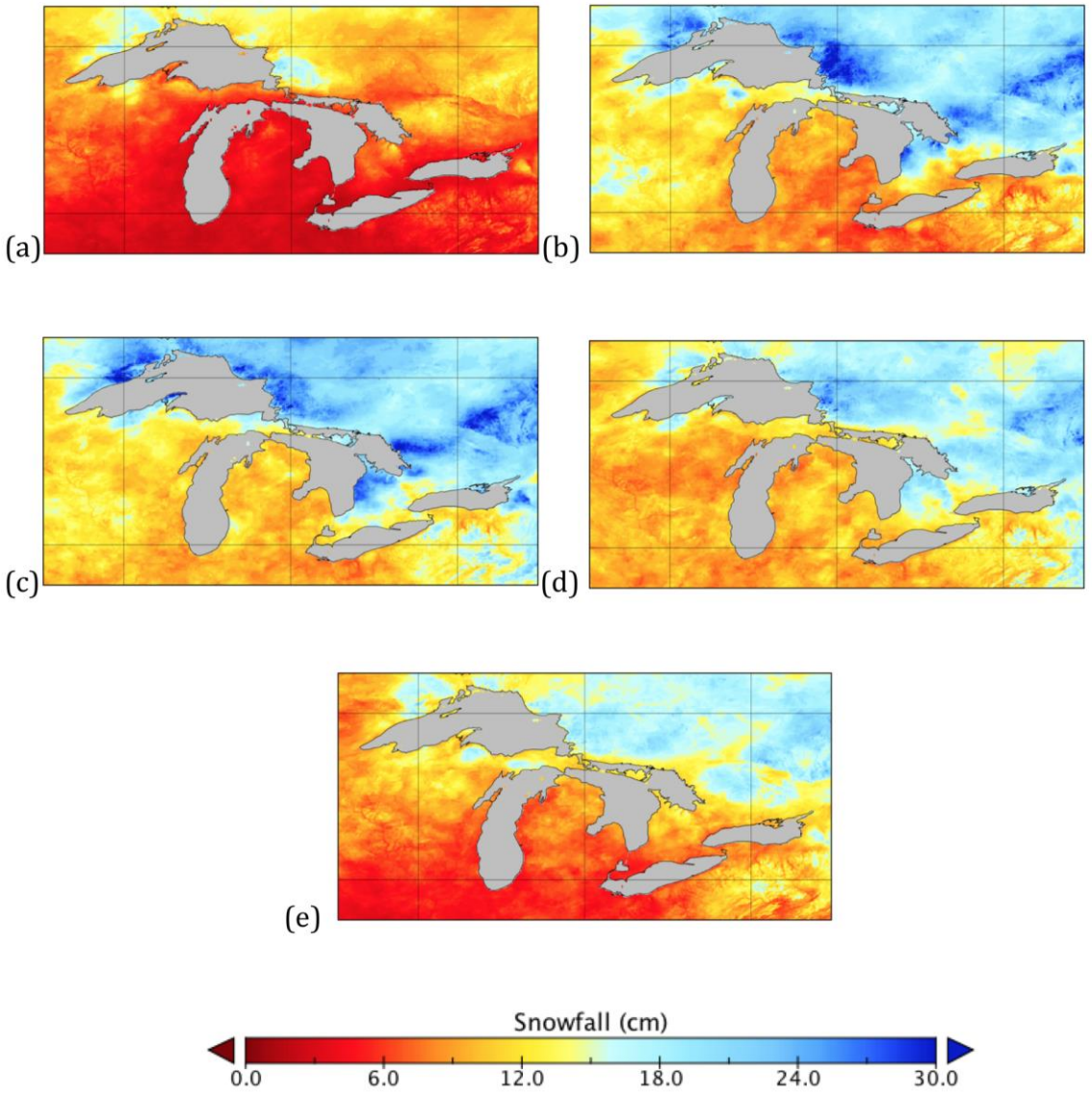

Figure 4.2: Extreme snowfall intensity for each month of the cold season, a) November, b) December, c) January, d) February, and e) March, defined as the 99th percentile of daily snowfall between 1980 and 2015.

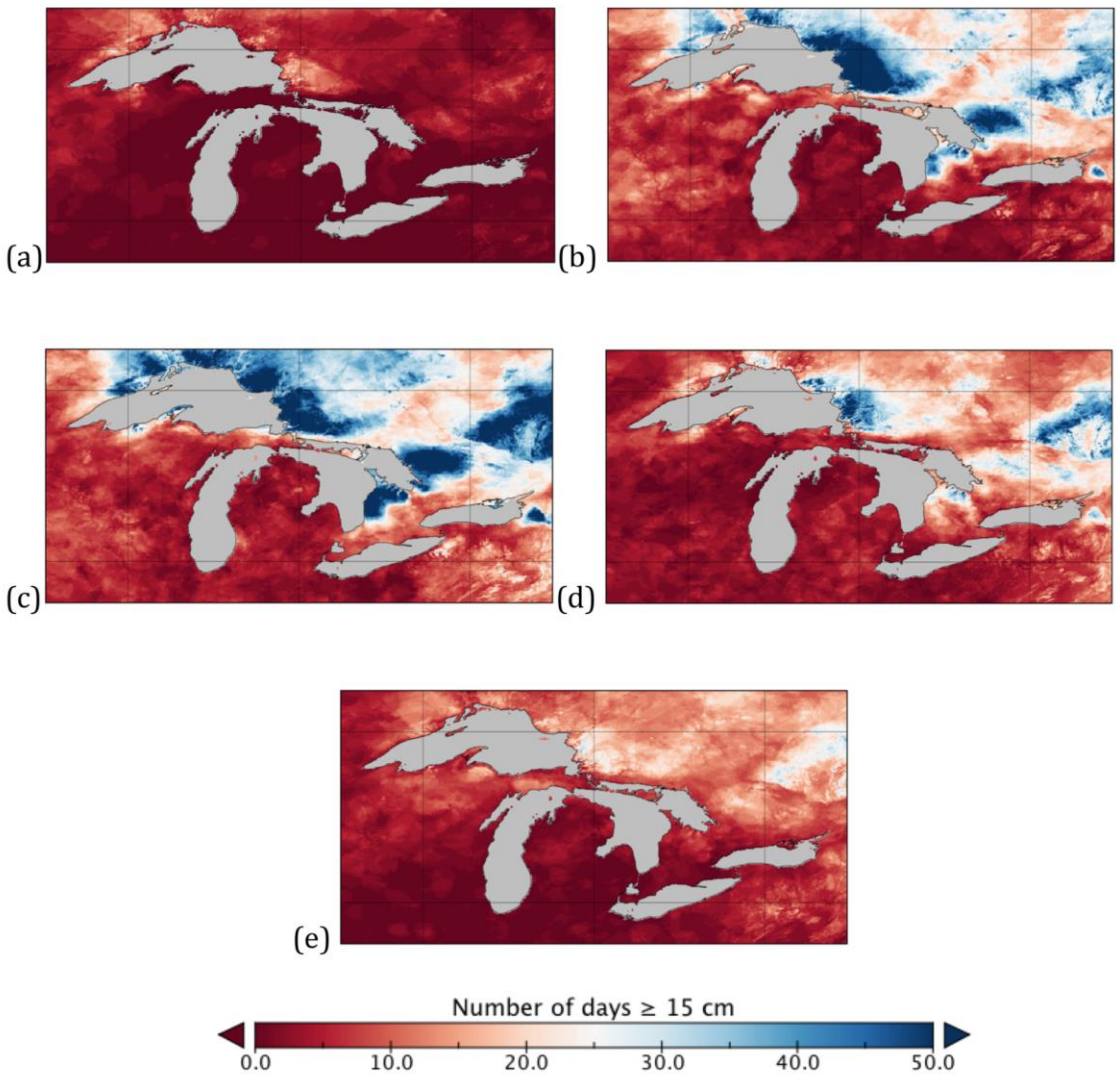

Figure 4.3: Extreme snowfall frequency for each month of the cold season, a) November, b) December, c) January, d) February, and e) March. Extreme snowfall frequency is defined as the number of days when daily snowfall amounts equaled or exceeded the extreme value threshold of 15 cm between 1980 and 2015.

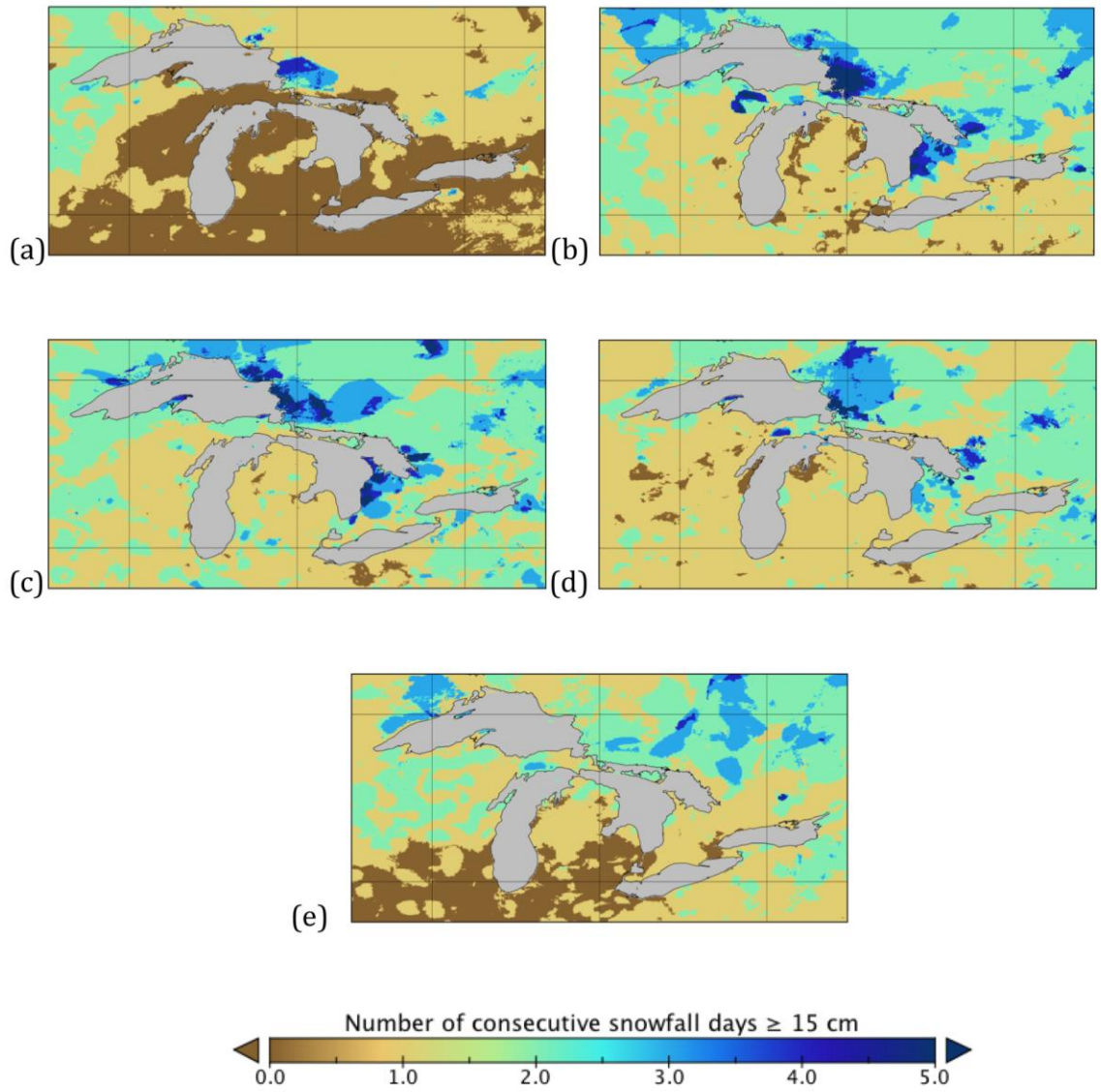

Figure 4.4: Extreme snowfall duration for each month of the cold season, a) November, b) December, c) January, d) February, and e) March. Extreme snowfall duration is defined as the maximum number of consecutive days for which daily snowfall amounts equaled or exceeded the extreme value threshold of 15 cm between 1980 and 2015.

4.3.4 Trends in Snowfall Extremes

This section evaluates the 1980 to 2015 spatiotemporal trends in extreme snowfall intensity, frequency, and duration for each month of the cold season, with a threshold extreme value of 15 cm/day. Baijnath-Rodino et al. (2018) showed clear, consistent, and contiguous spatiotemporal trends in monthly snowfall totals for Lake Superior's and Lake

Huron's snowbelts. However, spatiotemporal trends in monthly mean snowfall extremes are less coherent and less obvious to delineate.

4.3.4.1 November

Extreme snowfall intensity, frequency, and duration experience no significant changes over the GLB for the month of November. Although not significant, the snowfall intensity trends can provide indication of extreme snowfall evolution, shown in Figure 4.5. For instance, the northeastern shores of Lake Superior show a decrease in extreme snowfall intensity, while the southeastern shores present an increase, indicating the inconsistency of coherent spatial distribution along this snowbelt. Furthermore, there is a strong negative trend within the region of northeastern Ontario, which is father inland from the leeward shores of Lake Superior. This geographic location implies that the strong decrease in extreme snowfall trend may not be due to LES but perhaps to synoptic and extratropical scale snowstorms. The spatiotemporal trends for the month of November suggest that an increase in snowfall extremes in Northern Ontario is perhaps due to lake-induced processes and a decrease in extratropical and synoptic scale driven snowstorms.

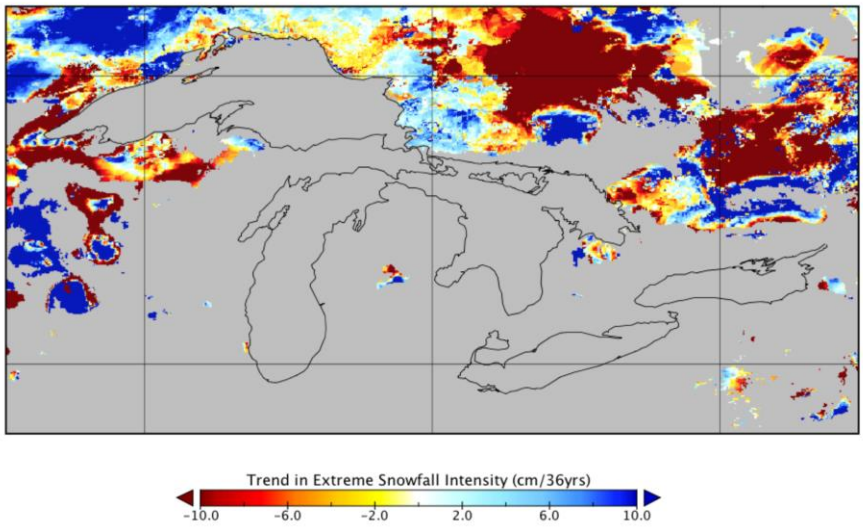

Figure 4.5: Trend in extreme snowfall intensity for the month of November. Gray pixels represent grid cells with no trend computed because region contains some years with no extreme snowfall values.

In Southern Ontario, most of this region does not experience daily extreme snowfall greater than 15 cm in November. Recall from Figure 4.2, the monthly mean extreme snowfall for November does not exceed 12 cm for most grid cells in Southern Ontario and is indicated by gray pixelated regions. Furthermore, extreme snowfall frequency and duration show no changes for the month of November and are not included in the results. December results provide more substantive evidence of trends in snowfall extremes for both snowbelt regions.

4.3.4.2 December

December exhibits the most coherent significant spatiotemporal trends in snowfall extremes for all months of the cold season. In December, Lake Superior's snowbelt displays two distinct trends. The southeastern shore reveals a significant decrease in extreme snowfall intensity, while the northeastern shore shows a highly localized significant increase (Figure 4.6a). Both the northeastern and southeastern shores exhibit a significant decrease in extreme snowfall frequency (Figure 4.6b). However, the northeastern shore displays a weaker negative trend. The duration also significantly decreases for the southeastern shore, with no change in extreme snowfall duration for the northeastern shore of Lake Superior's snowbelt (Figure 4.6c). During this month, the snowbelt of Lake Huron shows a highly localized decrease in snowfall intensity but no changes in extreme snowfall frequency and duration. It is evident that not only are spatiotemporal trends in snowfall extremes different for both snowbelts, but within the same snowbelt, trends in snowfall extremes are not spatially coherent.

4.3.4.3 January

The month of January shows less spatial coherency than December for both snowbelt regions. The northeastern shore of Superior shows a significant decrease in snowfall intensity (Figure 4.7a), frequency (Figure 4.7b), and duration (Figure 4.7c). Southern Ontario shows spatial incoherent negative trends in extreme snowfall intensity, while there are no changes in frequency and duration. Compared to December, the spatiotemporal trends in extreme snowfall are highly localized and, overall, less spatially coherent.

a)

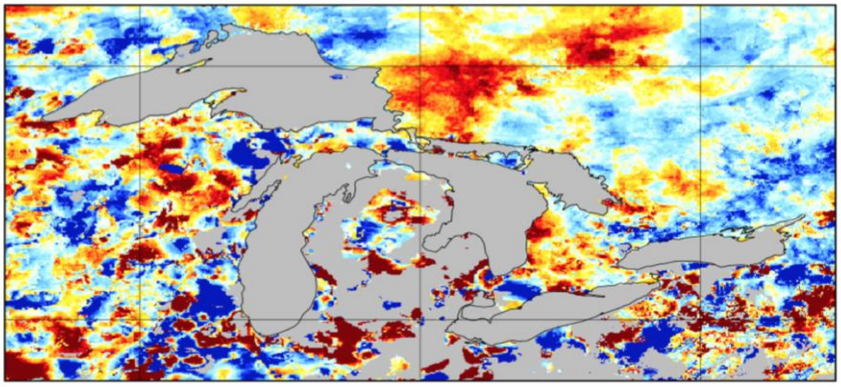

b)

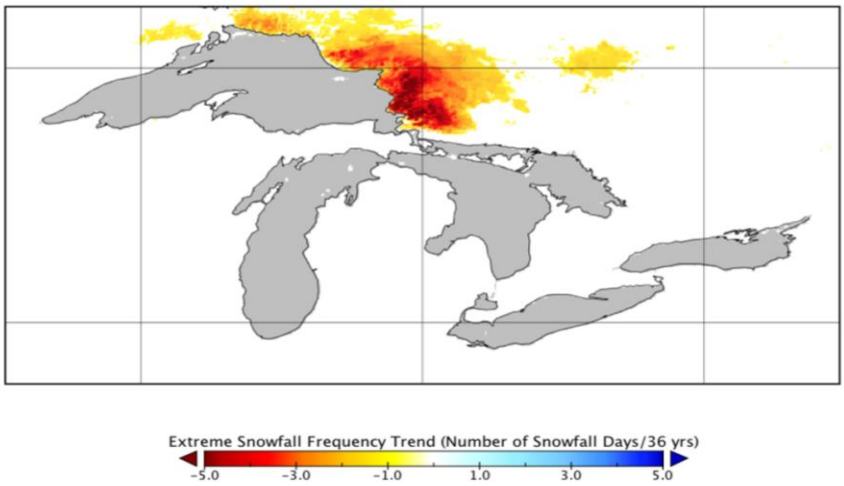

c)

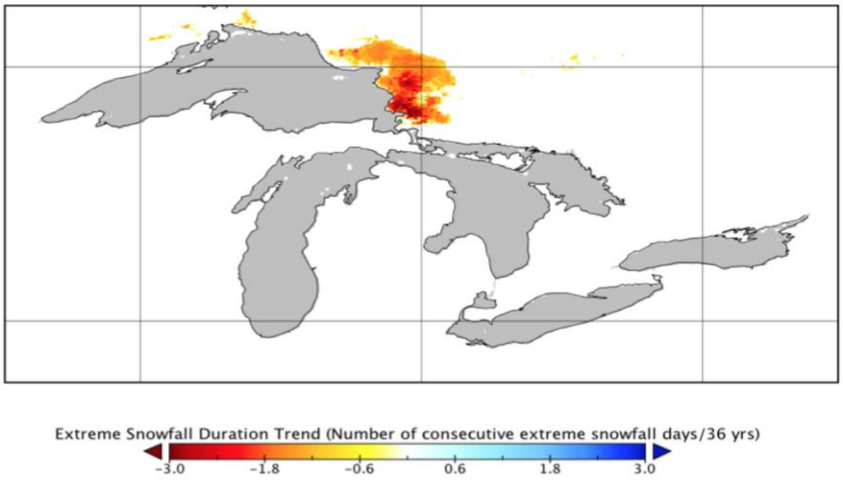

Figure 4.6: 1980 to 2015 trends in extreme snowfall a) intensity, b) frequency, and c) duration, for the month of December. Gray pixels represent grid cells with no trend computed because region contains some years with no extreme snowfall values.

a)

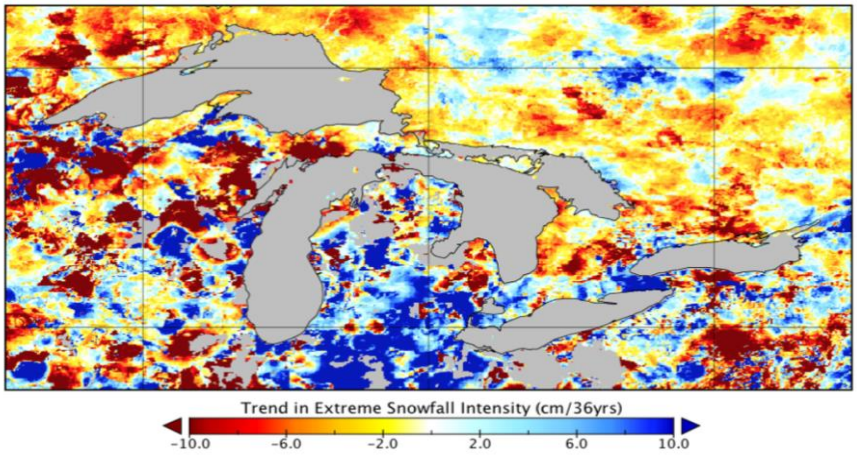

b)

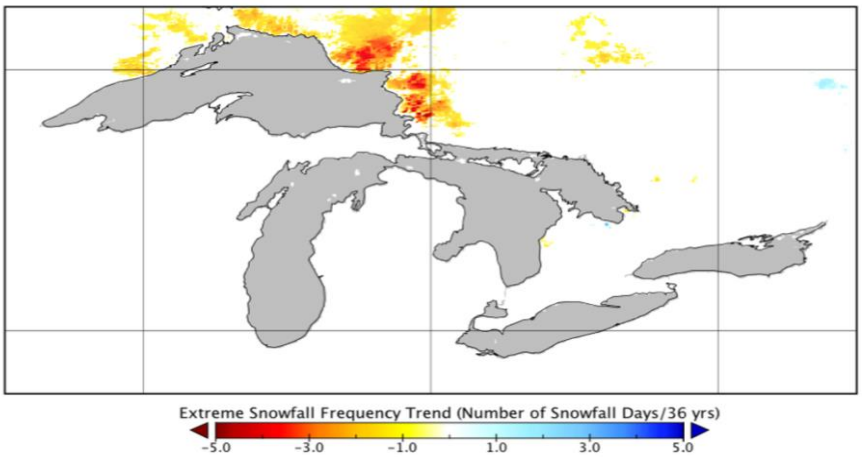

c)

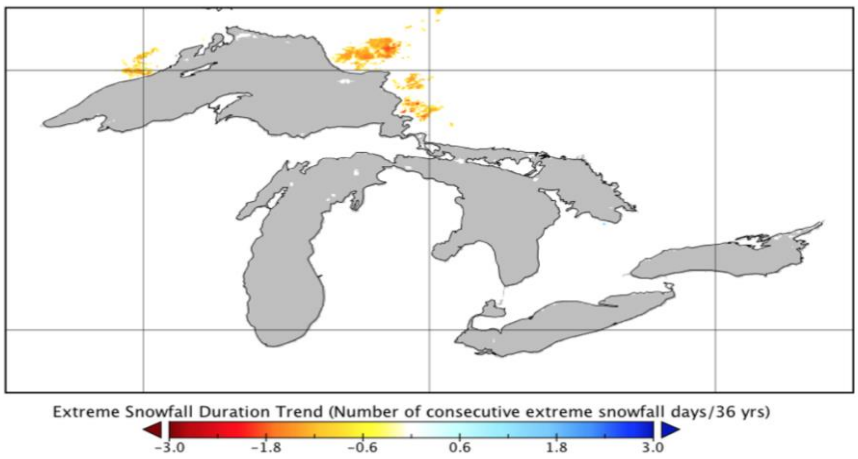

Figure 4.7: 1980 to 2015 trends in extreme snowfall a) intensity, b) frequency, and c) duration, for the month of January. Gray pixels represent grid cells with no trend computed because region contains some years with no extreme snowfall values.

4.3.4.4 February and March

The month of February shows incoherent spatial positive and negative trends in extreme snowfall intensity for both snowbelts (Figure 4.8a). Extreme snowfall frequency results show a highly localized decrease for the Superior snowbelt (Figure 4.8b), while there are no changes in extreme snowfall duration, not shown. There are also no changes in frequency and duration for Lake Huron's snowbelt.

a)

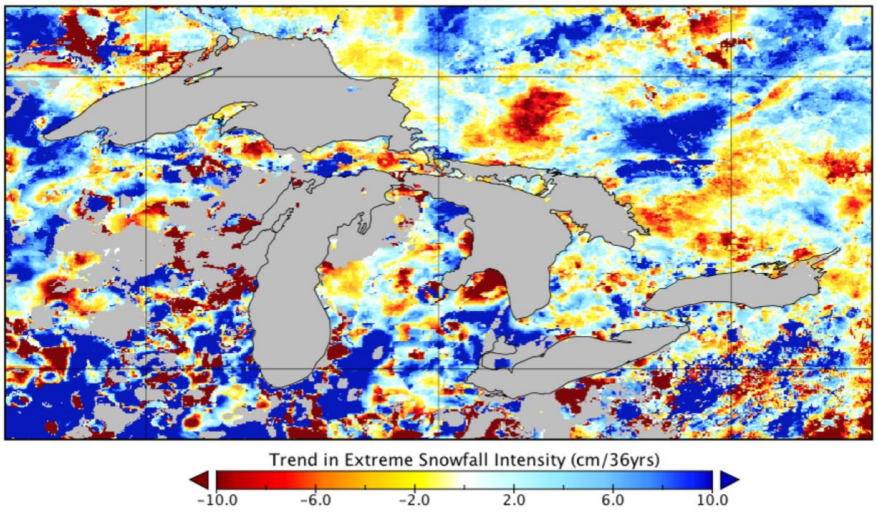

b)

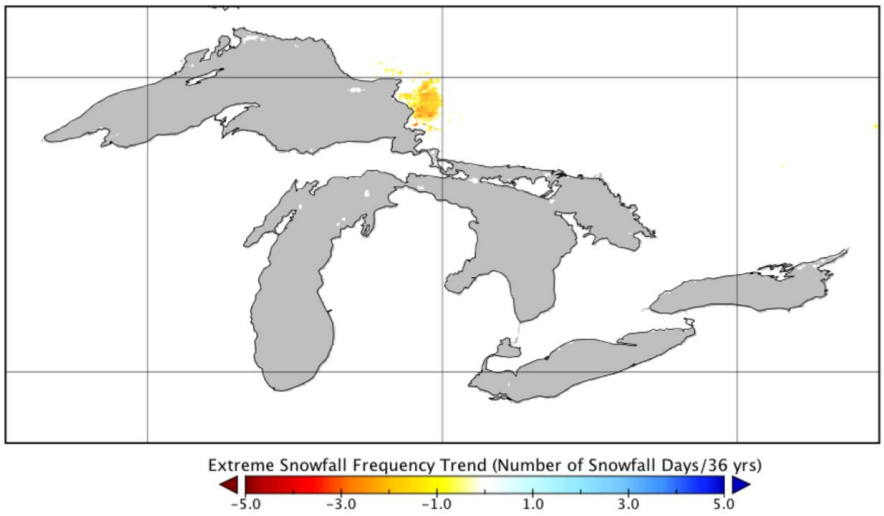

Figure 4.8: 1980 to 2015 trends in extreme snowfall a) intensity, and b) frequency, for the month of February. Gray pixels represent grid cells with no trend computed because region contains some years with no extreme snowfall values.

March exhibits a significant decrease in extreme snowfall intensity along the leeward shores of Lake Superior and farther inland, outside of the snowbelt zone (Figure 4.9). The geographic location and timing of this negative intensity trend suggest that the decrease in extreme snowfall intensity may not solely derive from LES, but perhaps as well from synoptic scale snowstorms. Frequency and duration in snowfall extremes exhibit no changes for this snowbelt, not shown. Lake Huron's snowbelt also shows negligible changes in snowfall extremes.

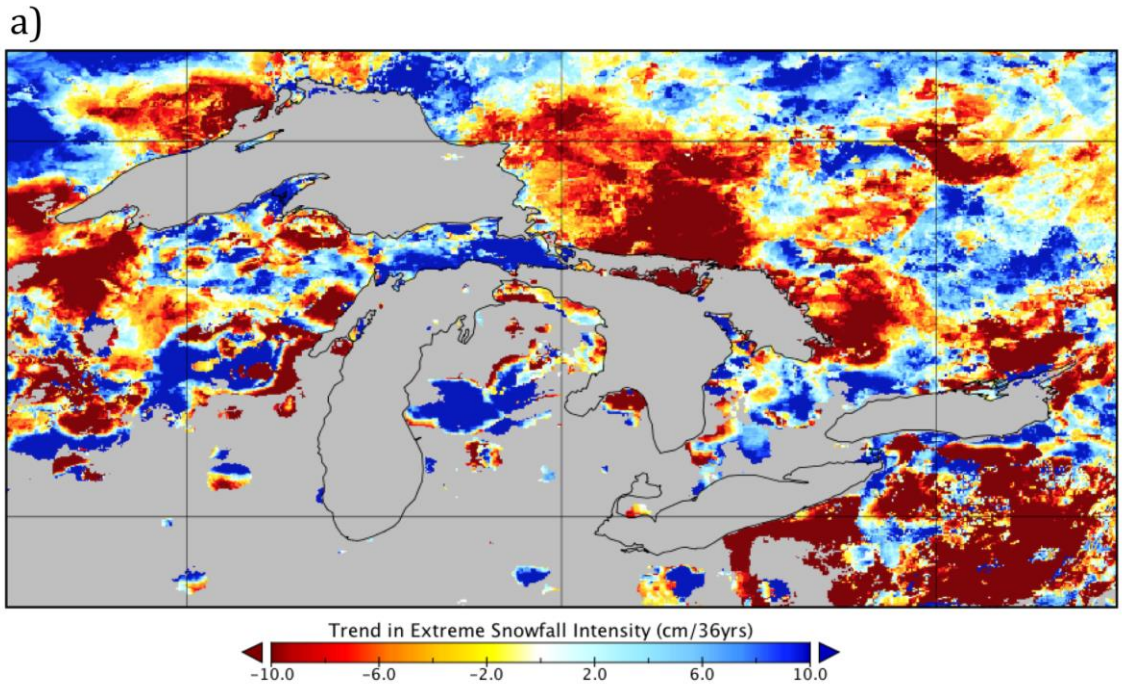

Figure 4.9: 1980 to 2015 trend in extreme snowfall intensity for the month of March. Gray pixels represent grid cells with no trend computed because region contains some years with no extreme snowfall values.

4.4 Discussion

4.4.1 Snowfall Intensity, Frequency, and Duration Extreme Values

The 36-year snowfall intensity, frequency, and duration, as determined by the daily 15 cm/day threshold are assessed over the Canadian domain of the GLB. The resultant

behavioural patterns in the spatial and temporal snowfall extremes suggest that they are predominantly attributed to lake-induced snowfall rather than extratropical storms. This is because the snowfall extremes exhibit similar temporal behaviours to that of LES. According to Eichenlaub (1979), these snowbelt regions experience high annual snowfall totals, exceeding 250 cm during the autumn and winter months due to LES. These spatial patterns in extreme snowfall are also seen for all cold months in this study, with the highest extreme snowfall intensities occurring during December and January. This is in agreement with the study by Braham and Dungey (1984), who suggest that LES within the GLB is most intense during December and January when there is maximum open water and cold Arctic air masses that facilitate the exchange of moisture and heat between the lake and atmosphere.

Results show a reduction in snowfall extremes in February and March. This is in agreement with they study by Notaro et al. (2013) who suggest that only approximately 14% of LES occurs downwind of Lakes Superior and Huron during February and March. This is attributed to the fact that ice cover is most extensive over the Great Lakes in February and March (Assel, 1990, 1999). As ice cover formation becomes more prominent, the dampening of the exchange in energy and moisture fluxes occurs, diminishing the production of snowfall (Niziol et al., 1995). Thus, lake ice is a regulator of LES (Brown and Duguay, 2010), and the change in ice cover fraction can also influence the spatial distribution and extent of LES.

From a spatial perspective, when compared to the rest of the Canadian GLB, the eastern shores of Lakes Superior and Huron exhibit the highest snowfall extremes, with a decrease in the snowfall extremes farther inland. The spatial patterns of the extreme snowfall resemble that of lake-induced snowfall near the leeward shores of Lakes Superior and Huron. LES does not fall very far inland and is dependent on wind shear at upper levels to determine the intensity and organization of snow bands. LES can produce the heaviest amounts of snow within 50 to 150 km of the leeward shore. Most moisture supplied from the lake to the upper atmosphere is removed through precipitation within this distance (Dewey, 1979; Rauber, 2005; Notaro et al., 2013).

Furthermore, in February, the spatial extent of extreme snowfall has substantially decreased for Lake Huron's snowbelt more so than Lake Superior's. In November, the onset of extreme snowfall has started to develop for Lake Superior's snowbelt but not for Lake Huron's. These differences in extreme snowfall behaviours are attributed to the surface-atmosphere features, affecting LES predictor variables, such as lake bathymetry and topography, thereby giving more credence that the resultant extremes in snowfall are mostly driven by lake-induced snowfall.

The Great Lakes have different geographic locations and lake morphometric properties, such as size, depth, and latitudinal extent that influence the onset of the unstable season and triggers LES along each snowbelt region. The unstable season refers to the period when the lake is warmer than the ambient air temperature. Lake Superior, for example, is larger, deeper, and farther north than the other Great Lakes and as a result, the warming season for Lake Superior begins relatively later in the spring and rarely ever attains the high LST values that are found for the lower Great Lakes. The prolonged unstable season over Lake Superior results in a longer LES season, lasting from mid November to early April (Notaro et al., 2013), indicative of what is being observed in the current study. Lake depth is also a controlling factor when considering ice freeze-up and ice break-up dates at high latitudes (Duguay et al., 2003; Duguay et al., 2006). In shallow lakes, LST rises faster than deeper lakes, allowing for strong evaporation to occur earlier in the thaw season (Rouse et al., 2005). In the fall and winter, shallower lakes permit rapid and early cooling of LST (Eichenlaub, 1979). These lakes also promote faster ice growth due to shorter thermal turnover rates, in the order of a week, as they store less heat. Thus, the spatiotemporal behaviours in snowfall extremes may vary among snowbelts because of lake bathymetry and other important factors.

Orographic lift is another factor that influences LES and can provide additional instability to an air parcel, affecting timing, and spatial distribution of precipitation (Campbell et al., 2016). As previously mentioned, orographic lift can add approximately 13 to 20 cm of mean annual snowfall for every 30 m increase in elevation. It can also double the snowfall

accumulation spawned from LES (Hill, 1979; Hartmann et al., 2013). The snowbelts of Lake Superior and the Tugg Hill Plateau produce the highest annual snowfall precipitation although the Tugg Hill Plateau is located farther south and experiences warmer air temperatures aloft than some of the other Great Lakes snowbelts (Eichenlaub, 1979). The plateau rises 500 m above the eastern shores of Lake Ontario, and even with its modest altitude, it can influence the distribution of lake effect precipitation off the long axis of the Lake Ontario. Mean annual snowfall in this area can exceed 700 cm on the western slope in Redfield, New York. This amount is more than twice the accumulation observed on the lowlands (Campbell et al., 2016).

Similar behaviours in extreme snowfall found in this study, for both Lake Superior's snowbelt and the Tugg Hill Plateau, further affirm that the extreme snowfall is produced by lake-induced processes and not solely by extratropical synoptic storms. If the extremes were mainly a product of large-scale frontal systems, then spatial distributions in snowfall extremes would follow climatologically persistent frontal boundaries and squall lines as opposed to snowbelt zones. The spatiotemporal snowfall extremes have been assessed for the 36-year duration, and the next step is to discuss whether there were any trends in these snowfall extremes.

4.4.2 Trends in Snowfall Extremes

Previous studies have shown an increase in the frequency of winter circulation patterns (between 1951 to 1982) such as 850 mb westerly winds, and super-adiabatic air temperature, which are both required for the development of LES and have given rise to an increase in LES events (Eichenlaub, 1970; Braham and Dungey, 1984; Norton and Bolsenga, 1993; Leathers and Ellis, 1996; Burnett et al., 2003). Comparatively, the last two decades of the 20th century and the first part of the 21st century show a significant decrease in monthly snowfall totals over the Canadian region of the Great Lakes Basin (Baijnath-Rodino et al., 2018). Recent trends in extreme snowfall over the Canadian domain of the Great Lakes are not as apparent and show less coherent spatiotemporal patterns. While overall, the results show a decrease in extreme snowfall intensity, frequency, and duration,

they are spatially inconsistent for each month and fluctuate between the snowbelts and non-lake-effect zones.

There are two apparent findings from this study. Firstly, both Canadian snowbelt zones exhibit different spatiotemporal trends in snowfall extremes. As discussed in the previous section, this is attributed to the geographic locations of the lakes, topography, lake bathymetry, and lake orientation that will influence fetch, ice cover, vertical temperature, and instability differently, thereby resulting in various spatial and temporal behaviours. It is therefore important to assess LES within each snowbelt separately, as the Laurentian Great Lakes and their locations have their own unique properties that influence LES and its ingredients such as lift, instability, and moisture.

Secondly, within each snowbelt, the spatiotemporal trends are not contiguously spatially coherent. The spatial variability within each snowbelt can result from local effects such as small scale surface-atmosphere meteorological factors, which include localized ice cover fraction, shifts in vertical and horizontal wind velocity in the lower PBL, and storm tracks from synoptic scale systems that lead to lake-enhanced snowfall. Furthermore, changes in the frequency and intensity of cold air outbreaks can affect the vertical temperature gradient and oscillation patterns, both of which influence the production of LES. Assessing trends in Arctic air outbreak is beyond the scope of this paper but worth examining in future lake effect and climate change studies.

4.5 Conclusion

The current study focused on examining the monthly cold season spatiotemporal extremes in snowfall intensity, frequency, and duration over the historical period of 1980 to 2015 for the Canadian GLB. The study has two folds; the first examines the 36-year period snowfall extremes, while the second explores the trends in snowfall extremes over the given period. In the first fold, extremes in snowfall intensity are derived by evaluating the 99^{th} percentile of all daily snowfall for each cold month of the 36-year period over the GLB domain. Based on the spatiotemporal results, a snowfall intensity of 15 cm/day was found as the ideal threshold to evaluate extremes in snowfall. Counting the number of snowfall days that

equaled or exceeded this extreme threshold value, the frequency of extreme snowfall days was determined. The maximum number of consecutive snowfall days that equaled or exceeded 15 cm/day represented the duration of extreme snowfall events. Spatiotemporal results show that the extremes in snowfall intensity, frequency, and duration are spatially coherent along the leeward shores of Lake Superior and Lake Huron. Results also indicate that snowfall extremes are most predominant for the months of December and January, suggesting that extremes in snowfall are attributed to lake effect processes rather than driven by extratropical storms.

In the second fold, there are two apparent findings in the spatiotemporal trends of snowfall extremes. Firstly, individual snowbelts behave differently when assessing spatiotemporal trends. Secondly, within each snowbelt, there are spatial variability and inconsistent snowfall patterns. The Great Lakes' topographical, geographical, and bathymetric features influence these results, in addition to, meso-scale and synoptic scale shifts in LES atmospheric predictor variables.

Baijnath-Rodino et al. (2018) noted that trends in monthly snowfall totals shifted from an increase in the first half of the 20th century to a decrease during the last part of the 20th and early 21st century. However, the current study suggests that not only are the totals in monthly snowfall decreasing along the Canadian leeward Shores of the Laurentian Great Lakes for the 1980 to 2015 period but, the extremes in snowfall intensity, frequency, and duration are also decreasing, albeit the spatial coherency is difficult to delineate.

Decrease in the intensity, frequency, and duration of extreme snowfall can result from influences in teleconnection patterns including El Niño-Southern Oscillation (ENSO), and North Atlantic Oscillation (NAO). These teleconnection patterns can influence Arctic air outbreaks and the trajectory of extratropical cyclones that can further affect the development of LES. For example, work by Wang et al. (2018) suggests that 1963-2017 ice cover over the Great Lakes responds linearly to Atlantic Multidecadal Oscillation (AMO) and quadratically to the Pacific Decadal Oscillation (PDO). As discussed previously, ice cover can influence the amount of energy into the PBL for producing LES.

Therefore, although Suriano and Leathers (2017) have investigated several synoptic scale patterns linked to lake-induced events, future work should continue to focus on examining the connection of oscillation patterns that influence the historical trends in snowfall extremes. Finally, as anthropogenic climate change continues to influence the Laurentian Great Lakes, conducting climate model validation studies are essential for testing model predictive capabilities in capturing future lake effect precipitation.

Chapter 5

Assessment of Coupled CRCM5-FLake on the Reproduction of Wintertime Lake-Induced Precipitation in the Great Lakes Basin

5.1 Introduction

This chapter is intended to fill the third gap, as described in Chapter 1. Lake-induced snowfall can produce un-expected whiteout snowsqualls and heavy snowfall accumulations in highly localized areas, thus warranting accurate lake-induced snowfall forecasts, specifically for the snowbelts in the Laurentian GLB. Although previous studies have evaluated LES processes using modelled simulations, many were conducted by employing coarse resolution global climate models (GCMs) and regional climate models (RCMs) that make it difficult to delineate meso-beta scale LES snow bands. For example, Notaro et al. (2013) used the 25 km RegCM4, with initial and lateral boundary conditions obtained from the NCEP-NCAR reanalysis (Kalnay et al., 1996). It was interactively coupled to the one-dimension Hostetler lake model to investigate historical (1976-2002) simulation snowfall across the GLB. This model was able to reproduce observed meso-beta features. Simulations showed the abundance of LES downwind of Lake Ontario and Lake Erie in response to cold surges associated with an anticyclone in the Central United States and a cyclone positioned over the northeastern United States. These results are consistent with observational studies by Niziol (1987), Leathers and Ellis (1996), and Ballentine et al. (1998). However, LES snowband dimensions can be extremely narrow, from a few km to approximately 50 km in width. These individual convective bands are difficult to capture and delineate in the 25 km RegCM4. Improved developments of a non-hydrostatic version of the RegCM are required for delineating highly localized snowbands. Experiments, analysing 45 km, 22 km, and 12 km resolutions using CRCM5 showed an increased skill in capturing LES and delineating snowbelts in the GLB at the 12 km resolution (Lucas-Picher et al., 2016). Therefore, this study evaluates the high resolution, 0.11° (12 km) CRCM5, interactively coupled to the one-dimensional Freshwater Lake model (FLake), to predict SWE and precipitation along the Canadian snowbelts of Lake Superior and Lake Huron.

In this paper, total monthly gridded SWE and wintertime precipitation were separately averaged over a 20-year (1995-2014) period and the root mean square difference (RMSD) and the mean bias difference (MBD) were computed between the simulated and gridded interpolated Daymet dataset. Furthermore, seven separate lake-induced snowfall events were examined to validate the model's performance in predicting the timing, location, and precipitation accumulation of the specific events for the snowbelts during the 2013-2014 (high) and 2011-2012 (low) ice seasons. An introduction describing the purpose of this study is provided in section 5.1. Data and methodology is provided in section 5.2 and outlines the multiple data sources and statistical approaches employed. The research findings and discussions of this study are presented in section 5.3. Lastly, section 5.4 provides a summary of the current study and discusses the limitations and potential for future related research.

5.2 Data and Methodology

Wintertime precipitation and SWE outputs were examined for the LES months of December and January (1995-2014). This time period was selected based on the availability of data. The lower time bound was limited by the availability of monthly LST data, with records starting from January 1995. The upper bound was limited by CRCM5 data, ending in December 2014. SWE and precipitation from CRCM5 were statistically compared to those from the Daymet gridded interpolated dataset. Key LES predictor variables were also compared between CRCM5 and additional datasets in order to understand the performance of the CRCM5 in predicting lake-induced snowfall. The predictor variables include 850 mb air temperature, LST, and ice cover concentration. Furthermore, model validation was also conducted on seven selected observed lake-induced events to determine whether the model could capture the timing, location, and precipitation accumulation of these events. In this section a description of the data sources employed are first explained, followed by an explanation of the model validation statistics.

5.2.1 Description of CRCM5

In this study, simulation outputs are produced from the latest version of CRCM, that is, Version 5. For several reasons the CRCM5 was selected for this lake-induced investigation study. It has a relatively high, 0.11° (12 km), spatial resolution that is capable of resolving narrower meso-beta snowsqualls, not possible by coarser RCMs. All CRCM5 simulations, by default, use 56 vertical levels (Lucas-Picher et al., 2016). Ten of these levels are below 850 mb and are important for capturing mesoscale convective features. The lateral boundary conditions are driven by the European Reanalysis (ERA) Interim from 1979 onwards (Dee et al., 2011) on a grid mesh of 0.75°. The ERA Interim fields that force CRCM5 at the lateral boundaries include the horizontal wind components, temperature, specific humidity, and surface pressure. These variables are available at 6-hour intervals with a linear temporal interpolation that is used for providing the CRCM5 with data at every time step (Lucas-Picher et al., 2016). One-hour outputs of CRCM5 data are available and will be used later in this this study when examining the seven lake-induced precipitation events.

The first version of CRCM was developed in 1991 at the Université du Québec à Montréal (UQAM). CRCM5 is based on the global numerical weather prediction model (GEM) of Environment and Climate Change Canada (ECCC), which employs the semi-Lagrangian transport and implicit marching scheme. It has a fully elastic non-hydrostatic formulation, and uses a vertical coordinate based on hydrostatic pressure (Laprise 1992; Yeh et al., 2002). In the CRCM5, the usual GEM land surface scheme is replaced by the Canadian land surface scheme (CLASS) Version 3.4 (Verseghy 2009) and then later by Version 3.5 that allows a mosaic representation of land surface types. While in NWP applications of GEM, LST and ice fraction are prescribed using the climatological Atmospheric Model Intercomparison Project (AMIP II), these prescriptions are inappropriate for climate change projections. Future climate projections require an interactive lake parameterization scheme (Martynov et al., 2012) so that accurate estimates of lake processes, including ice cover extent, can be used for improved predictions in climate studies (Scott et al., 2012). Thus, Martynov et al. (2012) tested and compared model simulations of CRCM5 interactively coupled to lake models. The CRCM5 has been coupled to the one-

dimensional freshwater lake model (FLake) (Mironov et al., 2010) and separately to the Hostetler model (HL) (Hostetler and Bartlein 1990; Hostetler, 1991 and 1995; Hostetler et al., 1993; Bates et al. 1993 and 1995). The CRCM5 simulations coupled to the two lake models are provided by UQAM – Canadian Network for Regional Climate and Weather Processes (CNRCWP) working group.

5.2.2 Description of FLake

The current study employs the CRCM5 model run coupled to the interactive Freshwater Lake model (FLake). FLake was chosen for this study because Martynov et al. (2010) showed that FLake outperformed other one-dimensional lake model predictions over the GLB. FLake is a one-dimensional column model with a two layered time varying temperature profile (Mironov, 2008; Mallard et al., 2014). The two layered water temperature profile has a mixed layer at the surface and a thermocline extending from the mixed layer to the bottom of the lake. A system of prognostic ordinary differential equations is solved to obtain the thermocline shape coefficient, temperature of active sediment layer, ice and snow temperatures, the surface and lower level water temperatures, and the mixed layer depth.

The mixed layer depth equation includes convective entrainment, wind driven mixing, and volumetric solar radiation absorption. The two-layer water temperature limits the lake model's performance for deep lakes because it does not resolve the hypolimnion layer between the thermocline and the lake bottom. A solution is to simulate a virtual bottom that is assigned between 40 and 60 m (Martynov et al., 2012; Mallard et al., 2014). In this CRCM5-FLake simulation, a maximum lake depth of 60 m is assigned for all lakes with depths greater than 60 m, such as the Laurentian Great Lakes (personal communication with Katja Winger 2017). Temperature changes in the deep abyssal zone is not appreciable, thus assigning a false bottom approximation produces satisfactory results (Gula and Peltier, 2012).

Furthermore, a snow module is included in FLake but is advised against using by the model developers until further improvement. However, a correction of the ice albedo, which takes

into account the influence of snow albedo is applied and is usually assigned a value between 0.2 and 0.3. Finally, FLake does not allow partial ice cover for each grid cell (Martynov et al., 2012). This could be a potential limitation in the analysis and will be elaborated on in the results and discussion section. FLake is well tested because it has been coupled to different NWPs and RCMs, such as studies conducted by Kourzeneva et al. (2008), Martynov et al. (2008), Mironov et al. (2010), Samuelsson et al. (2010) and has further been evaluated against other lake models, including studies by Martynov et al. (2010), Kheyrollah Pour et al. (2012), Semmler et al. (2012), and Mallard et al. (2014).

5.2.3 Description of Datasets Used for Validation

The CRCM5 modelled outputs were validated against several other datasets. These datasets comprise Daymet, NARR, the NOAA Great Lakes Ice Atlas and NOAA Coast Watch, and Environment and Climate Change Canada's (ECCC) historical data archives. Recall the description of the NARR dataset in Chapter 3. This paper uses the NARR dataset to also assess 850 mb air temperature over the GLB.

Gridded interpolated SWE and precipitation data were acquired from the Oak Ridge National Laboratory Daymet product. The description of Daymet was presented in the previous chapters. The Daymet product is employed because it offers a high spatial gridded resolution that is ideal for delineating localized precipitation bands indicative of lake effect snowfall events during the winter months. In this study, the Daymet data was up-scaled from its native grid to the coarser CRCM5, 0.11°, grid using bi-linear interpolation. This conversion enables spatial comparison between the gridded datasets. Refer to Chapter 3 for a description of the Daymet product used in this study.

Furthermore, SWE estimates are executed by employing a single calendar year of primary surface inputs, including daily maximum and minimum temperature, and daily total precipitation. Because higher latitude snow packs are normally underway at the beginning of the calendar year, the SWE algorithm uses data from a single calendar year to make a two year sequence of temperature and precipitation that predicts the evolution of the snowpack. This provides an estimate of the snowpack at day 365 as an initial condition for

the January 1st time step. However, because this approach ignores the dependence of January 1st snowpack on the preceding calendar year's temperature and precipitation conditions, it may generate potential biases in mid-season snowpack that can propagate to biases in late season timing of snowmelt. Additional information can be found at: https://daac.ornl.gov/DAYMET/guides/Daymet_V3_CFMosaics.html.

These limitations were considered when evaluating the performance of the CRCM5 with the Daymet data. This is why additional comparisons of snowfall were conducted by using doppler radar data, discussed later. Although, other SWE products are available, either the spatial resolution is too coarse to delineate snowfall within the relatively narrow snowbelt regions, or the temporal coverage is too short for the purposes of this study, examples include, Canadian Sea Ice Evolution (CanSISE) observation Version 2 and Snow Data Assimilation System (SNODAS) data product Version 2, respectively. Thus, for the purposes of this study, SWE generated by Daymet was the best option.

5.2.3.1 NOAA Ice Atlas and Coast Watch

Two data sources were used to provide the most comprehensive ice cover data. The electronic atlas of Great Lakes ice cover provided data for the years 1973 to 2005 and is available by NOAA Great Lakes Environmental Research Laboratory (GLERL). NOAA provides composite ice charts, which are a blend of observations from ships, shore stations, aircraft, and satellites to estimate ice cover data for the entire Great Lakes. The ice charts were digitized and made available at https://www.glerl.noaa.gov/data/ice/atlas/index.html.

Also, NOAA GLERL Coast Watch provides observed lake-wide averaged monthly mean LSTs and ice cover from 2008 to present. Coast Watch is a NOAA program that delivers environmental products and data in near-real time observations of the Great Lakes using three main satellite observations. NOAA'S Advanced Very High Resolution Radiometer satellite (AVHRR) provides 33 enhanced digital images of satellite-derived surface temperature, visible and near infra-red reflectance, brightness temperature, cloud masks, and satellite solar zenith angle data. The Geostationary Operation Environment Satellite (GOES) provides near-infrared, and water vapor data. Finally, the Moderate Resolution

Imaging Spectroradiometer (MODIS) satellite provides true colour 250 m resolution imagery of each Great Lake. Furthermore, in-situ measurements and modelled data, such as, marine meteorological observations, buoy from NOAA'S National Ocean Service, and Great Lakes Surface Environmental Analysis (GLSEA) composite charts, are acquired, produced, stored, and made available to the Great Lakes Coast Watch users. Further details are available at https://coastwatch.glerl.noaa.gov/overview/cw-overview.html.

Because the observed ice cover data was acquired from the electronic atlas of Great Lakes from 1973 to 2005 and then from NOAA GLERL Coast Watch from 2008 to present, the observational cold season of 2005/06 to 2007/08 are not available. However, this does not pose an issue, as the study focuses on in the inter-annual variability as opposed to climatic trends. Furthermore, the focus was to capture years of high and low ice cover concentrations and LST to determine whether the model was able to reproduce some of these annual observations. It is also acknowledged that CIS has a complete temporal coverage of monthly total accumulated ice cover. However, CRCM5 data comprises monthly mean ice cover. Therefore, to make ice cover comparisons consistent between CRCM5 and observations, the NOAA GLERL datasets were used because they also provide monthly mean ice cover.

5.2.3.2 Radar and Weather Station Data from ECCC

Specific lake-induced snowfall events were analysed by identifying observational data from ECCC's historical archive data, found at the National Climate Data and Information Archive, http://climate.weather.gc.ca. Historical ground-based weather observation stations and radar imagery were used to identify the location, duration, and precipitation accumulation of observed lake-induced events that were compared against model predictions. The weather observation stations provide the daily total precipitation in millimeters for the specified location observed. The daily total precipitation acquired from ECCC is defined as the sum of total rainfall and water equivalent of total snowfall in millimeters observed at the location (ECCC, 2018). In addition to the weather stations, a network of ground-based weather radars, which have a detection range of 250 km radius and a Doppler range of 120 km, were also used to determine the events. For cities analysed

along Lake Superior's snowbelt, the Montreal River (near Sault Ste. Marie) radar was utilized. For cities along Lake Huron's snowbelt, either King City (near Toronto), or Exeter (near London Ontario) radar was employed. The two ECCC sources, which are the ground observation stations and the radar networks, were applied in unison for identifying lake-induced snowfall in order to reduce common radar analysis errors such as overshooting beams and virga detection. Table 5.1 lists the cities and their associated weather station coordinates used for acquiring observed precipitation accumulations; snowbelts; observation radar; and grid cells for obtaining the predicted precipitation accumulation.

Table 5.1: Description of the cities and their associated weather station coordinates, snowbelt, radar, and modelled grid cell coordinates.

City	Weather Station Coordinates	Snowbelt	Radar	CRCM5 Grid Cell Location
Barrie	44.39, -79.74	Huron-Georgian Bay	King City	X=357 Y=281
Sault Ste. Marie	46.39, -84.5	Superior	Montreal River	X=357 Y=281
Wawa	47.9, -84.78	Superior	Montreal River	X =377 Y =308
Wiarton	44.75, -81.11	Huron-Georgian Bay	Exeter	X =385 Y=175

5.2.4 Assessment of Model Performance

The study regions of interest focused on the Canadian snowbelts of Lakes Superior and Huron. In order to delineate whether the model captures LES for the two snowbelt regions, gridded SWE and total precipitation were analysed for the entire Laurentian GLB within the coordinates of 94W, 74W, 40N, and 50N. SWE and precipitation were analysed by computing the monthly mean SWE and monthly precipitation totals for December and January (separately) for each of the 20 years (1995-2014). Statistical indices were employed followed by analyses of selected lake-induced events.

5.2.4.1 Statistical Validations

Three statistical indices of model performance were employed over the 20-year period and include, the 20-year SWE and precipitation averages for both CRCM5 and Daymet. The RMSD and MBD were computed. The 20-year averages were calculated for the monthly mean SWE and total precipitation for December and separately for January.

The RMSD was also computed for December and January and indicates the magnitude of the average difference, Equation (5.1). Additionally, RMSD was calculated for each grid cell within the GLB. Similarly, MBD is analysed, and given in equation (5.2). MBD describes the direction of the error bias; for example, a negative bias suggests that the model simulation under-estimates the prediction when compared to the observed output (Chow et al., 2006). In equations 5.1 and 5.2, pr represents the predicted value, o represents the observed value, and n is the number of data values used.

$$\text{RMSD} = \sqrt{\frac{\sum_{n=1}^{20}(pr-o)^2}{n}} \qquad (5.1)$$

$$\text{MBD} = \frac{\sum_{n=1}^{20}(pr-o)}{n} \qquad (5.2)$$

In order to understand the predictive performance of the model in capturing SWE and wintertime precipitation, 20-year time series were analysed for LES predictor variables followed by an examination of their RMSD and MBD. Monthly means of each predictor variable were computed separately for December and January for each year between 1995 and 2014. Table 5.2 shows the list of variables along with their temporal range and sources, which will be discussed in the results section.

Table 5.2: List of datasets with associated variables, sources and temporal availability used in this study.

Dataset	Temporal Availability	Variables	Source
CRCM5	January 1980 – December 2014	• SWE • Precipitation • Mixed layer depth (LST) • Ice cover • 850 mb air temperature	Université du Québec à Montréal
Daymet Version 3	January 1980 – December 2014	• SWE • Precipitation	https://daac.ornl.gov/DAYMET/guides/Daymet_V3_CFMosaics.html#revisions
NARR	January 1979 – December 2014	• 850 mb air temperature	https://www.esrl.noaa.gov/psd/data/gridded/data.narr.pressure.html
NOAA Coast Watch	November 1994 – December 2014	• LST	https://coastwatch.glerl.noaa.gov
NOAA Coast Watch	December 2008 – March 2014	• Ice cover concentration	https://coastwatch.glerl.noaa.gov
NOAA Great Lakes Ice Atlas	December 1973 – December 2005	• Ice cover concentration	https://www.glerl.noaa.gov/data/ice/atlas/daily_ice_cover/daily_averages/dailyave.html https://www.glerl.noaa.gov/pubs/tech_reports/glerl-135/Appendix2/DailyLakeAverages/
Historical Weather Radar	2007 – 2014	• Snowfall rate	http://climate.weather.gc.ca
Historical Weather Station Observations	2011 – 2014	• Precipitation accumulation	http://climate.weather.gc.ca/historical_data/search_historic_data_e.html

5.2.4.2 Assessment of Lake-Induced Snowfall Events

Further model assessments on predicting lake-induced snowfall were conducted by determining whether the model could capture the timing, location, and precipitation accumulation of selected events for the Lake Superior and Lake Huron snowbelt regions.

The selected events were narrowed down by snowfall that either occurred along Lakes Superior or Huron's snowbelt, during the LES months of December or January, and during years of either low or high ice season. This is because ice cover is a determining variable in producing LES. In total, seven events were analysed using four cities, two that represent the Superior snowbelt, Wawa and Sault Ste. Marie, and two that represent the Huron Georgian-Bay snowbelt, Barrie and Wiarton. Observations were limited to four cities and two LES seasons in order to reduce additional influences in LES predictions, such as microclimate influences, differences in station data gathering techniques, and climatic seasonal variations. These restrictions maintained a sense of consistency when comparing the model's performance in the different events.

Lake-induced snowfall events were determined when parallel snowsquall lines were observed, from radar images, along the leeward shores of Lakes Superior and Lake Huron Georgian-Bay and only precipitated approximately 100 km inland. If wide spread precipitation was noticed farther inland, this would not be considered a lake effect event. However, if localized squall lines developed after wide spread precipitation moved through the region, this was an indication of lake-enhanced precipitation and was considered as a lake-induced precipitation event.

When available extreme lake-induced snowfall events were selected for these analyses. Extreme daily precipitation accumulations were retrieved, providing that observed snowfall were ≥ 15 cm/ day (Baijnath-Rodino and Duguay, in review) or, if the equivalent liquid amount of 10 mm/day was recorded. The 10 mm liquid equivalent amount is determined by assuming that across the GLB, from December through February, the snow liquid ratio (SLR) is approximately 15:1 inches (Baxter et al., 2005), or, 38.1 cm of snow to 25.4 mm of water, thus a 15 cm snowfall would equal 10 mm of liquid water equivalent.

Apart from accumulation, timing was also documented by recording how long an event occurred in a particular location. The predicted precipitation accumulation amounts were best captured by determining the grid cell where the observed city was located and aggregating its hourly precipitation value within the day it occurred, starting at 0000 and

ending at 2300. The CRCM5 hourly snowfall prediction of the duration, location, and accumulation were compared against the observed events and analysed in the results and discussion section.

5.3 Results and Discussion

5.3.1 SWE and Precipitation

Model validation was first carried out by comparing SWE outputs. Figure 5.1 a and b show the averaged 1995 to 2014 December SWE totals for CRCM5 and Daymet, respectively. The spatial results indicate a predominant discrepancy in simulated SWE along the Canadian leeward shores of Lakes Superior and Huron. Higher Daymet SWE averages, of approximately 60 mm, are seen along Lake's Superior's snowbelt, whereas CRCM5 values, closer to 40 mm are predicted. Heavier Daymet SWE averages of 40 mm are also seen along Lake Huron's snowbelt, in contrast to values of approximately 20 mm shown in the CRCM5. RMSD values are upwards of 30 mm predominantly along both snowbelts (Figure 5.1c). MBD indicates negative bias upwards of 20 mm along both snowbelts, indicating that the model is under-predicting SWE along the Canadian leeward shores (Figure 5.1d).

Similarly, Figure 5.2 presents the averaged 1995 to 2014 January SWE totals. Unlike the CRCM5 prediction in Figure 5.2a, higher amounts of averaged SWE, upwards of 100 mm, are shown for Daymet (Figure 5.2b) along the leeward shores of the two snowbelts. The RMSD value indicates values closer to 60 mm along both snowbelts (Figure 5.2c) and a higher SWE MBD of 50 mm (Figure 5.2d). Thus, both LES months show a predominant under-estimation of simulated SWE along both Canadian snowbelts.

The resultant spatial discrepancy along the snowbelts suggests that lake effect snowfall and its processes may not be accurately predicted in the coupled Flake-CRCM5 simulation. Experiments conducted by Lucas-Picher et al. (2016) suggest that additional information can be extracted from CRCM5 when downscaling from a resolution of 0.44 to 0.11. The higher resolution CRCM5 improved the orography and allowed for higher accuracy of small-scale lake effect snow processes along the snowbelts. Despite the added value of the

higher resolution CRCM5, results of Figures 5.1 and 5.2 indicate that there is an under-estimation of simulated SWE, predominantly along the Canadian leeward shores of Lakes Superior and Huron. However, SWE is subject to snow metamorphosis processes, such as melting, re-freezing, densification, and re-distribution from surface winds. Therefore, to determine whether the model can accurately predict lake effect snowfall events, wintertime precipitation is also validated along with selected LES events.

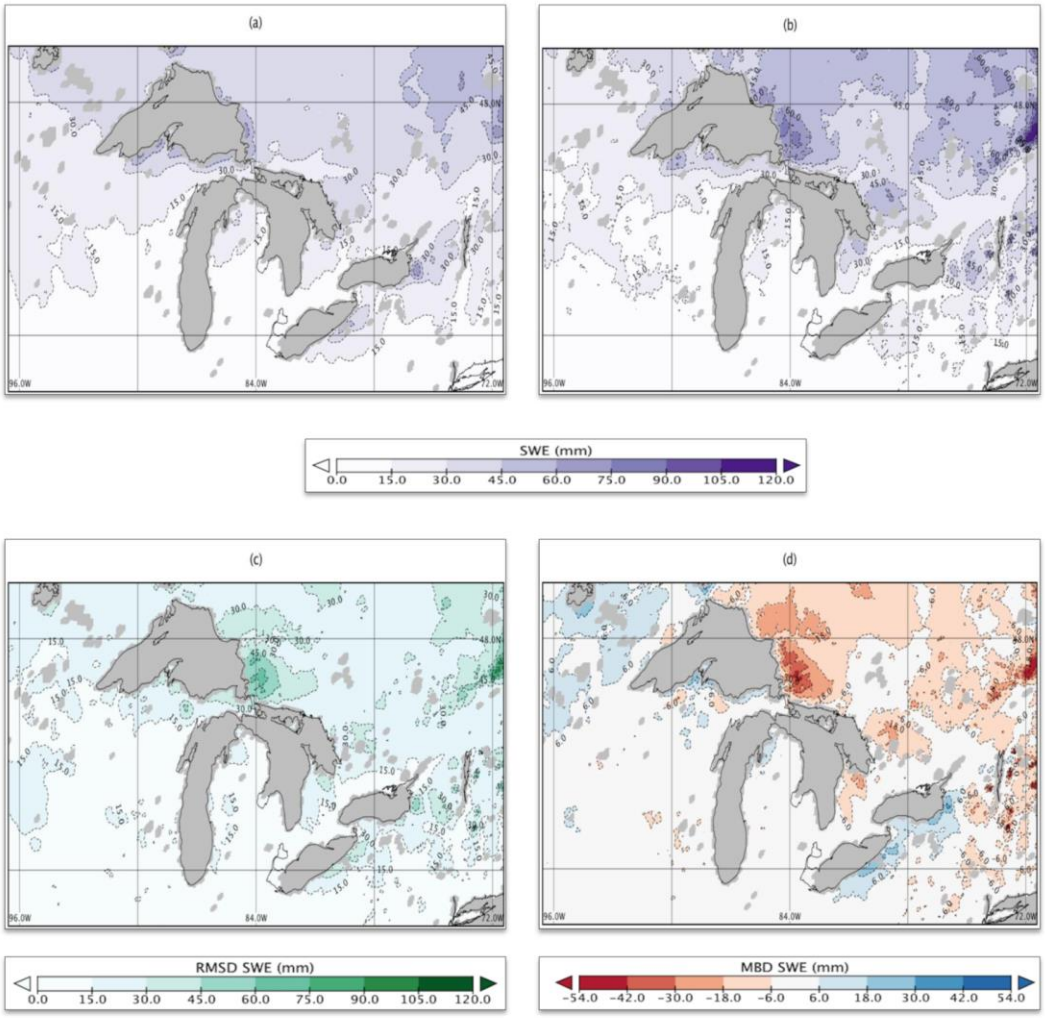

Figure 5.1: December mean SWE averaged over 1995 to 2014 for (a) CRCM5, (b) Daymet, (c) RMSD, and (d) MBD.

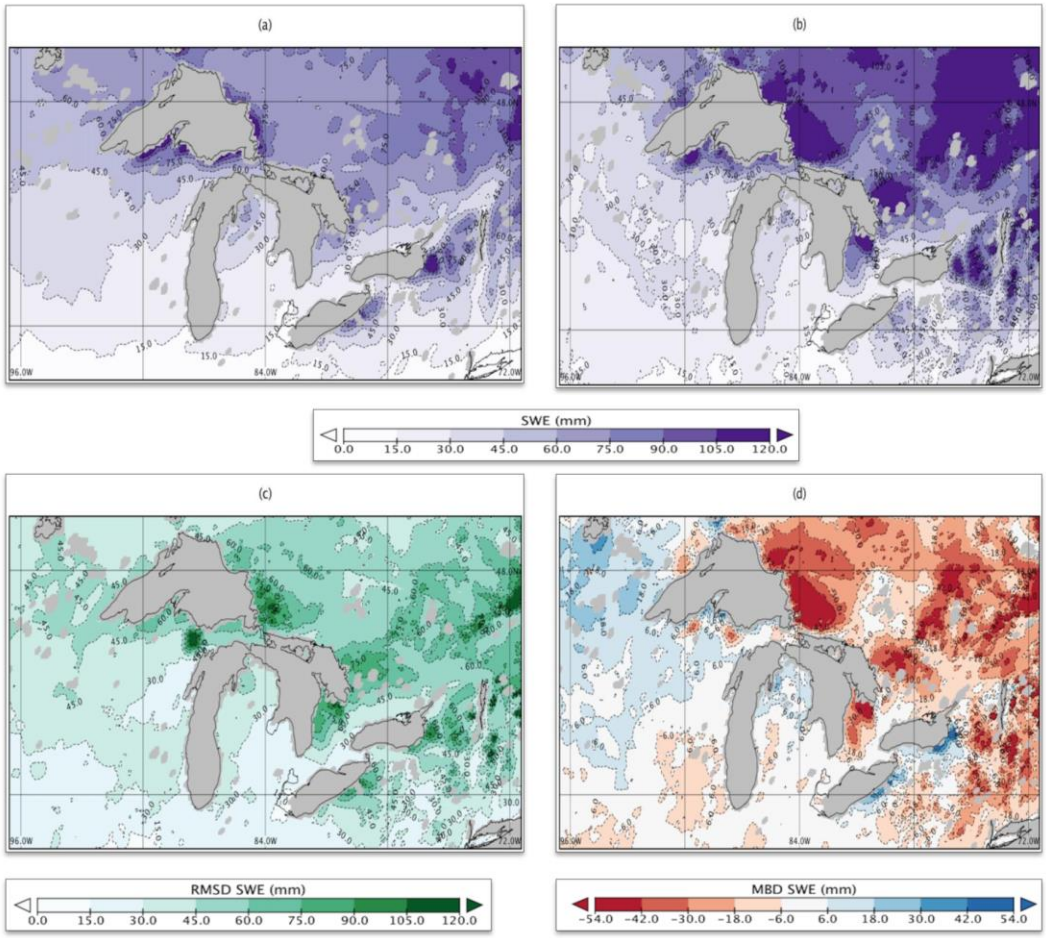

Figure 5.2: January mean SWE averaged over 1995 to 2014 for (a) CRCM5, (b) Daymet, (c) RMSD, and (d) MBD.

The averaged 1995 to 2014 December precipitation totals for CRCM5 and Daymet outputs are shown in Figures 5.3a and b, respectively. Although the CRCM5 captures higher amounts of precipitation along the snowbelts, relative to farther inland (Figure 5.3a) the location and amount are not accurately predicted. The RMSD shows values of approximately 40 mm along both snowbelts (Figure 5.3c). The MBD also indicates negative biases of approximately 30 mm along the southeastern shores of Lake Superior and 10 mm along Lake Huron's leeward shores (Figure 5.3d).

Furthermore, the January precipitation totals are computed and are presented in Figure 5.4. Relative to precipitation in December, results show less amounts of precipitation in January along Lake Superior's snowbelt (Figures 5.4a and b), respectively. The RMSD is relatively

low along Lake Superior's snowbelt (Figure 5.4c) compared to a higher RMSD values of 40 mm for Lake Huron's snowbelt. Figure 5.4d shows the MBD values, which are predominantly negatively biased along the leeward shores of Lake Huron, straddling the north and south shores of Georgian Bay.

Similar to the SWE results, precipitation validation indicates that the CRCM5 also under-estimates wintertime precipitation. The results, showing the location and accumulation discrepancy in wintertime precipitation along the Canadian leeward shores of Lake Superior and Lake Huron, further reinforce that the CRCM5 may not fully capture lake effect snowfall and its surface-atmosphere processes.

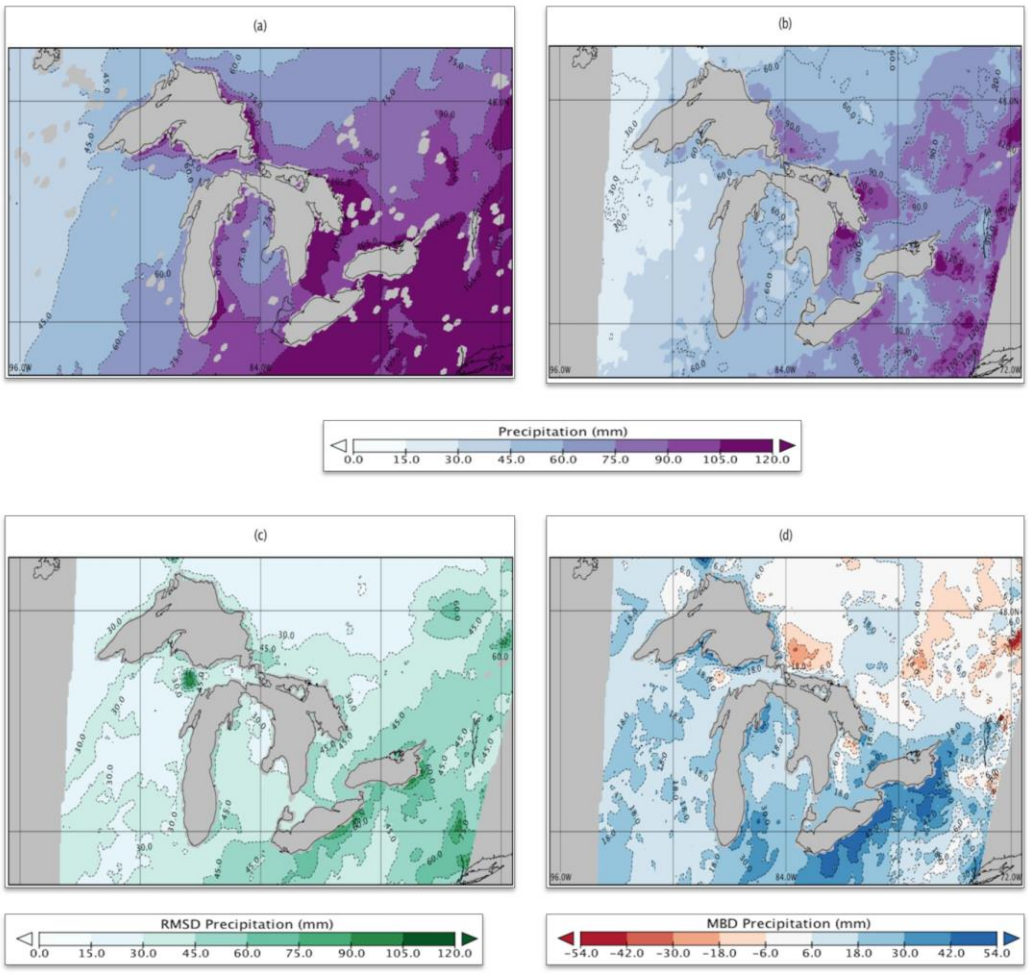

Figure 5.3: December total precipitation averaged over 1995 to 2014 for (a) CRCM5, (b) Daymet, (c) RMSD, and (d) MBD.

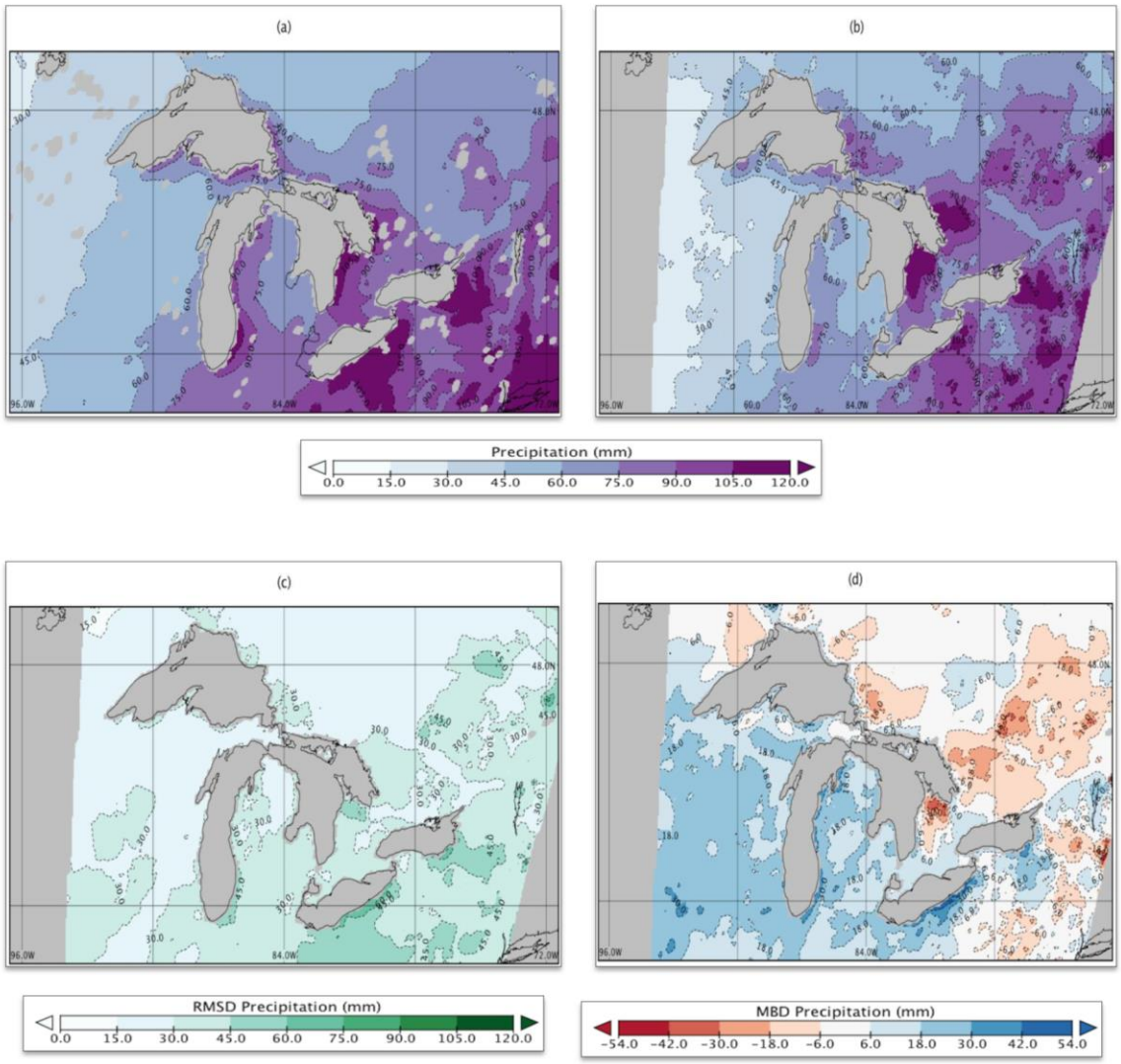

Figure 5.4: January total precipitation averaged over 1995 to 2014 for (a) CRCM5, (b) Daymet, (c) RMSD, and (d) MBD.

5.3.2 Assessment of Lake-Induced Snowfall Events

To further evaluate the model's predictive performance in capturing lake-induced snowfall, seven separate events were documented and analysed. Events 1 through 4 were taken during the high ice season of 2013-2014, during the months of December or January, and located on either the Superior or Huron snowbelt. Events 5a and 5b through event 7 were similarly examined, but for the low ice season of 2011-2012. Figure 5.5 shows a timestamp of each simulated and observed event, 1 through 7.

The first event was documented for Wawa on January 28, 2014. Event 1 was observed as an extreme lake-enhanced snowfall event for the Lake Superior snowbelt. The synoptic system moved through the region prior to 0000 January 28 and dissipated around 1800 on January 29 with snowsqualls lasting approximately 42 hours. Observed squall bands moved from south, along Superior's snowbelt, to north, bringing 10.4 mm of precipitation to Wawa. The model simulation also predicted that event 1 started prior to January 28 0000 and dissipated approximately 45 hours later. The simulated hourly aggregated daily precipitation, taken from January 28 0000 to January 28 2300, only summed 0.3 mm within the model's grid cell. The model's timing of the LES event is similar to that of observations, however the accumulation of precipitation is grossly under-estimated. This could be attributed to the wind direction of the predicted snowsqualls. For example, while the observations recorded winds from a west-southwest direction, which advected squalls northeastward towards Wawa, the predicted squalls showed a southwesterly flow, advecting precipitation farther south away from Wawa. Figure 5.5, Event 1, shows the observation and simulation of the event, respectively, for January 28, 2014 at 2100 EST, and show the different directions of the squall band locations as they move onshore of Lake Superior's snowbelt. In conclusion, the model under-estimates the daily precipitation accumulation for this event; it also misses the location of the squall bands, but produces a similar onset of the event.

The second event was recorded for Barrie along Lake Huron's snowbelt on January 6, 2014. This event was observed as an extreme lake-enhanced snowfall. A synoptic scale system moved through the GLB from January 5 into the early morning of January 6 and snow squalls developed behind the synoptic system, ushering snow squalls to Barrie off of Georgian Bay with a northwesterly flow. The squalls started by 0700 January 6 to approximately 0700 on January 8 with a duration of about 48 hours. The observed daily precipitation in Barrie on January 6 was 19.0 mm, making this an extreme lake-induced snowfall event. In contrast, the model recorded no precipitation for Barrie on this day and did not capture the observed extreme event for this location. Nevertheless, the model was able to capture the trajectory and timing of the synoptic system that moved through the GLB, followed later by squalls. The model kept lingering precipitation bands in the Huron

snowbelt region while the radar shows these bands moving farther north as the wind profile switches to a southeasterly flow. Figure 5.5, Event 2 shows the observed and simulated LES event respectively for January 6, 2014 at 2300 EST. In conclusion, the daily accumulation associated with this extreme event was not captured by the model, but the timing and the general vicinity of the squall lines moving through the snowbelt were similar to that of observations.

The third LES event was recorded for Sault Ste. Marie, along Lake Superior's snowbelt on December 31, 2013. This observed extreme event was suggested to form from a weak Alberta Clipper that moved through the GLB from 0000 December 31, 2013 to 0900 January 1, 2014, bringing 13.8 mm of precipitation to Sault Ste. Marie. However, the model prediction of only 0.6 mm was recorded. Figure 5.5, Event 3, shows the timestamp of this event on December 31, 2013 at 1800 EST. The squall lines in the model are visibly difficult to delineate for the Sault Ste. Marie region. Despite the under-prediction in the daily precipitation accumulation, the model accurately predicted the onset, duration and the general location of the squalls.

The fourth event was observed at Wiarton along Lake Huron's snowbelt on December 11, 2013 and was considered a pure lake effect event. The radar shows persistent lake effect squalls moving through Wiarton and then advecting southward away from the city. Snowfall started prior to 0000 December 11, 2013 and ended at approximately 0800 on December 12. It brought 8.1 mm of precipitation to the city. The model, however, predicted only 2.5 mm for that day. The predicted onset time was similar to that of the observed, except the model had squalls lingering until 2100 December 13. The locations of the squalls were within the general snowbelt region as can be seen by Figure 5.5, Event 4, with the timestamp of December 11, 2013 at 1900 EST. Overall, only the location of this LES event was well captured. The duration was over predicted and the daily accumulation was under predicted.

Event five was a lake-enhanced system that affected both Lakes Superior and Huron's snowbelts on January 19, 2012. Event 5a was analysed for Sault Ste. Marie and the Lake

Superior's snowbelt while event 5b was analysed for Wiarton and corresponds to Lake Huron's snowbelt. A synoptic system moved through the GLB overnight into the morning of January 19 and behind it was lake-enhanced squalls that developed around 1100 towards Sault Ste. Marie and persisted into the morning of January 20. The cold front associated with this system then moved through Southern Ontario, bringing squalls to Lake Huron's snowbelt and the city of Wiarton. The timing of the system moving through Southern Ontario was delayed in the model and did not appear until later in the evening. Figure 5.5, Event 5 shows the observed snowfall over Southern Ontario at 1100 EST, while the model shows the precipitation still farther to the west of Southern Ontario at this time. Observed daily precipitation for Sault Ste. Marie, along Lake Superior's snowbelt, was 9.2 mm, but the model only predicted 2.7 mm. Furthermore, Wiarton's observed precipitation measurements, along Lake Huron's snowbelt, was 8.0 mm, however the model only predicted 4.7 mm. In conclusion, the model under-estimates the accumulated daily precipitation associated with this lake-enhanced system. The onset of the system is also delayed in the model; however, the general locations of the squalls are accurate.

The sixth event was observed as pure LES over Wawa for the Superior's snowbelt on December 10, 2011. The observed event started the evening of December 8 and ended the morning of December 10, bringing 3.6 mm of precipitation to the city. The model predicted earlier development of the squalls, starting overnight and into the early morning of December 8 and persisting until the night of December 10. The model predicted 4.9 mm of daily precipitation for December 10. In comparison to all the other selected events, this is the only event for which the model over predicted the accumulation. The model also over-estimated the duration of this event, but accurately captured the location of the observed squalls, Figure 5.5, Event 6, with timestamp of December 10, 2011 at 1000 EST.

Finally, event 7 was a lake-enhanced snowfall event for Barrie along Lake Huron's snowbelt on December 16, 2011. A synoptic system moved over the GLB on December 15 and, behind this system, snowsqualls developed over Georgian Bay. Squalls started in the early morning of December 16 and persisted until noon of December 17, producing 5.0 mm of precipitation. The model's estimated onset and duration of the event were accurately

depicted, but it did not record any daily precipitation accumulation for Barrie on December 16. However, the model was able to capture the previous day precipitation accumulation for a larger synoptic system that moved through the region. The squall locations in the model are farther south towards Owen Sound and the squalls are short lived (Figure 5.5) Event 7, with a timestamp of December 16, 2011 at 0800 EST.

Overall these analyses suggest that the model seems to accurately predict the timing and, to an extent, the location of the snowsqualls, but drastically under-estimates the daily precipitation associated with the lake-induced snowfall events. The model mostly captures the onset of snow squalls and synoptic systems moving through the region. However, the model seems to prolong the duration of the event, extending the duration of the overall event longer than what was observed.

The model captures the general locations of squall lines moving towards the observed snowbelts. However, specific localized squalls are difficult to delineate by the model, such as squalls that occurred in Barrie, along Lake Huron's snowbelt, or Wawa, along Lake Superior's snowbelt. This could be that the 0.11° resolution of the model was too coarse to represent the highly localized squall lines associated with some of these LES bands. Perhaps higher resolution models, at resolutions of only 2-km would better capture these highly localized bands since squall lines can be as narrow as 1-2 km. Furthermore, the model consistently under predicts precipitation accumulation, despite the month of the LES season, or the ice season, with the exception of one event. These results are in agreement with the previous results (recall Figures 5.3 and 5.4) that suggest that precipitation is significantly under-predicted along the snowbelt regions of both Lake Superior and Huron. Thus, reasons for the predominant negative bias in lake-induced precipitation accumulations are explored by examining key LES predictor variables.


PRECIP - Snow - 2014-01-28, 21:00 EST, 9/13
Hornepayne
Manitouwadge
Marathon
White River
Peterbell
Dubreuilville
Foleyet
Wawa
Chapleau
Sultan
Gogama
Mattagama
Ranger Lake
Marquette
Sault Ste. Marie
Elliot Lake
Blind River
Thessalon
St. Ignace
Gore Bay

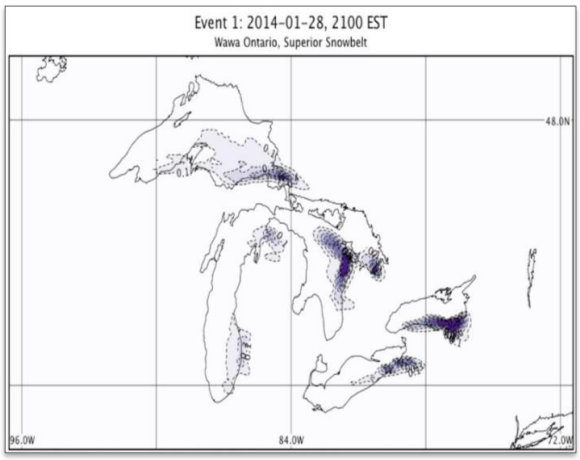
Event 1: 2014-01-28, 2100 EST
Wawa Ontario, Superior Snowbelt
48.0N
96.0W
84.0W
72.0W

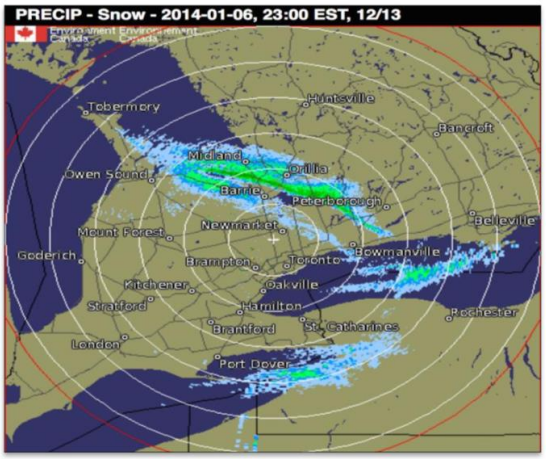
PRECIP - Snow - 2014-01-06, 23:00 EST, 12/13
Tobermory
Huntsville
Bancroft
Midland
Owen Sound
Orillia
Barrie
Peterborough
Belleville
Newmarket
Mount Forest
Goderich
Brampton
Toronto
Bowmanville
Kitchener
Oakville
Stratford
Hamilton
Rochester
Brantford
St. Catharines
London
Port Dover

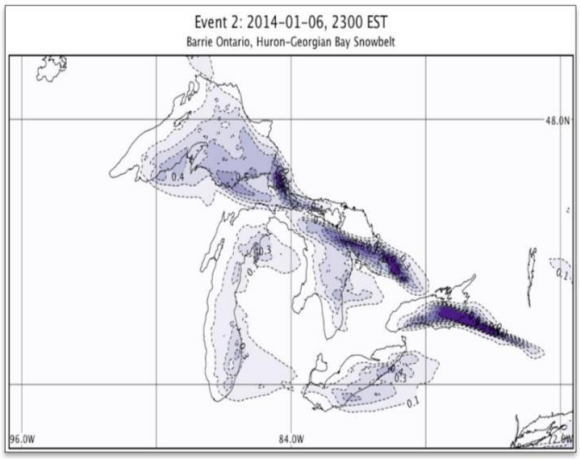
Event 2: 2014-01-06, 2300 EST
Barrie Ontario, Huron-Georgian Bay Snowbelt
48.0N
96.0W
84.0W
72.0W

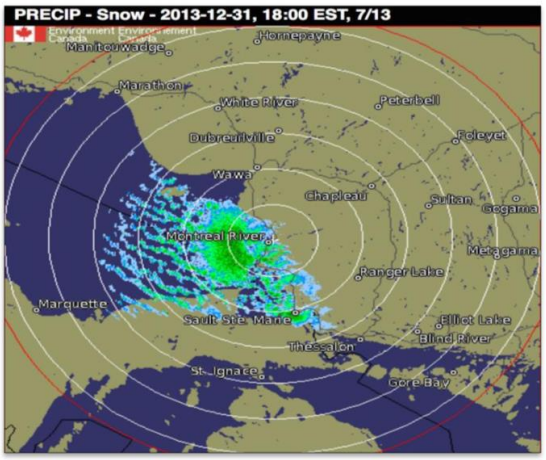
PRECIP - Snow - 2013-12-31, 18:00 EST, 7/13
Hornepayne
Manitouwadge
Marathon
White River
Peterbell
Dubreuilville
Foleyet
Wawa
Chapleau
Sultan
Gogama
Mattagama
Ranger Lake
Marquette
Sault Ste. Marie
Elliot Lake
Blind River
Thessalon
St. Ignace
Gore Bay

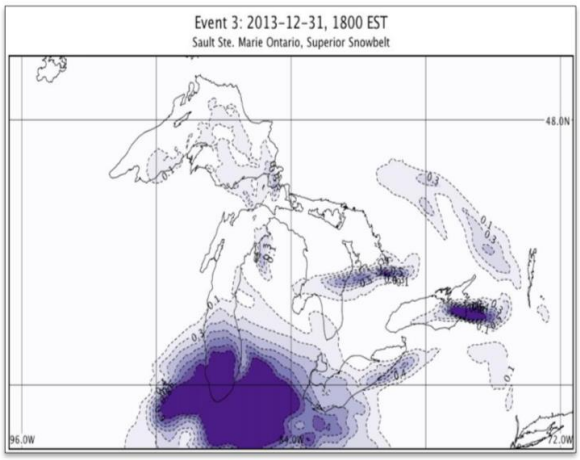
Event 3: 2013-12-31, 1800 EST
Sault Ste. Marie Ontario, Superior Snowbelt
48.0N
96.0W
84.0W
72.0W


PRECIP - Snow - 2013-12-11, 19:00 EST, 7/12
Environment Canada Environnement Canada
Tobermory
Owen Sound
Barrie
Kincardine
Newmarket
Mount Forest
Goderich
Listowel
Brampton
Toronto
Kitchener
Guelph
Grand Bend
Stratford
Hamilton
Sarnia
London
Brantford
St. Catharines
Port Colborne
St. Thomas
Port Dover
Windsor
Chatham
Leamington
Cleveland

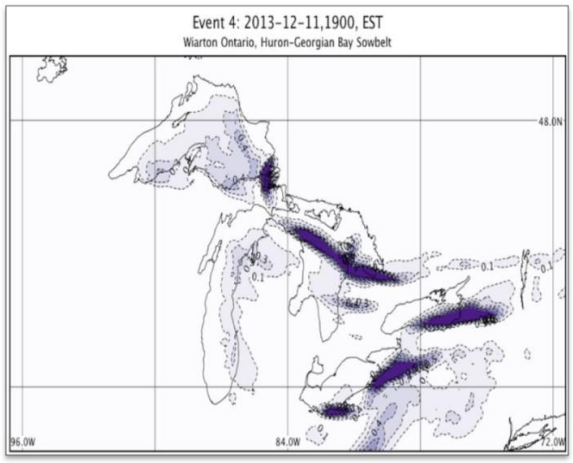
Event 4: 2013-12-11,1900, EST
Wiarton Ontario, Huron-Georgian Bay Sowbelt
48.0N
96.0W
84.0W
72.0W


PRECIP - Snow - 2012-01-19, 16:00 UTC, 12/13
Environment Canada Environnement Canada
100 KM
Timmins
Ottawa
Sudbury
Kingston
Dryden
Thunder Bay
Sault Ste. Marie
Orillia
Toronto
London
Windsor

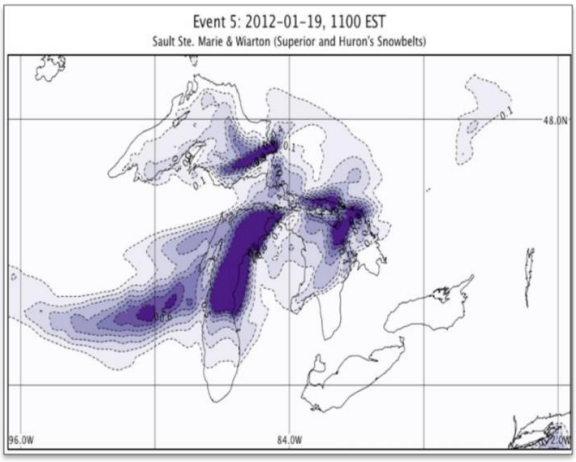
Event 5: 2012-01-19, 1100 EST
Sault Ste. Marie & Wiarton (Superior and Huron's Snowbelts)
48.0N
96.0W
84.0W


PRECIP - Snow - 2011-12-10, 10:00 EST, 11/13
Environment Canada Environnement Canada
Hornepayne
Manitouwadge
Marathon
White River
Peterbell
Dubreuilville
Foleyet
Wawa
Chapleau
Sultan
Gogama
Mattagama
Ranger Lake
Marquette
Sault Ste. Marie
Elliot Lake
Blind River
Thessalon
St. Ignace
Gore Bay

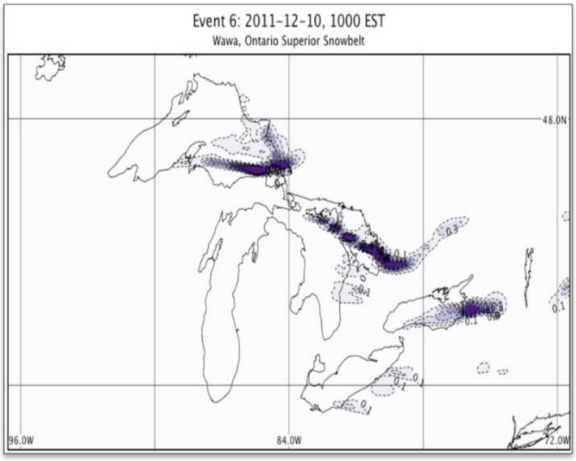
Event 6: 2011-12-10, 1000 EST
Wawa, Ontario Superior Snowbelt
48.0N
96.0W
84.0W

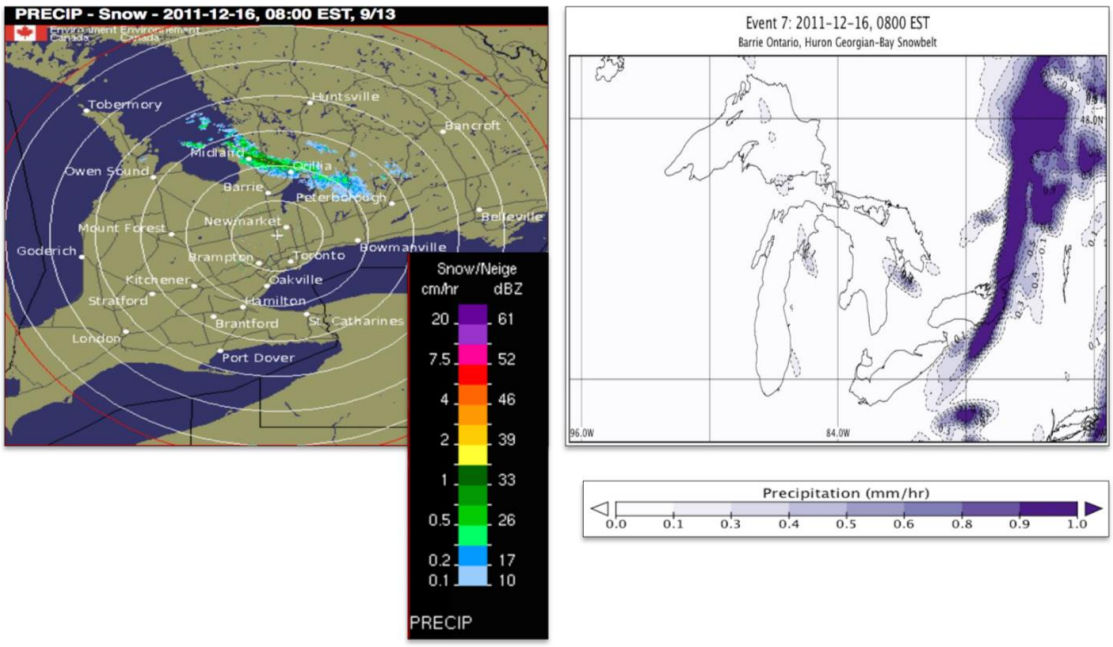

Figure 5.5: Lake-induced events 1 through 7 with radar observations (left) and CRCM5 predictions (right).

5.3.3 Atmospheric Predictor Variable

Key predictor variables, as suggested in previous literature, including Niziol et al. (1995), Cosgrove et al. (1996), Hamilton et al. (2006), Hartmann et al. (2013), and Notaro et al. (2013), Baijnath-Rodino et al. (2018), and Baijnath-Rodino and Duguay, (in review), are 850 mb air temperature, LSTs, and ice cover concentration. Temperature plays a multifaceted role in the development of LES by influencing precipitation type and vertical instability. Lake effect precipitation will usually fall as a solid state when temperatures at the 850 mb level are below freezing. The VTG, which is the difference between the LST and 850 mb temperature, is an indicator of instability in the planetary boundary layer. In meteorology, a VTG greater than 13 °C is a general indicator of an unstable lapse rate, which will induce moisture and energy fluxes into the lower PBL, inducing convection (Holroyd 1971; Niziol 1987; Theeuwes et al., 2010; and Hartman 2013). Thus, the 850 mb air temperature is an important feature that influences LES and is therefore warranted in this study.

In this paper, the CRCM5 and NARR outputs of 850 mb air temperature are represented on their native grids. This is because the NARR grid has a relatively coarse 32 km resolution and the CRCM5 would have to be up-scaled from 12 km, with the possibility of losing precise spatial information. The advantage of presenting 850 mb air temperature on its native grids allow the RCM to preserve high spatial details. Comparing modelled and reanalysis outputs on native grids were similarly employed by Lucas-Picher (2016).

Figure 5.6 compares averaged 1995 to 2014 mean December 850 mb air temperature from CRCM5 and reanalysis NARR outputs (Figures 5.6a, and b), respectively. The model output for December (Figure 5.6a) seems to be slightly warmer along the southwestern tip of Lake Superior and northern Lake Huron, where the 265 °K isotherm extends slightly farther north than the reanalysis output (Figure 5.6b). In Figures 5.6c, and 5.6d the same averaged 20-year duration is shown, but for January. Based on visual comparison, the CRCM5 captures well the 850 mb air temperature field over the GLB. The zonal isotherms are spatially aligned similarly between the CRCM5 and NARR.

The model also captures the colder southward air mass towards Lake Superior in January, (Figure 5.6c). Overall, there are no strong biases in the 850 mb air temperature between the CRCM5 and reanalysis for the months of December and January. This is, perhaps, expected as both of CRCM5 and the NARR are driven by observed atmospheric reanalysis data forced at the lateral boundaries by Era-Interim and NCEP, respectively. These results are in agreement with Martynov et al. (2013) who analysed averaged 1989 to 2008 predicted 2-m air temperature from CRCM5 coupled with the FLake model and found that the air temperature is generally reproduced over the whole annual cycle for the Great Lakes region. Evident from the current research, the 850 mb air temperature over the Great Lakes have minimal discrepancies and as a result, is not a factor that highly influences the modelled lake-induced snowfall biases. Other LES surface-atmosphere LES variables are thus explored to help determine the reasons for the aforementioned biases.

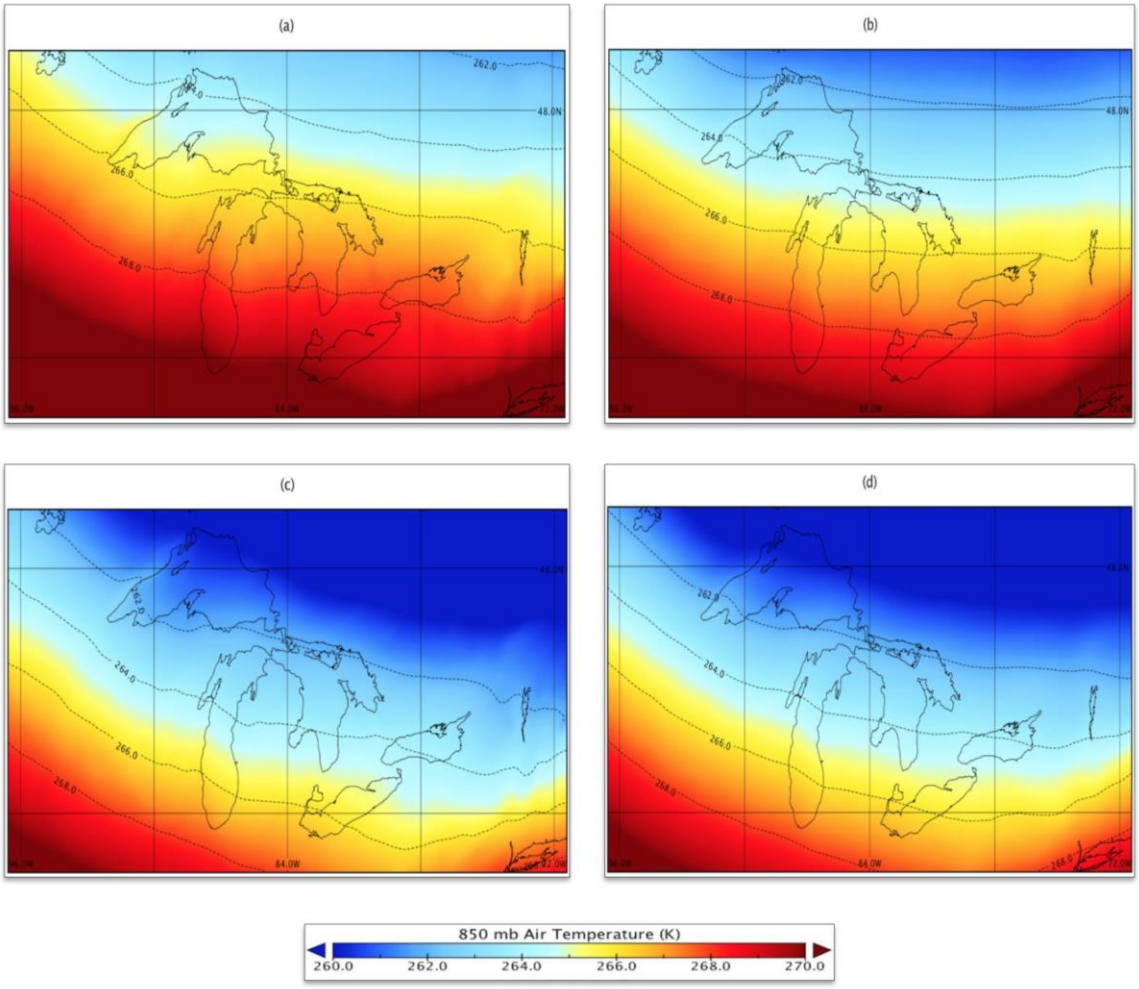

Figure 5.6: Monthly mean 850 mb air temperature averaged over 1995-2014, (a) CRCM5 December mean, (b) NARR December mean, (c) CRCM5 January mean, (d) NARR January mean.

5.3.4 Surface Predictor Variables

Twenty-year time series are plotted for monthly mean of lake-wide averaged LST and ice cover concentration for both observations and simulation. Figure 5.7 presents the time series for Lake Superior for the month of December. Figure 5.7a shows the averaged lake-wide LST. Results indicate that the CRCM5 captures a similar pattern of the observed inter-annual variability, with a peak LST in 1998 and a local minimum in 2008. Although the simulated LST follows that of the observed, the simulated LST is evidently warmer.

Table 5.3 shows that the RMSD of LST for Lake Superior in December is 2.13 and the MBD is 2.02, indicating that the RCM over-estimates the LST.

In Figure 5.7b, the lake-wide ice cover concentration is plotted. The simulated and observed inter-annual variability do not follow a similar pattern and show disagreement in peak ice cover years, from 1995 to 2004. For most years, the simulation shows lower ice cover concentrations than that of the observed, which could correspond to the warmer simulated LST temperatures. The RMSD is 1.10 with a negative MBD of 0.36, suggesting that the CRCM5 under-estimates ice cover (Table 5.3). The model's warmer LST and less ice cover over Lake Superior in December should, in theory, favour the production of LES along the leeward shores of Lake Superior. However, the 20-year averaged SWE and wintertime precipitation indicated a negative bias, recall Figures 5.1 and 5.3.

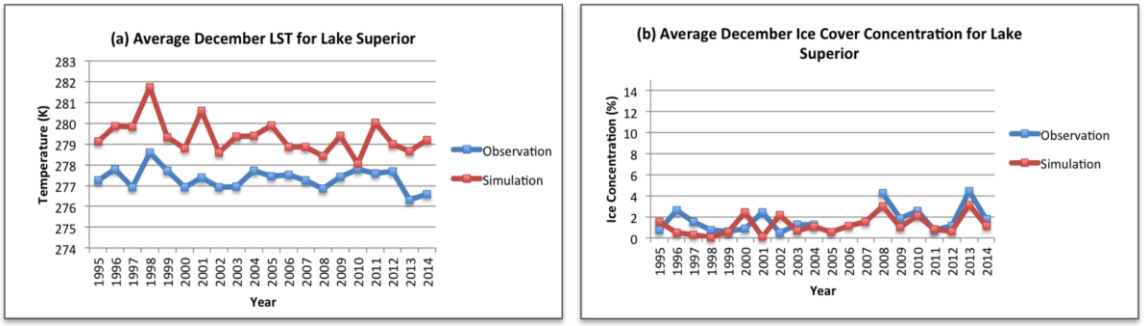

Figure 5.7: 1995 to 2014 time series of observed (blue) and simulated (red) December averaged (a) lake surface temperature and (b) ice cover concentration for Lake Superior.

Table 5.3. Statistical comparison of observed versus simulated outputs of December's LST and ice cover concentration, for Lake's Superior and Huron.

Variables	Root Mean Square Difference (RMSD)		Mean Bias Difference (MBD)	
December	Superior	Huron	Superior	Huron
LST	2.13	1.68	2.02	1.43
Ice Cover	1.10	5.63	-0.36	-3.73

Similarly, Figure 5.8 plots the 20-year December time series of LST (Figure 5.8a) and ice cover concentration (Figure 5.8b), respectively, for Lake Huron. Table 5.3 shows that the RMSD and MBD are both larger for Lake Superior's LST than Lake Huron's. However, there is a greater disagreement between the simulation and observation for Lake Huron's ice cover compared to that of Lake's Superior, indicating that the simulation under-estimates ice cover for Lake Huron more than Lake Superior.

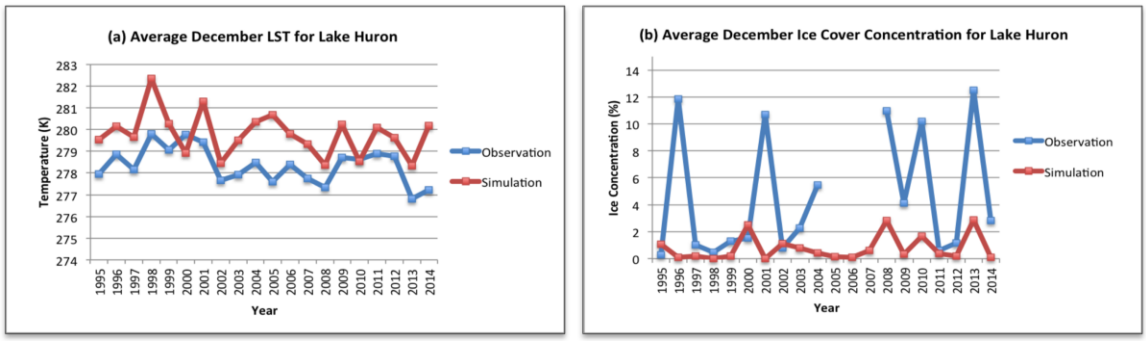

Figure 5.8: 1995 to 2014 time series of observed (blue) and simulated (red) December averaged (a) lake surface temperature and (b) ice cover concentration for Lake Huron.

Figure 5.9 shows January's LST and ice cover for Lake Superior (Figures 5.9a, and b), respectively. Results show that the inter-annual variability for simulated Lake Superior's LST and ice cover are slightly over-estimated in January (Table 5.4). Figure 5.10a shows the inter-annual variability in lake-wide LST for Lake Huron. There is a slight warmer bias in the model prediction for LST and an under-prediction in ice cover for Lake Huron. The biases in wintertime LST and ice cover are consistent with Martynov et al. (2012; 2013), who suggest that the FLake model over-estimates summertime temperatures for the Great Lakes, thereby, leaving lakes free of ice for a longer period, than that of observed, into the winter months and creating a warm wintertime bias. In the current study, for both lakes during both LES season, the model over predicts the LST. Ice cover predictions correspond to the warmer bias in the model's LST, by underestimating ice cover concentrations for both lakes, except for Lake Superior in January. Thus, the current results of the positive wintertime LST bias and negative ice cover bias, for the lakes, are in agreement with previous literature.

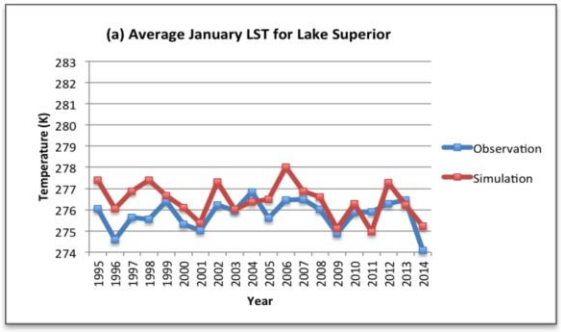

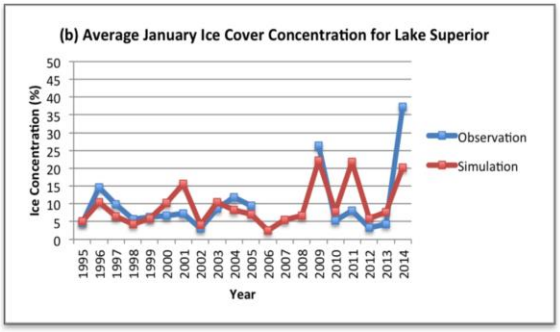

Figure 5.9: 1995 to 2014 time series of observed (blue) and simulated (red) January averaged (a) lake surface temperature and (b) ice cover concentration for Lake Superior.

Table 5.4: Statistical comparison of observed versus simulated outputs of January's LST and ice cover concentration, for Lake's Superior and Huron.

Variables	Root Mean Square Difference (RMSD)		Mean Bias Difference (MBD)	
January	**Superior**	**Huron**	**Superior**	**Huron**
LST	0.95	1.05	0.65	0.68
Ice Cover	6.22	11.94	0.05	-9.79

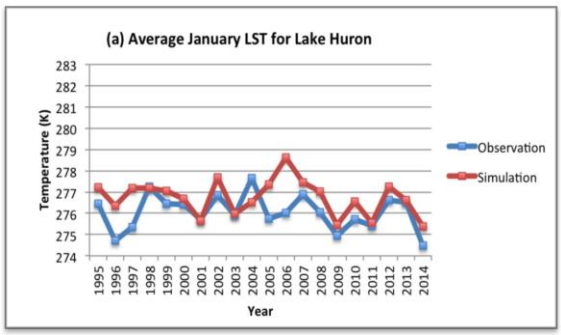

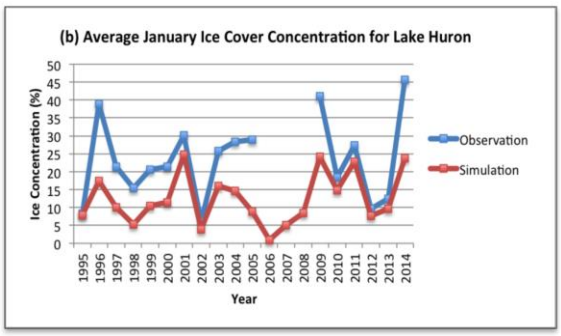

Figure 5.10: 1995 to 2014 time series of observed (blue) and simulated (red) January averaged (a) lake surface temperature and (b) ice cover concentration for Lake Huron.

Validation studies by Martynov et al. (2013) also suggest that precipitation rates are well represented by the CRCM5 over the whole Great Lakes domain in the summertime but is over-estimated during the autumn and winter months for the 1989 to 2008 period, and that the over-estimation in precipitation can be attributed to enhanced evaporation from the

overlying warm, ice-free surface of the Great Lakes. While this may be the case for the overall GLB, the current study suggests that precipitation is under-estimated for the Canadian snowbelts of Lakes Superior and Huron between 1995-2014.

Wright et al. (2013) assessed the impacts of both LST and ice in the Weather Research and Forecasting Model (WRF) and found that the increased ice cover and thickness suppressed the formation of LES because increased ice cover is shown to decrease sensible and latent heat fluxes into the atmosphere (Gerbush et al., 2008; Zulauf and Krueger, 2003). Warmer LST and lower ice cover should create high intensity and spatial cover of snowfall (Wright et al. 2013), relative to the observed results because lakes would be able to generate greater energy fluxes into the atmosphere.

It is suggested that sensible and latent heat fluxes representation within the model could also affect the production of LES. Sensible and latent heat fluxes are of primary importance for the development of LES because a transfer of both heat and moisture from the lake into the lower PBL produces an unstable lapse rate at the lower levels and creates conditions favourable for convection. Lower PBL instability occurs because water vapour ($H_2O_{(g)}$) has a lower molecular weight than atmospheric oxygen ($O_{2(g)}$). Therefore, an increase in water vapour into the lower PBL decreases the density of the air mass, and increases the instability of the air mass, inducing convection, the development of cloud formation, and lake effect precipitation. Furthermore, increased sensible and latent heat fluxes into the PBL increase both the air temperature and dew point temperature over the lake (Phillips, 1972). As a result, CAPE is increased within the above air parcel, inducing convection, and cloud formation, which are favourable for the development of LES. Therefore, these fluxes are important key factors in influencing the production of LES.

Also observed by Lofgren and Zhu, (2000), is that high outgoing sensible and latent heat fluxes are observed over the late fall and early winter, which drive strong cooling of the lake surface and consequent convective mixing within the lake water column. However, while the epilimnion layer, in FLake, can account for convective and mechanical mixing,

FLake does not represent these processes in the hypolimnion layer, which are present in large and deep lakes (Perroud et al., 2009; Balsamo et al., 2012; Mallard et al., 2014).

Thus, the large discrepancy in the predicted lake variables may be attributed to unrealistic parameterization schemes within the FLake model. For example, sensible and latent heat fluxes are calculated in the CRCM5 lake interface module and are based on parameters supplied by the model, such as surface temperature and ice cover. Martynov et al. (2012) explains that the influence of lakes on air temperature and humidity in lake rich regions is weakly simulated in FLake. Kourzeneva (2010) suggests that a basic issue of lake parameterization in numerical weather predictions and climate simulations is the need for external lake parameters, and that the most important lake parameter is the minimum depth required for lake models. Thus, assigning a virtual depth of only 60 m for Lake Superior, which, in actuality, has a maximum lake depth of 406 m, could cause significant biases in lake thermal process simulations (Gu et al. 2015), because lake depth is a controlling factor influencing ice freeze-up and ice break-up dates (Duguay et al., 2003; Duguay et al., 2006), as mentioned in previous chapters. Furthermore, FLake does not allow partial ice cover for each grid cell (Martynov et al., 2012), thus, local ice cover could be falsely represented, thereby influencing the production of localized lake-induced snowfall.

Although, lake ice and temperature sensitivity analyses with FLake, conducted by Martynov et al. (2010), showed that FLake outperformed other one-dimensional lake prediction models over the Great Lakes, the one-dimensional models failed to capture patterns of springtime warming in the Great Lakes. This failure suggests the absence of three-dimensional processes, such as lake currents, ice drift, and the formation of thermal bars, thereby negatively affecting the predictive capabilities of FLake (Mallard et al. 2014).

The one-dimensional lake model, FLake, is interactively coupled to the CRCM5 and despite providing satisfactory predictions of temperature and ice cover, it is limited compared to three-dimensional dynamical lake models that could simulate both horizontal and vertical circulation (Lucas- Picher et al., 2016). The quality of reproduced SWE, wintertime precipitation, and LES events along the Canadian leeward shores of Lake

Superior and Lake Huron are, thus, highly dependent on the performance of FLake (Martynov et al., 2013).

5.4 Conclusion

The purpose of this study was to validate a regional climate model (CRCM5) in predicting snowfall along Canadian snowbelts of Lakes Superior and Huron within the Laurentian GLB. Gridded outputs of total December and January SWE and, separately, precipitation, were averaged over the 20-year period of 1995 to 2014. Gridded RMSD and MBD were computed between the model and interpolated gridded dataset (Daymet). Results showed that the CRCM5 under-estimates both SWE and precipitation along both snowbelts in December and January. The negative biases in SWE and precipitation along the shores of these Great Lakes suggest that the processes of lake-induced snowfall were not properly represented by the model.

In order to understand the sources of these biases, seven lake-induced events along Lake Superior or Lake Huron's snowbelt were selected for the months of December or January during a high and low ice season to validate the model's performance in capturing the timing, location, and accumulation of each event. The results in this study showed that while the model generally predicted the onset of the squall bands and the general location of the trajected squall paths, it drastically under-estimated the daily total lake effect precipitation accumulation. The study further validated the model's capabilities in simulating LES predictor variables, which are key factors in the development of lake-induced precipitation.

The LES predictor variables included 850 mb air temperature, lake-wide LST, and lake-wide ice cover concentration. Time series of the simulated outputs of LST and ice cover were plotted against the observed dataset for each variable. While the model accurately simulates 850 mb air temperature, it over-estimates LST for both lakes in December and January, respectively. Ice cover is under-estimated in both lakes for December, but only for Lake Huron in January.

This study suggests limitations within the coupled lake-RCM. The CRCM5 is interactively coupled to the one-dimensional freshwater lake model (FLake), which is used to reproduce LST and ice cover concentration. The accuracy and precision of the simulated lake-induced events within the snowbelt regions of the Laurentian Great Lakes are highly dependent on the performance of the coupled lake model (Martynov et al. 2013). However, there are limitations within the one-dimensional FLake model, such as a virtual lake depth of only 60 m, and the inability to simulate both horizontal and vertical circulation, processes which can be reproduced by three-dimensional dynamical lake models. Moving forward, as three-dimensional lake models become more available, the interactive coupling of three-dimensional lake models to RCMs should be applied in order to assess the accuracy of LES forecasts.

Chapter 6
General Conclusions

6.1 General Summary

The purpose of this thesis was to explore the under-studied region of the Canadian Laurentian Great Lakes' snowbelts. This research conducted analyses of historical spatiotemporal trends in snowfall and LES predictor variables and examined the predictive performance of a RCM in capturing observed lake-induced snowfall events. These investigations were motivated by three noticeable gaps in the current scientific literature. The first gap identified the lack of snowfall research along the Canadian snowbelts of the GLB. Much LES research has been conducted for the GLB snowbelts in the United States but with minimal focus on Ontario's snowbelts along the leeward shores of Lakes Superior and Huron. The second gap identified the limited investigations on climatological, lake-induced, snowfall trends within the GLB. While most LES research focused on specific case study events, there has been an under-examination of climatological spatiotemporal trends in regional Great Lakes snowfall. The third gap highlighted the lack of RCM studies in LES for the Canadian snowbelt region. Previous studies that have utilized modelled simulations for analysing LES have employed coarse global climate models (GCMs) and regional climate models (RCMs) that make it difficult to delineate meso-beta scale LES snow bands. Thus, addressing these gaps is imperative because residential, agricultural, economic, and recreational sectors along the populated Canadian snowbelts can be adversely impacted by extreme snowfall within the GLB. The findings gained from this thesis will provide beneficial information for sustainability and adaptation studies as climate change continues to influence variability in precipitation over lake-rich regions well into the late 21st century.

Manuscript 1, presented in Chapter 3, aimed to determine historical spatiotemporal trends in snowfall over the under-studied Ontario snowbelts of Lakes Superior and Huron. Potential explanations into the resultant snowfall trends were explored by analysing additional spatiotemporal trends in key surface-atmosphere LES predictor variables. An algorithm was used to derive gridded snowfall by employing interpolated total daily

precipitation, as well as maximum and minimum temperatures provided by Daymet. The datasets were then used to compute monthly totals in snowfall and total precipitation over the 1980 to 2015 cold seasons (NDFJM).

Along the Ontario snowbelt of Lake Superior, results indicated a significant decrease in snowfall and total precipitation at rates of 40 cm/36 yrs and 20 mm/36 yrs, respectively, at the 95% confidence level. Similar spatiotemporal trends in snowfall and precipitation indicated that snowfall was not transitioning to a different precipitation state, but rather, there were changes in the overall moisture budget within the atmosphere. Furthermore, the study suggested that the negative trends in snowfall might be attributed to lake-induced processes because these trends were mostly dominant along the leeward shores of Lake Superior during the LES months of December and January. To test this hypothesis, trends in LES predictor variables were also analysed.

LES predictor variables showed a decrease in ice cover over both lakes, an increase in instability in the lower PBL, an increase in LST, and an increase in the 1000 mb air temperature over Lake Superior. This paper concluded that complex processes, such as inefficient moisture recycling and increased moisture storage in warmer air masses can inhibit the development of lake-induced snowfall along the immediate leeward shores of Lake Superior. These parcels can advect farther southwest before saturation and precipitation can occur. Based on these results, additional questions arose. For example, although monthly total snowfall has been decreasing over the past 36-years, does this suggest that the intensity, frequency, and duration of these snowfall events follow a similar trend? This question was the motivation for the second manuscript.

Manuscript 2, presented in Chapter 4, aimed to assess historical spatiotemporal trends in snowfall extremes for Lakes Superior and Huron's snowbelts by evaluating, 1980-2015, 99^{th} percentile of snowfall frequency, intensity, and duration. Discussions on various environmental controls and factors influencing regional snowfall were provided to explain the resultant extremes. Spatiotemporal snowfall and precipitation trends were computed using Daymet monthly gridded datasets. The extreme value for snowfall intensity was

calculated by taking the 99th percentile of daily snowfall over the 36-year time period. Frequency was defined as the number of days for which snowfall rates equaled or exceeded the extreme value. Duration was the maximum number of consecutive days for which snowfall intensity equaled or exceeded the extreme value.

The results indicated that mostly lake-induced processes, and not solely extratropical cyclones, drove the high intensity, frequency, and duration of these historic extreme events over the GLB. Results showed that the snowfall extremes have been decreasing along the Canadian leeward shores of Lake Superior. Furthermore, the Canadian snowbelts of Lake Superior and Lake Huron exhibited different spatiotemporal patterns, and even within a particular snowbelt region, trends in extreme snowfall were not spatially coherent. It is concluded that the differences in geographic location of the lakes, topography, lake bathymetry, and lake orientation influence the local and large-scale surface-atmosphere variables.

While manuscripts 1 and 2 examined historical spatiotemporal trends in monthly snowfall totals and extremes over the Canadian domain of the Laurentian Great Lakes, the final manuscript looked into whether RCMs could satisfactorily predict contemporary lake-induced snowfall events. In order to investigate future trends in lake-induced snowfall, high-resolution regional climate models need to be readily available and accurate at predicting historical snowfall events. Thus, the objective of Manuscript 3, presented in Chapter 5, determined whether a RCM could accurately predict the location, timing, and accumulation of observed lake-induced events within the Canadian snowbelts of the GLB. This study conducted an evaluation of the high resolution, 0.11°,CRCM5 interactively coupled to the one-dimensional Freshwater Lake model (FLake), to predict SWE and precipitation along the Canadian snowbelts of Lake Superior and Lake Huron. Total monthly gridded SWE and wintertime precipitation were separately averaged over a 20-year (1995-2014) period and the RMSD and the MBD were computed between the simulated and gridded interpolated Daymet dataset.

The findings in this paper showed that December SWE indicated a negative MBD ≤ -10 mm along both snowbelts, with values ≤ -30 mm in January. Similarly, December precipitation showed a MBD ≤ -5 mm and January's precipitation had an MBD ≤ -10 mm for both snowbelts. The results suggested that the model under predicts SWE and precipitation predominantly along the snowbelts of the Laurentian Great Lakes, indicating that the model may have difficulty predicting lake-effect processes associated with lake-induced precipitation in these regions.

Therefore, seven separate LES events were examined to validate the model's performance in predicting the timing, location, and accumulation of specific lake-induced precipitation events during the 2013-2014, high, and 2011-2012, low, ice seasons. Observations were taken from ECCC's archive weather observation stations and Ontario archive radar images. NARR and NOAA's Ice Atlas and Coast Watch provided additional datasets. Lake-induced events also showed that the model mostly under-predicted the daily accumulated precipitation associated with each event but tended to accurately capture the timing and the general location of the snowsqualls along the snowbelts, though not for highly localized snow bands.

This study also compared LES predictor variables, including 850 mb air temperature, LST, and ice cover concentration between data sources. The lake-wide results indicated over-estimations of LST for both lakes during December and January and under-estimations of ice cover concentrations for both lakes in December. The resultant biases in the model could be attributed to limitations within the coupled lake model, because the quality of reproducing LES in this region is highly dependent on the performance of the coupled one-dimensional lake model within the CRCM5. However, limitations within the one-dimensional FLake model in simulating both horizontal and vertical mixing can reduce the accuracy of LST and ice cover parameters required for input into the CRCM5. Meteorologists and climatologists are highly dependent on NWP and RCMs for snowfall predictions and projections; thus, it is imperative that they consider these model limitations in order to understand prediction uncertainties. Furthermore, as higher resolution regional

climate models become available, the need for more accurate and realistic parameterization schemes is required.

6.2 Limitations and Future Research Directions

This section reviews the overall limitations in the observed and simulated datasets and algorithms used in this thesis. Climatological snowfall studies are often challenging to conduct because of the lack of highly spatial and homogenized observed snowfall measurements for the regions of interest. As a result, this limited the number of cities, and the temporal period of analyses selected for the observed lake-induced events in Manuscript 3 because the weather stations were selected based on the availability of data for the periods of interest.

Therefore, Daymet was used in this thesis because it served as a useful gridded data source for examining snowfall for the 1980-2015 period due to its availability of high spatial and temporal meteorological data. However, Daymet output is interpolated from weather stations, sometimes from regions of sparse networks, such as the far north. Therefore, a system is established to have the search radius of stations reduced in data-rich regions and increased in data-poor regions.

Furthermore, it is acknowledged that there are uncertainties within Daymets dataset estimates. For example, cross-validation statistics conducted for 2°x2° tiles containing the Canadian snowbelts of Lakes Superior and Huron indicate the standard deviation over the 36-year period of precipitation, T_{max}, and T_{min}. The standard deviation of Daymet's precipitation is of 0.05 for both snowbelts. The standard deviation for T_{max} for both Lakes Superior and Huron's snowbelt are 0.5 and 0.6, respectively and for T_{min}, 1.0 and 0.9, respectively. Thus, the uncertainty in the Daymet datasets are low and gives confidence to using them for deriving snowfall estimates.

Gridded snowfall estimates were derived using daily precipitation and daily T_{mid}, which were calculated from daily T_{max} and T_{min} values. Standard deviation of the computed T_{mid} values was 2.0 and 3.7 for Lakes Huron and Superior's snowbelts, respectively. The

uncertainty values of precipitation and T_{mid} were inputted to the derivative of the snowfall estimate algorithm to determine the sensitivity among the variables used in the algorithm. The sensitivity of new snowfall to the variables used in the algorithm were low and within a reasonable range of uncertainty. The low errors provided confidence that the derived snowfall height algorithm employed was an appropriate approach.

Another assumption that was applied was the definition of an extreme. While environment Canada defines an extreme snowfall event as 15 cm/12 hours, in Chapter 4 an extreme event was defined as 15 cm/day. This is because the highest temporal resolution for the Daymet data was daily. The results also showed that the extreme snowfall events, at the 99th percentile, were approximately 15 cm/day, thus, giving credence to using that threshold. Despite these limitations, this research was able to determine spatiotemporal trends in monthly precipitation and snowfall totals and extremes for the under-studied regions of the Canadian snowbelt. Furthermore, this research was able to evaluate a high resolution CRCM5 model in predicting LES events for the purpose of determining its performance in conducting future LES predictions.

There are evident limitations within the coupled CRCM5-FLake in predicting the timing, location, and accumulation of lake-induced precipitation. Reproducing lake-induced precipitation within the snowbelt regions of the Laurentian Great Lakes is highly dependent on the performance of the coupled lake model (Martynov et al., 2013). However, limitations within the one-dimensional FLake model, such as a virtual lake depth of only 60 m, and the inability to simulate both horizontal and vertical circulation make it difficult to accurately predict lake-induced precipitation. However, these mixing processes can be reproduced in three-dimensional dynamical lake models, such as the Nucleus for European Modelling of the Ocean (NEMO) ocean model, a tool that should be employed in future LES coupled lake-atmosphere simulation studies. Recent studies have employed offline simulations of NEMO in the Laurentian Great Lakes, such as ECCC that explored complex air-lake interactions with this model (Dupont et al., 2012). Furthermore, studies at UQAM are also underway to test NEMO coupled to the CRCM5 in determining its ability to predict

certain LES predictor variables. However, these investigations are still in the preliminary stages.

Now that historical LES trends and model evaluation studies have been conducted, continued work should aim to assess future projections in LES trends along the Lake Superior and Lake Huron Georgian-Bay's snowbelts. These analyses should be conducted by coupling new and improved three-dimensional lake models to high resolution RCMs in order to examine possible improvements in LES predictions. Furthermore, oscillation patterns can affect the location and intensity in cold air outbreaks. Thus, future work should investigate predictive shifts in oscillation patterns to determine changes in teleconnections and its influence on lake-induced snowfall within the GLB.

References

Anyah, R.O., and Semazzi, F.H.M. 2004. Simulation of the sensitivity of Lake Victoria basin climate to lake surface temperature. *Theoretical and Applied Climatology,* 79 (1-2): 55-69, DOI: 10.1007/s00704-004-0057-4.

Assel, R.A. 1990. An ice-cover climatology for Lake Erie and Lake Superior for the winter seasons 1897–98 to 1982–83. *International Journal of Climatology*,10(7):731–748.

Assel, R.A. 1999. Great Lakes ice cover. In Lam D.C.L., and Schertzer, W.M. (Eds.), *Potential Climate Change Effects on Great Lakes Hydrodynamics and Water Quality* (pp. 1-21). American Society of Civil Engineers: ISBN-10: 0784404135.

Assel, R.A., Cronk, K., and Norton, D. 2003. Recent trends in Laurentian Great Lakes ice cover. *Climatic Change,* 57 (1-2): 185–204.

Austin, J.A., and Colman, S.M. 2007. Lake Superior summer water temperature are increasing more rapidly than regional air temperatures: a positive ice-albedo feedback. *Geophysical Research Letter,* 34(6): 1-5, DOI:10.1029/2006GL029021.

Baijnath-Rodino, J.A., and Duguay C.R. in review. Historical spatiotemporal trends in snowfall extremes over the Canadian Domain of the Great Lakes Basin. *Advances in Meteorology.*

Baijnath-Rodino, J.A., Duguay, C.R., and LeDrew, E. 2018. Climatological trends of snowfall over the Laurentian Great Lakes Basin. *International Journal of Climatology*, Early view, DOI: 10.1002/joc.5546.

Ballentine, R.J., Stamm, A.J., Chermack, E.F., Byrd, G.P., and Schleede, D. 1998. Mesoscale model simulation of the 4–5 January 1995 lake-effect snowstorm. *Weather and Forecasting,* 13: 893–920.

Balsamo, G., Salgado, R., Dutra, E., Boussetta, S., Stockdale, T., and Potes, M. 2012. On the contribution of lakes in predicting near-surface temperature in a global weather forecasting model, *Tellus*, 64, 15829, DOI:10.3402/tellusa.v64i0.15829.

Bard, L., and Kristovich, D.A.R. 2012. Trend in Lake Michigan contribution to snowfall. *Journal of Applied Meteorology and Climatology,*51: 2038-2046.

Barjenbruch, K., Hiltbrand, R., Kosarik, J., and LaPlante, R. 1997. Examination of a lake-effect snow event with the focus on new technology. *Eastern region technical attachment, no 97-98.*

Bates, G.T., Giorgi, F., and Hostetler, S.W.1993. Toward the simulation of the effects of the Great Lakes on regional climate. *Monthly Weather Review,* 121: 1373–1387.

Bates, G. T., Hostetler, S.W., and Giorgi, F. 1995. Two-year simulation of the Great Lakes region with a coupled modeling system. *Monthly Weather Review,* 123: 1505-1522.

Baxter, M.A., Graves, C.E., and Moore, J.T. 2005. A Climatology of Snow-to-Liquid Ratio for the Contiguous United States. *Weather and Forecasting*, 20: 729-744.

Blanken, P.D., Spence, C., Hedstrom, N., and Lenters, J.D. 2011. Evaporation from Lake Superior: 1. Physical controls and processes. *Journal of Great Lakes Research,* 37(4): 707–716.

Bluestein, H.B. 1992. *Synoptic-dynamic meteorology in midlatitudes: Principles of kinematics and dynamics* (Volume 1, pp. 246-247). New York, NY: Oxford University Press.

Braham, R.R. Jr., and Dungey, M.J. 1984. Quantitative estimates of the effect of Lake Michigan on snowfall. *Journal of Applied Meteorology and Climatology*, 23(6): 940–949.

Brown, L.C., and Duguay, C.R. 2010. The Response and role of ice cover in lake climate interactions. *Progress in Physical Geography,* 34(5), DOI: 10.1177/0309133310375653.

Burnett, A.W., Kirby, M.E., Mullins, H.T., and Patterson, W.P. 2003. Increasing Great Lake-effect snowfall during the twentieth century: A regional response to global warming? *Journal of Climate,* 16: 3535-3542.

Byrd, G.P., Anstett, R.A., Heim, J.E., and Usinski, D.M.1991. Mobile sounding observations of lake-effect snowbands in western and central New York. *Monthly Weather Review*, 119(9): 2323–2332.

Cairns, M.M., Collins, R., Cylke, T., Deutschendorf, M., and Mercer, D. 2001. A lake effect snowfall in Western Nevada- Part I: Synoptic setting and observations. *Paper presented at the 18th Conference on Weather Analysis and Forecasting/14th Conference on Numerical Weather Prediction,* Fort Lauderdale.

Campbell, L.S., Steenburgh, W.J., Veals, P.G., Letcher, T.W., and Minder, J.R. 2016. Lake effect mode and precipitation enhancement over the Tug Hill Plateau during OWELes IOP2b," *Monthly Weather Review*, 144(5):1729-1748.

Carpenter, D.M. 1993. The Lake Effect of the Great Salt Lake: Overview and Forecast Problems. *Weather and Forecasting,* 8 (2):191-193.

Chow, F.K., Weigel, A.P., Street, R.L., Rotach, M.W., and Xue, M. 2006. High resolution large eddy simulations of flow in a steep alpine valley. Part one: Methodology, verification, and sensitivity experiments. *Journal of Applied Meteorology and Climatology,* 45: 63-86.

Cogley, J. 1979. The albedo of water as a function of latitude. *Monthly Weather Review*,107: 775-781.

Cohen, S.J., and Allsopp, T.R.1988. The potential impacts of a scenario of CO2-induced climatic change on Ontario, Canada. *Journal of Climate,* 1: 669–681.

Comet. 2015. Accessed 2015. Website of the University Corporation for Atmospheric Research (UCAR) [Available online since 1997 - www.meted.ucar.edu].

Cosgrove, B.A., Colucci, R.J., and Waldstreicher, J.S. 1996. Lake effect snow in the Finger Lakes region. Preprints, *15th Conf. on Weather Analysis and Forecasting*, Norfolk, VA, American Meteorological Society: 573–576.

Croley, T.E., II 1989. Verifiable evaporation modeling on the Laurentian Great Lakes. *Water Resources Research,* 25:781–792.

Cubasch, U. and co-authors. 2013. Introduction. In: Climate change 2013: The physical science basis. Contribution of Working Group I to the Fifth Assessment Report of the Intergovernmental Panel on Climate Change. Cambridge University Press, Cambridge, United Kingdom and New York, NY, USA. Accessed March, 2018. [Available online at http://www.ipcc.ch/pdf/assessment-report/ar5/wg1/WG1AR5_Chapter01_FINAL.pdf].

Current Results. 2017. Weather and science facts, Barrie snowfall totals and snowstorm averages. Accessed 15 January 2017. [Available online https://www.currentresults.com/Weather/Canada/Ontario/Places/barrie-snowfall-totals-snowstorm-averages.php.].

Cuxart, J., Jimenez, M.A., Telisman Prtenjak, M., and Grisogono, B. 2014. Study of a sea-breeze case through momentum, temperature, and turbulence budgets. *Journal of Applied Meteorology and Climatology,*53: 2589-2609.

Dee, D.P. et al. 2011. The ERA-Interim reanalysis: configuration and performance of the data assimilation system. *Quarterly Journal of the Royal Meteorological Society*, 137(656): 553-597, DOI:10.1002/qj.828.

Dewey, K.F. 1979. An objective forecast method developed for Lake Ontario induced snowfall systems. *Journal of Applied Meteorology* 18(6): 787–793.

Dobiesz, N.E., and Lester, N.P. 2009. Changes in mid-summer water temperature and clarity across the Great Lakes between 1968 and 2002. *Journal of Great Lakes Research,* 35(3): 371-384.

Duguay, C.R., Flato, G.M., Jeffries, M.O., Ménard, P., Morris, K., and Rouse, W.R. 2003. Ice covers variability on shallow lakes at high latitudes: model simulation and observations. *Hydrological Process*, 17(17): 3465–3483.

Duguay, C.R., Prowse, T.D., Bonsal, B.R., Brown, R.D., Lacroix, M.P., and Ménard, P. 2006. Recent trends in Canadian lake ice cover. *Hydrological Process*, 20(4): 781-801.

Dupont, F., Chittibabu, P., Fortin, V., Rao, Y.R., and Lu, Y. 2012. Assessment of a NEMO – Based Hydrodynamic Modelling System for the Great Lakes. *Water Quality Research Journal of Canada* 47(3-4), DOI: 10.23266 54.

ECCC. 2015. Environment and Climate Change Canada. Accessed 2015. [Available online https://weather.gc.ca/analysis/index_e.html].

ECCC. 2017a. Environment and Climate Change Canada, Public Alerting Criterion. Accessed 15 January 2017. [Available online at http://www.ec.gc.ca/meteo weather/default.asp?lang=En&n=d9553ab5-1#snowFall.].

ECCC. 2017b. Environment and Climate Change Canada, Great Lakes Quickfacts. Accessed 15 January 2017. [Available online https://www.ec.gc.ca/grandslacsgreatlakes/default.asp?lang=En&n=B4E65F6F-1.].

ECCC. 2017c. Environment and Climate Change Canada, Lake Ice Climatic Atlas for the Great Lakes 1981-2010. Accessed 9 February 2017. [Available online at http://www.ec.gc.ca/glaces-ice/default.asp?lang=En&n=F1596609-1&offset=1&toc=show].

ECCC. 2018. Environment and Climate Change Canada, Glossary. Accessed April 2018. [Available online at http://www.climate.weather.gc/glossary_e.html#totalPrec].

Eichenlaub, V.L. 1970. Lake effect snowfall to the lee of the Great lakes: Its role in Michigan. *Bulletin of the American Meteorological Society,*51: 403-412.

Eichenlaub, V.L. 1979. *Weather and climate of the Great Lakes region.* Notre Dame, Indiana: The University of Notre Dame Press. ISBN 0-268-01929-0.

Ellenton, G.E., and Danard, M.B. 1979. Inclusion of sensible heating in convective parameterization applied to lake-effect snow. *Monthly Weather Review,* 107: 551–565.

Ellis, A.W., and Johnson, J.J. 2004. Hydroclimatic analysis of snowfall trends associated with the North American Great Lakes. *Journal of Hydrometeorology,* 5: 471–486.

Gerbush, M.R., Kristovich, D.A.R., and Laird, N.F. 2008. Mesoscale boundary layer and heat flux variations over pack ice-covered Lake Erie. *Journal of Applied Meteorology and Climatology,* 47: 668–683.

Gilbert, R.O. 1987. *Statistical methods for environmental pollution monitoring.* New York, NY: John Wiley & Sons Inc. ISBN: 978-0-471-28878-7.

Gorman, P.A. 2014. Contrasting response of mean and extreme snowfall to climate change. *Nature*, 512(7515): 416-418.

Gu, H., Jin, J., Wu, Y., Ek, M.B., and Subin, Z.M. 2015. Calibration and validation of lake surface temperature simulations with the coupled WRF- lake model. *Climatic Change,* 129(3-4): 471-483 DOI: 10.1007/s/110584-013-0978-y.

Gula, J., and Peltier, R. 2012. Dynamical downscaling over the Great Lakes Basin of North America using the WRF regional climate model: The impact of the Great Lakes system on regional greenhouse warming. *Journal of Climate,* 25: 7723-2242, DOI: 10.1175/JCLI-D-11-00388.1.

Hamilton, R.S., Saff, D., Nizol, T. 2006. A catastrophic lake effect snow storm over Buffalo, NY October 12-14, 2006 Cast study. *NOAA National Weather Service, Buffalo, NY. 22nd Conf. on Weather Analysis and Forecasting/18th Conf. on Numerical Weather Prediction.* [Available online at https://ams.confex.com/ams/22WAF18NWP/techprogram/paper_124750.htm]\

Hartmann, H., Livingstone, J., and Stapleton, M.G. 2013. Seasonal forecast of local lake-effect snowfall: The case of Buffalo, U.S.A. *International Journal of Environmental Research,* 7(4): 859-867.

Hartnett, J.J., Collins, J.M., Baxter, M.A., and Chambers, D.P. 2014. Spatiotemporal snowfall trends in Central New York. *Journal of Applied Meteorology and Climatology,* 53: 2685-2697, DOI: 10.1175.

Hill, J.D. 1971. Snow squalls in the lee of Lakes Erie and Ontario. *NOAA Technical Memorandum, NWS* ER-43.

Hjelmfelt, M.R. 1990. Numerical study of the influence of environmental conditions on lake-effect snowstorms over Lake Michigan. *Monthly Weather Review,* 118: 138–150.

Hjelmfelt, M.R., and Braham, R.R. Jr.1983. Numerical simulation of the airflow over lake Michigan for a major lake effect snow event. *Monthly Weather Review* 111: 205-219.

Holroyd, E. W. III. 1971. Lake effect cloud bands as seen from weather satellites. *Journal of the Atmospheric Sciences* 28(7): 1165-1170.

Hostetler, S.W., 1991: Simulation of lake ice and its effect on the late-Pleistocene evaporation rate of Lake Lahontan. *Climate Dynamics,* 6: 43-48.

Hostetler, S. W., 1995: Hydrological and thermal response of lakes to climate: description and modeling. In Lerman, A., Imboden, D., and Gat, J. (Eds.), *Physics and Chemistry of Lakes* (pp.63-82). Berlin, Germany. Springer-Verlag.

Hostetler, S.W., and Bartlein, P.J. 1990: Modeling climatically determined lake evaporation with application to simulating lake-level variations of Harney-Malheur Lake, Oregon. *Water Resources Research*, 26: 2603-2612.

Hostetler, S.W., Bates, G.T., and Giorgi, F. 1993: Interactive coupling of a lake thermal model with a regional climate model. *Journal of Geophysical Research,* 98: 5045-5057.

Hozumi, K., and Magono, C. 1984. The cloud structure of convergent cloud bands over the Japan Sea in winter monsoon period," *Journal of the Meteorological Society of Japan*, 62(3): 522–53.

Hunter, T.S., Clites, A.H., Campbell, K.B., and Gronewold, A.D. 2015. Development and application of a North American Great Lakes hydrometeorological database – part1: precipitation, evaporation, runoff, and air temperature, *Journal of Great Lakes Research,* 41: 65-77.

iWeatherNet.com. 2017. Accessed 2017. [Available online http://www.iweathernet.com/educational/lake-effect-snow-great-lakes].

Jensen, O.P., Benson, B.J., Magnuson, J.J., Card, V.M., Futter, M.N., Soranno, P.A, and Stewart, K.M. 2007. Spatial analysis of ice phenology trends across the Laurentian Great Lakes region during a recent warming period. *Limnology and Oceanography,* 52(5): 2013-2026.

Kalnay, E., and Coauthors, 1996. The NCEP/NCAR 40-Year Reanalysis Project. *Bulletin of the American Meteorological Society*,77:437–471.

Karl, T.R., and Knight, R.W. 1998. Secular trends of precipitation amount, frequency, and intensity in the United States, *Bulletin of the American Meteorological Society*, 70(2): 231-241, 1998.

Kendall, M.G. 1975. Rank Correlation Methods. *4th edition,* London, England: Charles Griffin.

Kennedy, A.D., Dong, X., and Xi, B. 2011. A comparison of MERRA and NARR Reanalyses with the DOE ARM SGP Data. *Journal of Climate*, 24: 4541-4557.

Kheyrollah Pour, H., Duguay, C.R., Martynov, A., and Brown, L.C. 2012. Simulation of surface temperature and ice cover of large northern lakes with 1-D models: A comparison with MODIS satellite data and in situ measurements. *Tellus Series A-Dynamic Meteorology and Oceanography*, 64, DOI: 10.3402/tellusa. v64i0.17614.

Kourzeneva, E.P. 2010: External data for lake parameterization in numerical weather prediction and climate modeling. *Boreal Environment Research,* 15:165–177.

Kourzeneva, E.P., Samuelsson, P., Ganbat, G., and Mironov, D. 2008: Implementation of lake model Flake into HIRLAM. *HIRLAM Newsletter, 54: 54–64.* [Available http://hirlam.org/index.php/component/docman/doc_view/195-hirlam-newsletter-no-54-paper-07- kourzeneva.

Krasting, J., Broccoli, A., Dixon, K., and Lanzante, J. 2013. Future changes in northern hemisphere snowfall. *Journal of Climate,* 26: 7813-7828.

Kristovich, D.A.R., and coauthors, 2000. The lake induced convection experiments and the snowband dynamics project. *Bulletin of the American Meteorological Society,*81: 519-542.

Kristovich, D.A.R., and Hjelmfelt, M.R. 2003. Convective evolution across Lake Michigan during a widespread lake-effect snow event. *Monthly Weather Review*, 131(4): 643–655.

Kristovich, D.A.R., and Laird, N.F. 1998. Observations of widespread lake effect cloudiness: Influence of lake temperature and upwind conditions. *Weather and Forecasting,* 13: 811-821.

Kristovich, D.A.R., and Spinar, M.L. 2005. Diurnal variations in lake-effect precipitation near western Great Lakes. *Journal of Hydrometeorology*, 6(2): 210-218.

Kunkel, K.E., and coauthors, 2013. Monitoring and understanding trends in extreme storms: state of knowledge. *Bulletin of the American Meteorological Society*, 94(4): 499–514.

Kunkel, K.E., Palecki, M., Ensor, L., Hubbard, K.G., Robinson, D., Redmond, K., and Easterling, D. 2009. Trends in 20th Century U.S. snowfall using a quality-controlled data set. *Journal of Atmospheric and Oceanic Technology,*26: 33–44.

Kunkel, K.E., Wescott, N.E., and Kristovich, D.A.R. 2000. Climate change and lake effect snow. Preparing for a changing climate: The potential consequences of climate variability and change. *Journal of Great Lakes Research,* 28: 521-536.

Kunkel, K.E., Wescott, N.E.,and Kristovich, D.A.R. 2002. Assessment of potential effects of climate change on heavy lake-effect snowstorms near Lake Erie, *Journal of Great Lakes Research*, 28(4): 521-536.

Lacey, M.A., Riseng, C.M., Gronewold, A.D., Rutherford, E.S., Wang, J., Clites, A., Smith, S.D.P., and McIntyre, P.B. 2016. Fine-scale spatial variation in ice cover and surface temperature trends across the surface of the Laurentian Great Lakes. *Climatic Change,* 138: 71-83, DOI: 10.1007/s10584-016-1721-2.

Lackmann, G.M. 2001. Analysis of a surprise Western New York snowstorm. *Weather Forecasting, 1*6: 99-114.

Laird, N.F. 1999. Observation of coexisting mesoscale lake-effect vortices over the western Great Lakes. *Monthly Weather Review,* 127: 1137–1141.

Laird, N.F., Desrochers, J., and Payer, M. 2009. Climatology of lake-effect precipitation events over Lake Champlain. *Journal of Applied Meteorology and Climatology*, 48: 232-250.

Laird, N.F., and Kristovich, D.A.R. 2004. Comparison of observations with idealized model results for a method to resolve winter lake-effect mesoscale morphology. *Monthly Weather Review,* 132 : 1093-1103.

Laird, N.F., Kristovich, D.A.R., and Walsh, J.E. 2003a. Idealized model simulations examining the mesoscale structure of winter lake-effect circulations. *Monthly Weather Review*, 131:206–221.

Laird, N.F., Sobash, R., and Hodas, N. 2010. Climatological conditions of lake-effect precipitation events associated with the New York State Finger Lakes. *Journal of Applied Meteorology and Clim*atology, 49: 1052-1062. DOI: 10.1175/2010JAMC2312.

Laird, N.F., Walsh, J.E., and Kristovich, D.A.R. 2003b. Model simulations examining the relationship of lake effect morphology to lake shape, wind direction, and wind speed*. Monthly Weather Review*, 131:2102–2111.

Laprise, R. 1992. The Euler equation of motion with hydrostatic pressure as independent coordinate. *Monthly Weather Review,* 120: 197-207.

Lavoie, R.L. 1972. A mesoscale numerical model of lake-effect storms. *Journal of the Atmospheric Sciences, 29:* 1025–1040.

Leathers, D.J., and Ellis, A.W. 1993. Relationships between synoptic weather type frequencies and snowfall trends in the lee of Lakes Erie and Ontario. *Proceedings, 61st Annual Western Snow Conference,* Quebec City, Canada, CRREL, 325-330.

Leathers, D.J., and Ellis, A.W. 1996. Synoptic mechanisms associated with snowfall increases to the lee of Lakes Erie and Ontario. *International Journal of Climatology,*16: 1117–1135.

Legates, D.R., and Willmott, C.J. 1990. Mean seasonal and spatial variability in gage-corrected global precipitation. *International Journal of Climatology,* 10: 111–133.

Livingstone, D.M., Adrian, R., Blenckner, T., George, D.G., and Weyhenmeyer, G.A. 2010b. *Lake ice phenology.* In *The impact of climate on European Lakes. Aquatic Ecology Series 4.* (pp. 51-61). Dordrecht (Netherlands). Springer.

Lo, J.F., Yang, Z.L., and Pielke, R.A. Sr. 2008. Assessment of three dynamical climate downscaling methods using the Weather Research and Forecasting (WRF) model. *Journal of Geophysical Research,* 113, DOI: 10.1029/2007JD009216.

Lofgren, B.M. 2006. Land surface roughness effects on lake effect precipitation. *Journal of Great Lakes Research*, 32: 839-851.

Lofgren, B.M., and Zhu, Y. 2000. Surface energy fluxes on the Great Lakes based on satellite-observed surface temperatures 1992 to 1995. *Journal of Great Lakes Research,* 26 (4): 305-314.

Long, Z., Perrie, W., Gyakum, J., Caya, D., and Laprise, R. 2007. Northern lake impacts on local seasonal climate. *Journal of Hydrometeorology, 8:* 881-896.

Lucas-Picher, P., Laprise, R., and Winger, K. 2016. Evidence of added value in North American regional climate model hindcast simulations using ever-increasing horizontal resolutions. *Climate Dynamics,* DOI: 10.1007/s00382-016-3227-z.

Maesaka, T.G., Moore, W.K., Liu, Q., and Tsuboki, K. 2006. A simulation of a lake effect snowstorm with a cloud resolving numerical model. *Geophysical Research Letter,* 33: L20813, DOI:10.1029/2006GL026638.

Magnuson, J.J., Robertson, D.M., and Benson, B.J. 2000. Historical trends in lake and river ice cover in the northern hemisphere. *Science,* 289(5485): 1743-1746, DOI: 10.1126/Science.289.5485.1743.

Mahoney, K.M., and Lackmann, G.M. 2007. The effect of upstream convection on downstream precipitation. *Weather and Forecasting*, 22: 255-277, DOI:10.1175/WAF986.1.

Mallard, M.S., Nolte, C.G., Bullock, O.R., Spero, T.L., and Gula, J. 2014. Using a coupled lake model with WRF for dynamical downscaling. *Journal of Geophysical Research-Atmospheres,*119: 7193-7208, DOI:10.1002/2014JD021785.

Martynov, A., Laprise, R., and Sushama, L. 2008. Off-line lake water and ice simulations: A step towards the interactive lake coupling with the Canadian

Regional Climate Model. *Geophysical Research Abstract, 10, EGU2008-A-02898, EGU General Assembly*. Vienna, Austria.

Martynov, A., Laprise, R., Sushama, L., Winger, K., Separovic, L., and Dugas, B. 2013. Reanalysis-driven climate simulation over CORDEX North America domain using the Canadian Regional Climate Model, version 5: model performance evaluation. *Climate Dynamics,* 41:2973-3005.

Martynov, A., Sushama, L., Laprise, R. 2010. Interactive lakes in the Canadian Regional Climate Model (CRCM): present state and perspective. 44th Annual CMOS Congress, May 31-June 4, 2010, Ottawa.

Martynov, A., Sushama, L., Laprise, R., Winger, K., and Dugas, B. 2012. Interactive Lakes in the Canadian Regional Climate Model, version 5: The Role of Lakes in the Regional Climate of North America. *Tellus,* 64: 16226, DOI: 10.3402/tellusa.v64i0.16226.

Mendez, J., Hinzman, L. D., and Kane, D. L. 1998. Evapotranspiration from a wetland complex on the Arctic coastal plain of Alaska. *Nordic Hydrology*, 29: 303–330.

Menne, M.J., Durre, I., Korzeniewski, B., McNeal, S., Thomas, K., Yin, X., Anthony, S., Ray, R.,Vose, R.S., Gleason, B.E., and Houston, T.G. 2012(b). Global historical climatology network -daily (GHCN-daily), version 3.22, NOAA National Climatic Data Center, [Available online at ://doi.org/10.7289/V5D21VHZ.].

Menne, M.J., Durre, I., Vose, R.S., Gleason, B.E., and Houston T.G. 2012(a). An overview of the global historical climatology network-daily database. *Journal of Atmospheric and Oceanic Technology*, 29(7): 897-910.

Mesinger, F. 2006. North American Regional Reanalysis. *Bulletin of the American Meteorological Society*, 87: 343–360.

Miner, T.J., and Fritsch, J.M. 1997. Lake-effect rain events. *Monthly Weather Review,* 125: 3231–3248.

Mironov, D.V., 2008. Parameterization of lakes in numerical weather prediction, Description of a lake model, COSMO. *Technical Report No.11*. (pp. 41). Deutscher Wetterdienst, Offenbauch am Main, Germany.

Mironov, D., Heise, E., Kourzeneva, E., Ritter, B., Schneider, N., and Terzhevik, A. 2010. Implementation of the lake parameterisation scheme FLake into the

numerical weather prediction model COSMO. *Boreal Environment Research,* 15: 218-230.

Mote, T.L., Ramseyer, C.A., and Miller, P.W. 2017. The Saharan air layer as an early rainfall season suppressant in the Eastern Caribbean: The 2015 Puerto Rico Drought. *Journal of Geophysical Research,* 122, [https://doi.org/10.1002/2017JD026911].

National Geographic. 2017. Accessed 2017. [Available online https://www.nationalgeographic.org/media/lake-turnover/].

Niziol, T.A. 1987. Operational forecasting of lake effect snow in western and central New York. *Weather and Forecasting,* 2(4): 310-321.

Niziol, T.A., Snyder, W.R., and Waldstreicher, J.S. 1995. Winter weather forecasting throughout the Eastern United States, Part4: Lake effect snow. *Weather and Forecasting.* 10: 61-77.

NOAA. 2017. National Oceanic and Atmospheric Administration, Great Lakes Environmental Research Laboratory, About our lakes. Accessed 15 January 2017. [Available online at https://www.glerl.noaa.gov/education/ourlakes/intro.html.]

Norton, D., and Bolsenga, S. 1993. Spatiotemporal trends in lake effect and continental snowfall in the Laurentian Great Lakes, 1951-1980. *Journal of Climate,* 6: 1943-1956, DOI: 10.1175/1520-0442(1993)006<1943:STILEA>2.0.CO;2.

Notaro, M., Bennington, V., and Vavrus, S. 2015. Dynamically downscaled projections of lake-effect snow in the Great Lakes basin. *Journal of Climate.* 28:1661–1684, DOI: 10.1175/JCLI-D-14-00467.1.

Notaro, M., Zarrin, A., Fluck, E., Vavrus, S., and Bennington, V. 2013. Influence of the Laurentian Great Lakes on regional Climate. *Journal of Climate,* 26: 789-804, DOI: 10.1175/JCLI-D-12-00140.1.

Notaro, M., Zarrin, A., Vavrus, S., and Bennington, V. 2013. Simulation of heavy lake-effect snowstorms across the Great Lakes Basin by RegCM4: Synoptic climatology and variability. *Monthly Weather Review.* 141: 1990-2014.

NWS. 2014. National Weather Service, Lake-Effect Summary. Accessed 9 February 2017. [Available online at www.weather.gov/buf/]

Obolkinm, V.A., and Potemkin, V.L. 2006. The Impact of Large Lakes on Climate in the Past: a Possible Scenario for Lake Baikal. *Hydrobiologia,* 568: 249–252.

Oke, T.R. 1987. *Boundary layer climates*. Second edition (p. 12). New York, NY: Methuena and Co. in association with Metheuna, Inc.

OWO. 1994. Lake Effect Snow Decision Trees. *Ontario Weather Office,* Toronto, Canada: Author. Accessed 2012.

Passarelli, R.E. Jr., and Braham, R.R. Jr. 1981. The role of the winter land breeze in the formation of Great Lake snow storms. *Bulletin of the American Meteorological Society.* 62: 482–491.

Payer, M., Desrochers, J., and Laird, N.F. 2007. A lake-effect snowband over Lake Champlain. *Monthly Weather Review*, 135 (11): 3895-3900.

Pease, S.R., Lyons, W.A., Keen, C.S., and Hjelmfelt, M.R. 1988. Mesoscale spiral vortex embedded within a Lake Michigan snow squall band: High resolution satellite observations and numerical model simulations. *Monthly Weather Review,* 116: 1374-1380.

Perroud, M.S., Goyette, S., Martynov, A., Beniston, M., and Anneville, O. 2009. Simulation of multiannual thermal profiles in deep Lake Geneva: A comparison of one-dimensional lake models. *Limnology and Oceanography,* 54: 1574-1594.

Phillips, D.W. 1972. Modification of Surface Air Over Lake Ontario in Winter. *Monthly Weather Review*, 100(9): 662-670.

Rauber, R.M., Walsh, J.E., and Charlevoix, D.J. 2005. *Severe & hazardous weather – An introduction to high impact meteorology*. Second Edition. New York, NY: Oxford University Press, Inc.

Rawlins, M.A., Willmott, C.J., Shiklomanov, A., Linder, E., Frolking, S., Lammers, R.B., and Vörösmarty, C.J. 2006. Evaluation of trends in derived snowfall and rainfall across Eurasia and linkages with discharge to the Arctic Ocean. *Geophysical Research Letter,* 33: L07403, DOI:10.1029/2005GL025231.

Rouse, W.R., Oswald, C., Binyamin, J., Schertzer, W., Blanen, P., Bussieres, N., and Duguay, C.R. 2005. Role of northern lakes in a regional energy balance. *Journal of Hydrometeorology,* 6(3): 291-305.

Samuelsson, P., Kourzeneva, E., and Mironov, D. 2010. The impact of lakes on the European climate as simulated by a regional climate model. *Boreal Environment Research,* 15: 113-129.

Schertzer, W.M. 1997. *Freshwater lakes.* Montreal, Quebec, Canada: McGill-Queen's University Press.

Schroeder, J.J., Kristovich, D.A.R., and Hjelmfelt, M.R. 2006. Boundary layer and microphysical influences of natural cloud seeding on a lake-effect snowstorm. *Monthly Weather Review*, 134(7)1842–1858.

Scott, A.K., Buehner, M., and Caya, A. 2012. Assimilation of ASMR-E brightness temperatures for estimating sea ice concentration. *Monthly Weather Review*, 140: 997-1010, DOI: 10.1175/MWR-D-11-00014.1.

Scott, D., and Kaiser, D. 2004. Variability and trends in United States snowfall over the last half century. Preprints, *15th Symp. on Global Climate Variations and Change,* Seattle, WA, American Meteorological Society, CD-ROM, 5.2.

Semmler, T., Cheng, B., and Yang, Y., Rontu, L. 2012. Snow and ice on Bear Lake (Alaska)-Sensitivity experiments with two lake ice models. *Tellus Series A-Dynamic Meteorology and Oceanography*, 64, 17339, DOI: 10l.3402/tellusa.v64i0.17339.

Shi. J.J., and coauthors, 2010. WRF simulations of the 20–22 January 2007 snow events over eastern Canada: Comparison with in situ and satellite observations. *Journal of Applied Meteorology and Climatology,* 49: 2246–2266.

Sousounis, P.J., and Fritsch, J.M. 1994. Lake aggregate mesoscale disturbances. Part II: A case study of the effects on regional and synoptic-scale weather systems. *Bulletin of the American Meteorological Society,*75: 1793–1811.

Spence, C., Blanken, P.D., Hedstrom, N., Fortin, V., and Wilson, H. 2011. Evaporation from Lake Superior: 2: spatial distribution and variability. *Journal of Great Lakes Research,* 37(4): 717–724.

Spinar, M.L., and Kristovich, D.A.R. 2007. Multiscale interaction in a lake-effect snowstorm. In *12th Conference on Mesoscale Processes.*

Steenburgh, W. J., Halvorson, S.F., and Onton, D.J. 2000: Climatology of lake-effect snowstorms of the Great Salt Lake. *Monthly Weather Review*, 128: 709–727.

Surdu, C.M., Duguay, C.R., and Brown, L.C., Fernández, Priesto, D. 2014. Response of ice cover on shallow lakes of the North Slope of Alaska to contemporary climate conditions (1950 – 2011): radar remote-sensing and numerical modeling data analysis. *Cryosphere,* 8: 167-180, DOI:10.5194.

Suriano, Z.J., and Leathers, D.J. 2016. Twenty-first century snowfall projections within the eastern Great Lakes region: detecting the presence of a lake-induced snowfall signal in GCMs. *International Journal of Climatology,* 36: 2200-2209. DOI: 10.1002/joc/4488.

Suriano, Z.J., and Leathers, D.J. 2017. Climatology of lake-effect snowfall conditions in the eastern Great Lakes region. *International Journal of Climatology*, 37(12): 4377-4389.

Theeuwes, N.E., Steeneveld, G.J., Krikken, F., and Holtslag, A.M. 2010. Mesoscale modeling of lake effect snow over Lake Erie – sensitivity to convection, microphysics and the water temperature. *Advances in Science and Research,* 4: 15-22.

Thornton, P.E., Hasenaur, H., and White, M.A. 2000. Simultaneous estimation of daily solar radiation and humidity from observed temperature and precipitation: an application over complex terrain in Austria. *Agricultural and Forest Meteorology,* 14: 255-271.

Thornton, P.E., Running, S.W., and White, M.A. 1997. Generating surfaces of daily meteorological variables over large regions of complex terrain. *Journal of Hydrology,* 190: 214–251.

Thornton, P.E., Thornton, M.M., Mayer, B.W., Wei, Y., Devarakonda, R., Vose, R.S., and Cook, R.B. 2016. Daymet: Daily surface weather data on a 1-km grid for

North America, Version 3. ORNL DAAC, Oak Ridge Tennessee, USA. Accessed January, 2018. [Available online http://dx.doi.org/10.3334/ORNLDAAC/1328].

Titze, D.J., and Austin, J.A. 2014. Winter thermal structure of Lake Superior. *Limnology and Oceanography,* 59 (4):1336-1348.

Tripoli, G.J. 2005. Numerical study of the 10 January 1998 lake effect bands observed during lake-ice. *Journal of the Atmospheric Sciences,* 62: 3232–3249.

Vavrus, S., Notaro, M., and Zarrin, A. 2013. The role of ice cover in heavy lake-effect snowstorms over the Great Lakes Basin as simulated by RegCM4. *Monthly Weather Review,* 141:148-165.

Vavrus, S., Walsh, J.E., Chapman, W.L., and Portis, D. 2006. The behavior of extreme cold air outbreaks under greenhouse warming. *International Journal of Climatology,* 26 :1133-1147, DOI : 10.1002/joc.1301.

Verseghy, D.L. 2009. *CLASS-The Canadian Land Surface Scheme (Version 3.4)-technical documentation (version 1.1).* (pp.183). Internal report. Climate Research Division, Science and Technology Branch, Environment Canada.

Wang, J., and coauthors. 2018. Decadal variability of Great Lakes ice cover in response to AMO and PDO, 1963-2017. *Journal of Climate,* in press.

Wang, J., Bai, K., Hu, H., Clites, A., Colton, M., and Lofgren, B., 2012. Temporal and spatial variability of Great Lakes ice cover, 1973–2010. *Journal of Climate,* 25: 1318–1329, DOI:10.1175/2011JCLI4066.1.

Wang, J., Eicken, H., Yu, Y., Bai, X., Zhang, J., Hu, H., Wang, D.R., Ikeda, M., and Mizobata, K. 2014. Abrupt climate changes and emerging ice-ocean processes in the Pacific Arctic region of the Bering Sea. In Grebmeier, J., and Maslowski, W. (Eds.) *The pacific arctic region* (pp. 65-99). Dordrecht, Netherlands. Springer.

Wang, J. Ikeda, M., Zhang, S., and Gerdes, R. 2005. Linking the northern hemisphere sea-ice reduction trend and the quasi-decadal arctic sea-ice oscillation. *Climate Dynamics*, 24: 115-130, DOI: 10.1007/s00382-004-0454-5.

Warner, T.T., and Seaman, N.L., 1990. A real-time, mesoscale numerical weather prediction system used for research, teaching, and public service at the Pennsylvania State University. *Bulletin of the American Meteorological Society,*71: 792–805.

Wetzel, R.G. 1975. *Limnology.* W.B. Saunders CO., Philadelphia, London, and Toronto, xii. © the Association for the Sciences of Limnology and Oceanography, Inc.

Wiggin, B.L. 1950. Great snows of the Great Lakes. *Weatherwise,* 3, 123-126.

Wilson, J.W. 1977. Effect of Lake Ontario on precipitation. *Monthly Weather Review,*105. 207-214.

Wright, D.M., Posselt, D.J., and Steiner, A.L. 2013. Sensitivity of lake effect snowfall to lake ice cover and temperature in the Great Lakes region. *Monthly Weather Review,* 141: 670-689, DOI: 10.1175/MWR-D-12-00038.1.

Yeh, K.-S., Côté, J., Gravel, S., Méthot, A., Patoine, A., Roch, M., and Staniforth, A. 2002. The CMC-MRB global environmental multiscale (GEM) model. Part III: Nonhydrostatic formulation. *Monthly Weather Review*, 130(2): 339–356.

Zadra, A., Caya, D., Ducas, B., Jones, C., Laprise, R., Winger, K., and Caron, L.-P. 2008. The next Canadian regional climate model. *La Physique Au Canada,* 64(2): 74-83.

Zamg. 2017. Numerical parameters for synoptic to mesoscale systems: Vertical Motion-Omega Equation. Accessed 9 February 2017. [Available online http://rammb.cira.colostate.edu/wmovl/vrl/tutorials/satmanueumetsat/SatManu/Basic/Parameters/Omega.htm].

Zhang, X., Hogg, W.D., and Mekis, E. 2001. Spatial and temporal characteristics of heavy precipitation events over Canada. *Journal of Climate*, 14(9)1923–1936.

Zulauf, M. A., and Krueger, S.K. 2003.Two-dimensional cloud-resolving modeling of the atmospheric effects of Arctic leads based upon midwinter conditions at the surface heat budget of the Arctic Ocean ice camp. *Journal of Geophysical Research,* 108: 4312, DOI: 10.1029/2002JD002643.